460

Locomotion of Herring and Plaice Larvae

A thesis submitted to the University of Stirling for the degree

of Doctor of Philosophy

by

Robert Steven Batty

Scottish Marine Biological Association

Dunstaffnage Marine Research Laboratory

P.O. Box 3,

Oban,

Argyll, Scotland.

February 1983

CONTENTS

ACKNOWLEDGEMENTS

ABSTRACT

The swimming of larval plaice *Pleuronectes platessa* L was recorded using silhouette cinematography and that of larval herring *Clupea harengus* L by television and video recorder.

The swimming style of herring was found to change with growth. The amplitude of swimming movements of very young larvae increased linearly towards the tail, so that resistive rather than inertial forces were the more important. At a length of 20 mm when caudal and dorsal fins had developed, a new type of swimming was adopted in which amplitude increased more rapidly along the length of the body so indicating the greater importance of inertial forces.

. Plaice larvae used pectoral fins and body waves simultaneously at cruising speeds. The fins did not produce thrust but counteracted recoil and so prevented yaw of the head. This was achieved by synchronized tail and fin movements with a 180° phase difference between the strokes of each fin. Body wave speed: swimming speed ratio u/v was low increasing from 0.2-0.4 as the larvae swam faster. At burst speeds plaice larvae changed swimming style and used very high tail beat frequencies. The pectoral fins were not used and the length of the body wave lengthened.

A new kinematic model, based on the angle between segments of the body and direction of motion, was fitted to a swimming herring larvae 22 mm in length. This model demonstrated both variation in wavelength and speed of the propulsive wave within the tail beat cycle.

The distribution of red and white muscle fibre types of
larval herring changed during growth. On hatching, when the larva
was dependent on cutaneous respiration, red muscle fibres were
arranged as a single layer under the skin. The adult distribution
with red mucle concentrated along the mid-flank developed after
the gills and circulation became fully functional.

Locomotion of Herring and Plaice Larvae

A thesis submitted to the University of Stirling for the degree

of Doctor of Philosophy

by

Robert Steven Batty

Scottish Marine Biological Association

Dunstaffnage Marine Research Laboratory

P.O. Box 3,

Oban,

Argyll, Scotland.

February 1983

CONTENTS

ACKNOWLEDGEMENTS

ABSTRACT

The swimming of larval plaice *Pleuronectes platessa* L was
recorded using silhouette cinematography and that of larval herring
Clupea harengus L by television and video recorder.

The swimming style of herring was found to change with growth.
The amplitude of swimming movements of very young larvae increased
linearly towards the tail, so that resistive rather than inertial
forces were the more important. At a length of 20 mm when caudal
and dorsal fins had developed, a new type of swimming was adopted
in which amplitude increased more rapidly along the length of the
body so indicating the greater importance of inertial forces.

.   Plaice larvae used pectoral fins and body waves simultaneously
at cruising speeds. The fins did not produce thrust but counteracted
recoil and so prevented yaw of the head. This was achieved by
synchronized tail and fin movements with a 180° phase difference
between the strokes of each fin. Body wave speed: swimming speed
ratio u/v was low increasing from 0.2-0.4 as the larvae swam faster.
At burst speeds plaice larvae changed swimming style and used
very high tail beat frequencies. The pectoral fins were not used
and the length of the body wave lengthened.

A new kinematic model, based on the angle between segments of
the body and direction of motion, was fitted to a swimming herring
larvae 22 mm in length. This model demonstrated both variation in
wavelength and speed of the propulsive wave within the tail beat cycle.

The distribution of red and white muscle fibre types of larval herring changed during growth. On hatching, when the larva was dependent on cutaneous respiration, red muscle fibres were arranged as a single layer under the skin. The adult distribution with red mucle concentrated along the mid-flank developed after the gills and circulation became fully functional.

SYMBOLS

a coordinate running along a larva's body.

b phase.

c_f frictional drag coefficient.

L body length.

m virtual mass.

P vector of thrust along direction of motion.

Q vector of thrust normal to direction of motion (lateral force).

R_L Reynold number based on length.

t time.

T total thrust.

u forward swimming speed.

u_p velocity of tail tip tangential to tail blade.

v backwards velocity of propulsive wave.

w velocity of tail tip normal to tail blade.

α angle of attack.

δ boundary-layer thickness.

γ angle between a tangent to any part of the body on an arbitrary x axis.

η_p propeller efficiency.

θ angle between a tangent to any part of the body and the direction of motion.

θ^1 angle between a tangent to any part of the body and the instantaneous direction of motion.

λ_a wavelength of the wave on the body measured along a.

λ_b wavelength of the wave on the body measured along x.

ρ density.

μ viscosity.

INTRODUCTION

The study of fish swimming has a long history, the earliest reference dating from about 600 B.C. Hora (1935) reports a passage from the Susrutasamhita (an ancient hindu work) in which body forms of fishes are correlated with patterns of locomotion and thus with their ecology. Other early work is reviewed by Gray (1968). It was not until cinephotography was developed that much advance could be made on these simple observations. Marey (1895) used ciné techniques to record the movements of many animals including fish. He observed the basic pattern of fish swimming in which waves pass down the body from head to tail at greater speed than the fish swim forwards. It can also be seen from his photographs that amplitude increases from head to tail and that about one wavelength is included within the body.

During this century many aspects of fish swimming have been investigated both by biologists and applied mathematicians; this work is reviewed by Gray (1968), Webb (1975), and Wardle and Videler (1980). It is surprising that despite the large amount of work on adult fish there has been very little on larval fish and none is reported in these reviews.

There are several reasons for the relative neglect of swimming of fish larvae. They are nearly transparent and therefore difficult to photograph (Blaxter and Staines, 1971). This problem could not be overcome until specialized techniques were developed (Hunter,

1972; Arnold and Nuttall-Smith, 1974). Also live fish larvae
are not readily available for experiments. They are difficult
to obtain from the wild since they are very delicate and so
rarely survive capture. Thus detailed studies of swimming of
fish larvae rely on captive rearing in aquaria.

Locomotion plays an important part in many aspects of
behaviour of fish larvae that is vital to their survival. Mortality
of larvae in the sea may be caused by starvation, predation,
mechanical damage and genetic defects. Locomotion is essential for
avoiding the first three of these causes of mortality. Herring
larvae are negatively buoyant (Ehrlich,1972) and swim as soon as
they hatch. The amount of time herring larvae spend swimming
upwards is correlated with their sinking rate and therefore it is
most likely that swimming of yolk sac stage herring larvae is for
depth control. Weihs (1980b) found that the swimming movements of
yolk-sac anchovy larvae were also for depth control. Once the
yolk-sac has been absorbed larval herring are observed to swim
almost continuously at light intensities adequate for feeding
(Blaxter and Staines, 1971).

Swimming is important in the avoidance of predators by using
bursts of high speed but the cruising swimming speeds normally
employed by larvae have an effect on their susceptibility to
predation (Bailey and Batty, 1983). It was shown that the
orientation of swimming,either horizontal or vertical, had a dramatic
effect on the encounter rate of herring larvae with one of their

predators, the medusa *Aurelia aurita*; encounter rate was very
much higher when the medusa swam horizontally and the larva
vertically.

Swimming movments

Few studies have been made of the swimming movements of
fish larvae. Rosenthal (1968) filmed the swimming behaviour
of herring larvae. From his pictures it is obvious that herring
larvae have much more flexible bodies than adults and have somewhat
different swimming motions, but a detailed analysis was not made.
Apart from a comparison of speed, tailbeat frequency and amplitude
in anchovy by Hunter (1972), using a silhouette illumination
technique, and an application of a hydrodynamic model for the
energetic cost of swimming using the same film by Vlymen (1974)
there have been no kinematic analyses of swimming in fish larvae.

Swimming speeds

Observations of swimming speed may be divided into three
categories; a) Burst speeds; very greatly in excess of maximum
cruising speed, using anaerobic energy and approaching maximum
possible speed. b) Prolonged and critical speeds; endurance is
measured over a range of speeds and a "critical" speed (as defined
by Brett, 1964) is found which is an indication of the limit of
aerobic activity. c) Sustained or cruising speeds; this is a
simple observation of the self-imposed swimming speed employed in

food searching, migration etc and is usually much less than

maximum cruising speed which is the maximum swimming speed which can

be supported by aerobic respiration.

A number of measurements of larval swimming speeds have been

made using a variety of techniques. Although burst speeds may be

measured experimentally (Blaxter, 1962; Ryland, 1963; Radakov, 1964;

Hunter, 1972), it is difficult to obtain the maximum burst speed.

Hunter (1972) gives the results of a number of measurements of larval

anchovy of which two exceed 25 lengths per second ($L.s^{-1}$). This

was considerably faster than any of the other speeds measured to date

and may still not be a maximum speed.

Wardle (1974) tested the isotonic contraction time of fish

white muscle from adults of a number of species and found it

positively related to fish length; in other words, smaller fish

should be able to produce higher tailbeat frequencies and hence

their maximum burst speeds expressed as specific speeds (i.e. body

lengths per second) will be higher. Wardle's results predicted

that fish of 10 cm length could swim at 25 $L.s^{-1}$ but 1 m long fish

may only manage 6 $L.s^{-1}$. He showed television pictures of a 10 cm

sprat swimming at its maximum speed of 2.5 $m.s^{-1}$.It is therefore

possible that fish larvae,because of their small size,may be able

to swim even faster than has been observed to far.

Prolonged speeds have been measured in larvae by Bishai (1959),

Boyar (1961), Houde (1969), Glova and McInerney (1977), and

Laurence (1972). Specific speeds were found to be higher than in

adult fish. Interestingly, Laurence (1972) found that starvation caused considerable reduction in the critical speed of largemouth bass larvae.

Musculature

The development of the musculature has been thoroughly studied in Zebra fish *(Brachydanio rerio)*. Waterman (1970) examined the fine structure and found that on hatching larvae had two structurally dissimilar types of muscle cells whose appearance suggested development into the superficial red and deep white muscle portions of the adult. Van Raamsdonk et al. (1974, 1976), described the development of the myotomes in the zebra fish. They were initially simple curved plates but which developed into the complex adult form described by Alexander (1969) and Kashin and Smolyaninov (1969).

Scope of this study

It is the aim of this study to examine the movements of herring and plaice larvae in detail. These species were chosen because of their dissimilar larval forms. While the herring has an eel-like larva, plaice larvae are much shorter and deeper bodied. Arnold (1969) noted that plaice larvae may also use their pectoral fins for swimming, which suggests further interesting contrasts between the swimming of the two species. The musculature of herring larvae is also examined and the distribution of aerobic muscle fibres

related to earlier work on the respiration of herring larve by
de Silva (1973).

M E T H O D S

Rearing Techniques

Herring

   In March spawning herring were caught on the Ballantrae Bank, in the Clyde Sea, by RV Calanus using a trawl net. The gonads were excised from a number of ripe male and female fish and stored, dry, in glass jars on ice. These gonads were transported back to Oban to be fertilized within 12 h.

   Fertilizations were carried out according to the methods described by Blaxter (1968). The surface of herring eggs become adhesive on contact with water. Glass plates (45 x 15 cm) were laid in a rectangular plastic container (52 x 52 x 20 cm) under 10 cm of seawater. Eggs were then picked up on a dry spatula and scattered in the water over the plates to give approximately 4 eggs.cm^{-2}. Any clumps of eggs, that might cause anaerobic conditions and eventually the death of the eggs, were removed.

   These plates of eggs were placed in a bath of seawater, containing the sperm from between 5 and 10 males, for 10 to 20 min. After rinsing in a bath of seawater for 5 to 10 min the fertilized eggs were placed in the rearing tanks. About 12 plates could be accommodated in each tank in pairs, back to back resting on the bottom and leaning against the wall of the tank.

   Round black plastic tanks were used in two sizes: the

smaller were 62 cm in diameter by 50 cm holding 130 ℓ and the larger one were 75 cm in diameter by 60 cm holding 220 ℓ. Temperature was not controlled and depended on the incoming seawater temperature, flow rate into the tanks and air temperature in the aquarium. For this reason the seawater temperature was recorded daily and temperatures from fertilization onwards are shown for the three years 1977, 1978, 1979 in Fig. 1.

The plates of eggs were moved to tanks of clean seawater every second day until hatching started when an outflow screen, made of a short length of perspex tube with a mesh on one end, was attached to the drain tube by a hole in the wall of the outflow screen with the mesh beneath the water surface. This device prevented larvae being lost down the drain. When most of the larvae had hatched the plates were removed.

Plaice

In 1977 and 1978 fertilized plaice eggs were kindly supplied by both the White Fish Authority, Ardtoe and by University Marine Station, Port Erin, Isle of Man. By 1979 both these organisations had stopped rearing plaice but the WFA offered to give us their brood stock which was removed to Oban on 28 February 1979.

There was no suitable cage, with a plain surface for the fish to rest on, available to keep these fish in the sea. Since

Fig. 1.   Temperatures in larval rearing tanks during

1977 ■ , 1978 ▲ , 1979 O .

it is essential that flatfish experience a natural cycle of photo-period if they are to remain in spawning condition, it was necessary to set up a light-tight enclosure over their tank within which photo-period could be maintained. Two tanks (1.6 m diameter, 0.5 m deep) were set up with separate lighting systems controlled by solar dial clocks which provided a day length corresponding to latitude 54° north.

The fish were marked using freeze-branding (Everest and Edmundson, 1967) so that individual females could be identified and males could be distinguished from females before removal from the tank. Drikold (Solid CO_2) was broken up into small pieces and put in a wide neck vacuum flask and then 74 op. industrial methylated spirit was poured over the drikold. Brass branding tools were immersed in the alcohol for about 1 min to cool before applying to the fishes skin for 15 s.

Eggs were stripped from ripe females by gently pressing on the sides of the fish and running the hands from the tail towards the head. Ripe females would easily shed their eggs which were caught in a glass beaker held below the oviduct. Sperm was collected from ripe males by gently squeezing the region of the testes between finger and thumb and so pushing the sperm out. A second person collected the sperm in a syringe. The eggs from 3 females and sperm from 3 males were mixed dry and, after 5 min, seawater was added. Fertilized eggs float and were removed from the surface with a tea strainer, rinsed, and then

it is essential that flatfish experience a natural cycle of photo-period if they are to remain in spawning condition, it was necessary to set up a light-tight enclosure over their tank within which photo-period could be maintained. Two tanks (1.6 m diameter, 0.5 m deep) were set up with separate lighting systems controlled by solar dial clocks which provided a day length corresponding to latitude 54° north.

The fish were marked using freeze-branding (Everest and Edmundson, 1967) so that individual females could be identified and males could be distinguished from females before removal from the tank. Drikold (Solid CO_2) was broken up into small pieces and put in a wide neck vacuum flask and then 74 op. industrial methylated spirit was poured over the drikold. Brass branding tools were immersed in the alcohol for about 1 min to cool before applying to the fishes skin for 15 s.

Eggs were stripped from ripe females by gently pressing on the sides of the fish and running the hands from the tail towards the head. Ripe females would easily shed their eggs which were caught in a glass beaker held below the oviduct. Sperm was collected from ripe males by gently squeezing the region of the testes between finger and thumb and so pushing the sperm out. A second person collected the sperm in a syringe. The eggs from 3 females and sperm from 3 males were mixed dry and after 5 min, seawater was added. Fertilized eggs float and were removed from the surface with a tea strainer, rinsed, and then

floated in the rearing tanks.

Plaice eggs fertilized in the laboratory were immediately placed in the rearing tanks which were similar to those used for herring but smaller i.e. 43 cm diameter by 25 cm deep and holding 30 ℓ. Care was taken during the incubation period to ensure that eggs did not accumulate in one corner of the tank and to remove dead eggs with a siphon. An outflow screen, of the type described for use in the herring tanks, was used from the moment the eggs were introduced.

Fertilized eggs from Ardtoe or Port Erin were invariably in water of a higher salinity than our aquarium water. To prevent them from sinking and then dying on the bottom of the tank, these eggs were floated in seawater adjusted to the same salinity as the water they had arrived in, by adding sodium chloride to aquarium water. These tanks were kept in a temperature controlled room at 10°C. The antibiotics Penicillin (1 g) and Streptomycin (0.5 g) (Shelbourne, 1966) were added to 30 ℓ water to prevent bacterial growth; the water was changed every 3 days and the antibiotics were renewed. When the larvae had hatched the tanks were connected to the laboratory seawater circulation.

Maintenance and Feeding

The seawater supply to the rearing tanks ran via a degassing tower (Currie, Blaxter and Joyce, 1976) which emptied into a

header tank of 220 ℓ capacity. In addition to aeration in the degassing tower the water in the header tank was vigorously aerated. This was necessary to remove supersaturated oxygen and nitrogen present in the seawater supply. Seawater passed from the header tank to either of three intermediate small (2 ℓ) header/manifold tanks 0.5 m above the water surface of the rearing tanks. These manifold tanks allowed air bubbles introduced in the header tank to be removed, the water to be filtered and for the flow to the rearing tanks to be easily controlled. Seawater was delivered to the bottom of the rearing tanks by glass tubes.

Outflow screens were removed and cleaned daily to prevent blockage with food or debris and consequent overflow and loss of larvae. The bottom of the tanks were cleaned and dead larvae removed with a siphon. A oily film tended to build up on the water surface and could trap gas bubbles which might be ingested by larvae. To remove this film a desk lamp was positioned to shine on one part of a tank which would attract the majority of the larvae. The oily film was then removed by skimming with a glass beaker.

Feeding started once the yolk sac was resorbed at about 10 days from hatching. In 1977 *Balanus* nauplii were offered, during the first 2 weeks of feeding, until feeding was established with *Artemia* nauplii. Throughout development larvae were fed on *Artemia* but in 1977 the harpacticoid copepod *Tigriopus* was

collected from rock pools to supplement the diet from June onwards. Natural plankton was also provided in all 3 years; living zooplankton attracted to light was separated and sieved to remove predators and over-large food organisms.

Photography

Fish larvae are difficult to photograph because they are nearly transparent. This means that it is necessary to use special techniques designed to give increased contrast. Silhouette or shadow-graph photography techniques were developed and Fig. 2 shows three such techniques.

The most simple method of high-speed silhouette photography, developed by Edgerton (1970) and used to photograph small rapidly moving organisms (Edgerton, 1977) and to identify zooplankton (Ortner *et al.*, 1979), has been adapted here to photograph fish larvae (Fig. 2A). This same technique can also be used for measurement of fish larvae (Neave and Batty, 1982).

The two other techniques used here have already been used by other workers to make cine films of fish larvae. Fig. 2B shows the method used by Hunter (1972) for anchovy larvae. A single or double condenser is used to focus the light source on the camera lens, with the subject placed between the condenser and the camera. The third method (Fig. 2C), shadow cinematography, was developed and used by Arnold and Nuttal-Smith (1974) to film plaice larvae. In this method the subject is inserted between the collimator and condenser lens. This allows for a large depth of field but the

Fig. 2.   Three silhouette photography methods:

           A, a simple shadow method using no lenses (Edgerton 1977),

           B, using a condenser lens and camera,

           C, Shadowgraph method (Arnold and Nuttall-Smith 1974).

A

B

C
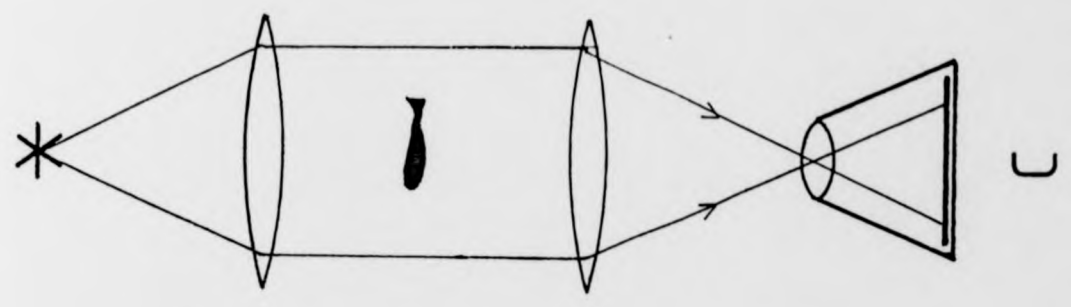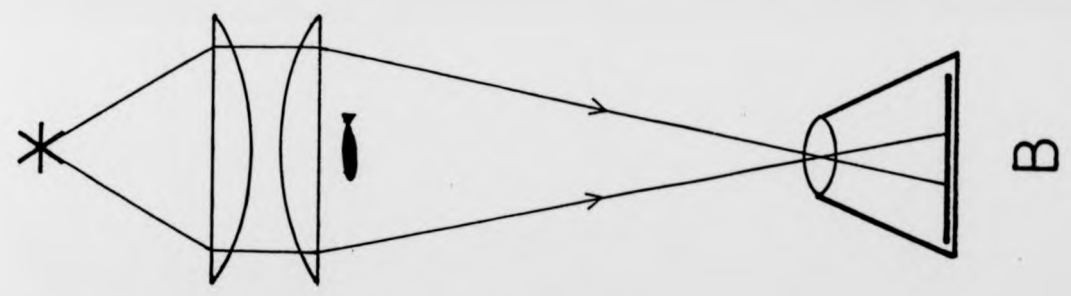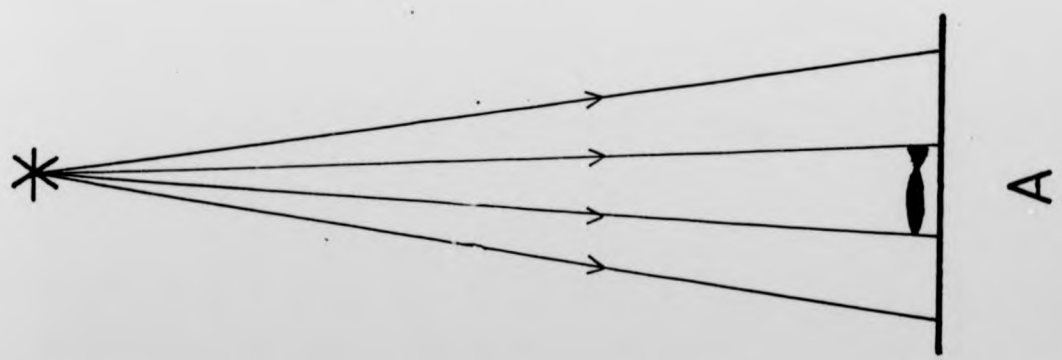
quality of the lenses may limit resolution and contrast.

The simple method (Fig. 2A) is probably the best for taking still photographs and was used here to make photographs of herring and plaice larvae for measuring their fin areas and body dimensions. None of these silhouette methods seemed appropriate for filming herring larvae which grow to 40 mm at metamorphosis. Either the depth of water in the tank or the field of view are limited or, in the case of Arnold and Nuttal-Smith's method, expensive purpose-made lenses are required. Another technique was therefore adopted.

Wardle and Reid (1977) used a reflective background to produce silhouette images of adult fish swimming. In this technique a strobe light source is positioned next to a cine or TV camera lens and "Scotchlite" (the retroreflective material used on vehicle number plates and road signs) is used as the background on the floor of the tank. Scotchlite reflects within 4° of the incident light and therefore the simple technique used by Wardle and Reid would not work at the smaller camera-to-subject distances which were necessary when filming larval fish.

Their technique was modified by inserting a semi-silvered mirror or a sheet of uncoated optical glass between the lens and the subject at 45° to the light path. In effect the light source and camera lens share the same optical axis. This allows light from the strobe to be reflected towards the subject and the subject to be observed by the camera Fig. 3.
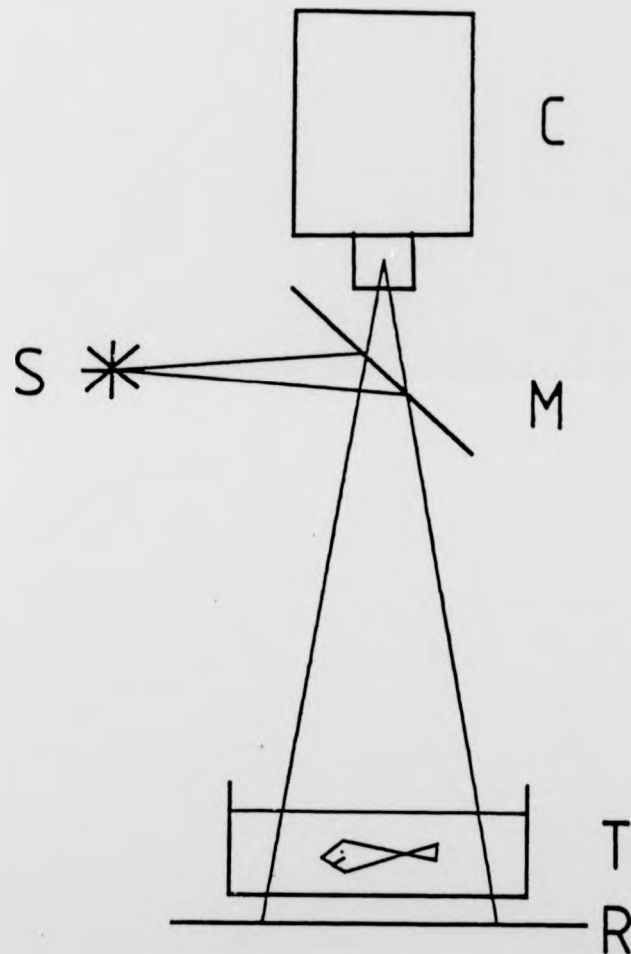
Fig. 3. A diagram showing the apparatus used to record larval

swimming movements. C, TV camera; S. strobe lamp

(synchronized with TV field pulse); M, semi-silvered

mirror, T. small tank containing subjects;

R, retro-reflector ('Scotchlite').

For detailed analysis of a high film speed of at least
50 frames s^{-1} is required in order to have sufficient frames per
tailbeat. When ciné film is used at these speeds a 30 m roll
of film can be used in 2 min. Therefore, unless the subjects can
be confined to the field of view, a great deal of film could be
wasted for few results. Closed circuit television can be used
with a video tape recorder for up to 1 h of continuous recording
at 50 fields.s^{-1}.

In the present experiments a television camera fitted with a
newvicon tube was used with a National Panasonic slow motion
video tape recorder. This type of tube has less smearing
than the cheaper vidicon tube but the effective shutter speed is
still greater than 1/50th s. To get sharp images a strobed light
source was used. This device was synchronized to the television
field pulses and provided 10 μs flashes of 0.15J from a
Wotan XE15, 15W strobe tube.

Still photographs

Eastman Kodak 35 mm Fine Grain Release Positive film 5302
was used, a length being loaded into a 35 mm cassette. The
leader was fixed to the spool of another cassette so that a
length of film could be drawn from one cassette, exposed and then
wound into the other cassette. In this way a number of
exposures could be made, and then developed together on one
length of film.

Larvae were carefully removed from their tanks and placed in seawater which had been filtered through a glass fibre filter (GFC3) to eliminate light-scattering particles in the water. Larvae were transferred by pipette through two beakers of this water before being placed in a tank made of microscope glass stuck along the edges with 'araldite' (37 x 25 x 74 x 1 mm thick). Top views were taken in this way but for profiles the larvae were anaesthetized with benzocaine. Benzocaine was dissolved in acetone at 50 g.ℓ^{-1} and this solution was added to filtered seawater to give a dilution of 1:40,000 and then filtered again. This anaesthetic-seawater solution was used in the photographic tank. Larvae were quickly anaesthetized and then tended to lay on their sides so allowing the profile photographs to be easily obtained. Once returned to pure seawater the larvae recovered quickly.

Silhouette cinématography

Preliminary work on the swimming of plaice larvae was carried out using the television technique described in the previous section. The pictures obtained showed that pectoral fins were used simultaneously with body movements and that their movement was, in some way, synchronized with tail movement. No clear fin outline could be discerned and therefore no more than this simple observation could be made.

High speed silhouette photography would be ideal for recording

larval swimming if the film could move continuously past the
subject and an intermittent light source such as a strobe used
to expose the film. A simple machine was therefore built to
achieve this as shown in Fig. 4. Film, wound on spool A with a
long leader of approximately 15 m of scrap film, is drawn over
the large diameter drum to spool B. The drum and take-up spool
are driven by separate motors both operated at full power. The
drum is driven via a reduction gearbox to give a full speed of
600 rpm, and the take-up spool is driven directly by a 12,000 rpm
motor. The final speed is controlled by the larger motor which
drives the drum.

Exposures are made by a strobe flash of the same type used
for the TV recording but driven by a variable speed triggering
circuit. The 'frame rate' is controlled by the frequency of
the strobe so that successive fields do not overlap. Above the
drum and spools is the lid which also forms the mask and
observation tank. In the present apparatus 70 mm film is used to
give a large field of view 58 x 58 mm of the entire tank. This
format allows 70 frames.s^{-1} at full speed. A print of a single
frame from a negative is shown in Fig. 5.

Histology

Herring and plaice larvae were sampled at frequent intervals
during their development. Frozen sections were cut in a cryostat
and then histochemical staining methods were used to demonstrate

Fig. 4.   The silhouette "camera". (A) plan view, (B) side view,
          c container for subjects, d drum, f 70 mm film, l lid,
          m drum motor, n take up spool motor, r rubber coupling,
          s supply spool, t take up spool.

20 cm
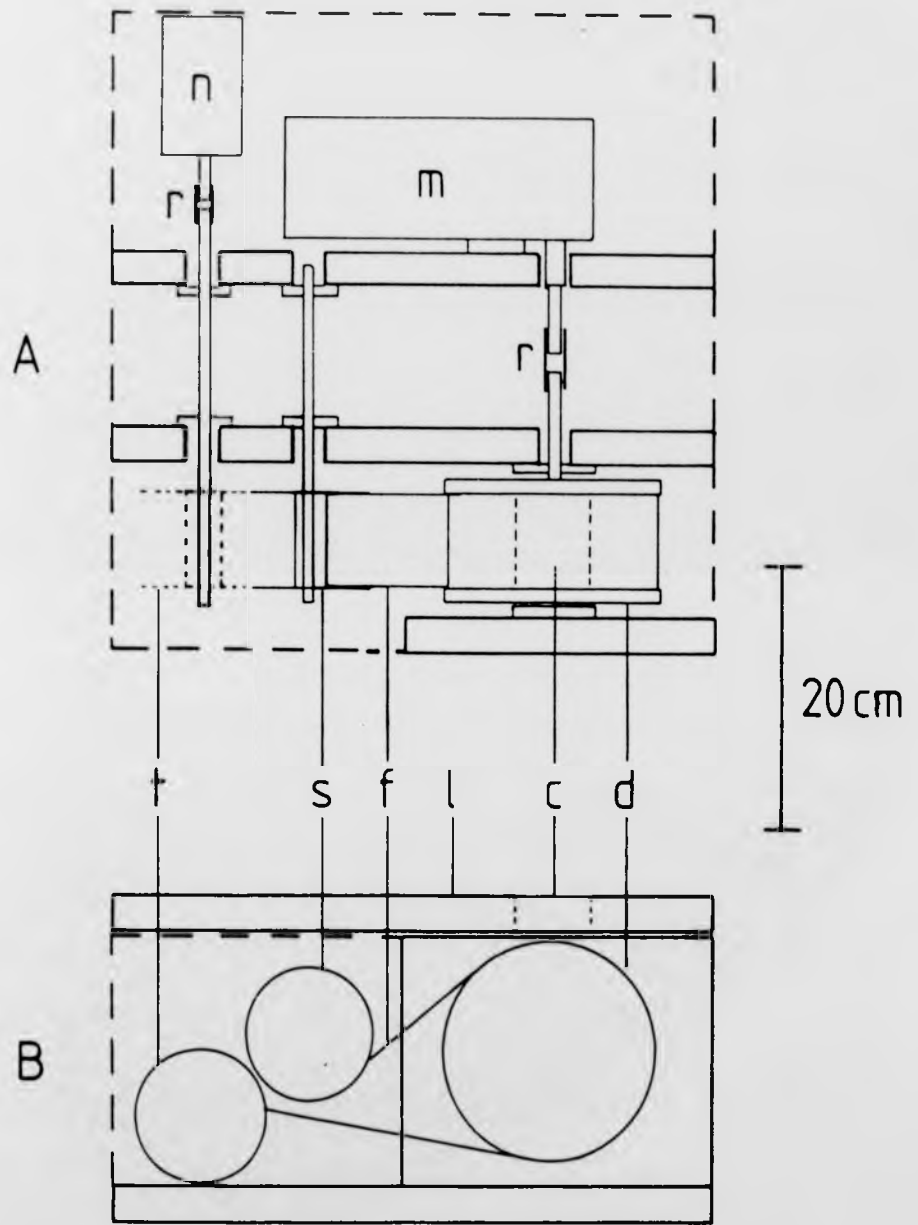
Fig. 5.   A print from one frame of a silhouette film

showing plaice larvae at various stages.   The

reference scales have 1 cm divisions and are

5 cm long.

the occurrence and distribution of different muscle fibre types in larval muscle.

Cryostat Sections.

Larvae were carefully removed from the rearing tanks with a pipette or a beaker and then anaesthetized and killed with an overdose of benzocaine. Larvae of less than 12 mm could be attached to the block while others had to be cut into one or more pieces. Larvae were mounted on the block by holding one end of a length of body between forceps and touching the other to a drop of water on a block. The material was carefully held in this position until freezing was complete. Once the end of the larva had frozen and adhered to the block freezing was accelerated using a freon aerosol spray directed at the larva and the block.

In order to add strength to the specimen and prevent it cracking up during sectioning, a column of ice was slowly built up around the specimen, by adding very small quantities of water taking care not to thaw the specimen. Sections were then cut using a wedge microtome knife and individually transferred to microscope slides where they were allowed to dry in air. The sections were not fixed before staining.

Staining

(a) Succinic dehydrogenase

Initially the methods described by Chayen et al. (1969) and

Pearse (1972) were tried with adult herring and with larvae. They were unsuccessful with the larvae and the results were variable with adult herring. Often the intensity of staining would diminish towards the skin. The simple methods described rely on the use of an excess of nitroblue tetrazolium, but if phenazine methosulphate (PMS), which acts as a hydrogen acceptor taking hydrogen from the flavoprotein of the dehydrogenase, is added to the reagent, then an enhanced reaction results and the nitroblue tetrazolium concentration can be reduced to one fifth.

This improved method did not, however, provide good staining in adult muscle or larval muscle of herring. The reason for this is that PMS is effectively competing with oxygen for hydrogen atoms, since succinate dehydrogenase is directly linked to the electron transfer chain. When incubations were carried out in a desiccator which was evacuated and then filled with nitrogen only a slight improvement resulted, but the sections often became detached from the slide and were lost.

Cyanide, a respiratory poison, blocks the electron transfer chain by inhibiting cytochrome a + a_3, the final stage in the electron tranfer chain where oxygen is reduced to water; PMS is now free to react with the flavoprotein of succinate dehydrogenase without any competition from oxygen via the electron transfer chain. The reactions involved in this method are summarized in Fig. 6.

The following incubation medium was developed to demonstrate

Fig. 6.   Reactions in the SDHase staining incubation.
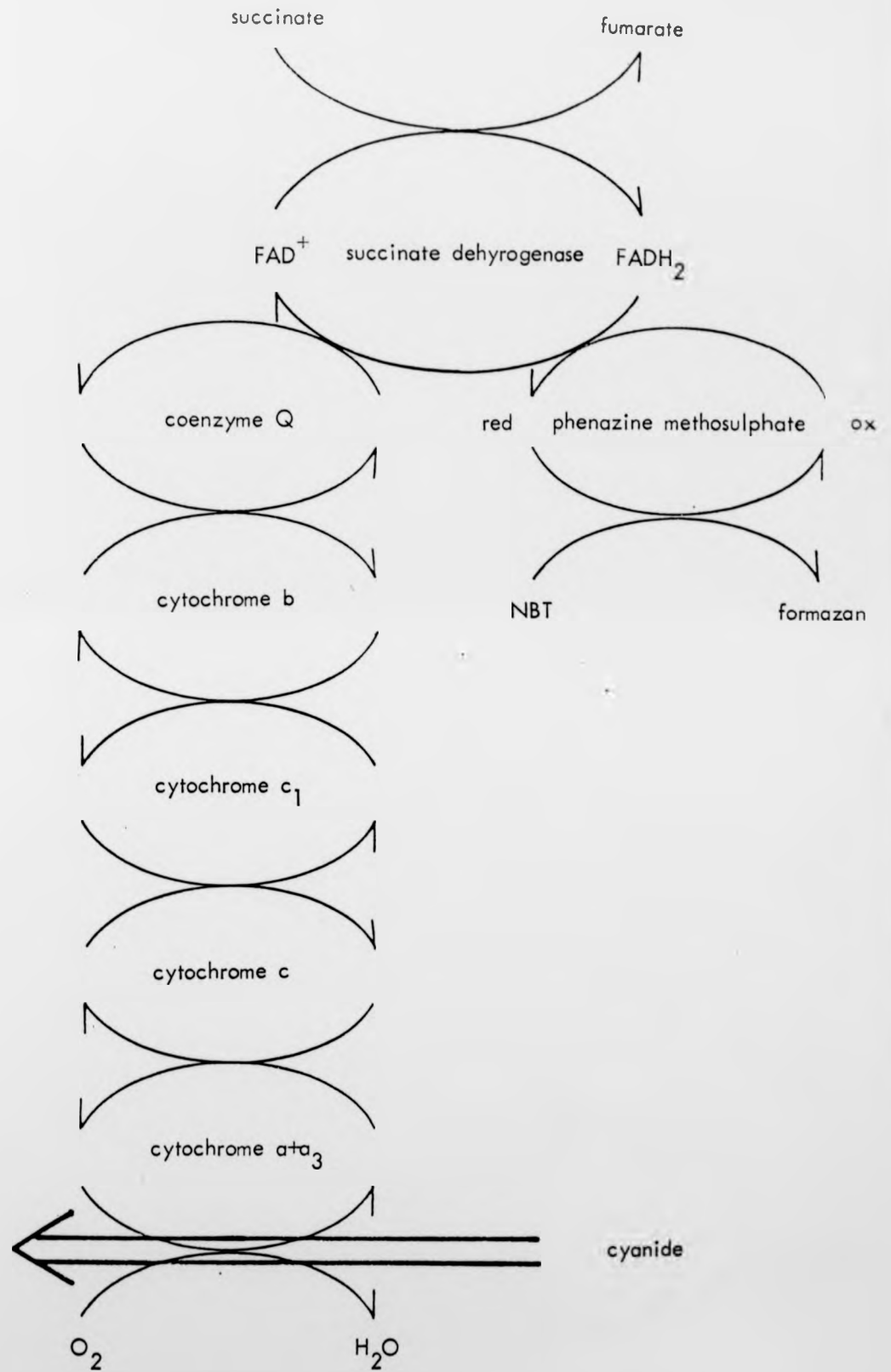
succinic dehydrogenase reliably in larval muscle. The two reagents A and B were mixed in equal proportions on the slide and incubated for 20 min at 20°C.

A

Phosphate buffer 0.5 m pH 7.4	20 ml
Nitroblue tetrazolium HCl	7 mg
Phenazine methosulphate	2 mg
Succinate	0.68 g

B

Phosphate buffer 0.5 m pH 7.4	20 ml
Potassium cyanide	10 mg

For control incubations malonate, an inhibitor of succinate dehydrogenase, was used. Malonate competes with succinate for the active site of succinate dehydrogenase. Control slides were given a 20 min pre-incubation with the following solution:

Phosphate buffer 0.5 mm pH 7.4	20 ml
Malonate	0.14 g

These slides were then incubated with the reagent A poisoned with malonate and equal quantity of reagent B, for 20 min.

Reagent A	20 ml
Malonate	0.14 g

Nitroblue tetrazolium is reduced by PMS to form an insoluble

formazan which is deposited in the tissue at the site of the reaction and so stains the sites where the enzyme occurs a dark blue. The rest of the tissue remains clear.

To preserve the sections and to allow counterstaining, slides were fixed in 10% phosphate-buffered formalin for 10 min. Initially an aqueous eosin was used as the counterstain but this was found to fade very quickly, leaving the tissue background completely unstained. It was felt that a mordant stain would give more permanent results. Nuclear fast red, with aluminium sulphate as the mordant, was used and could not be washed out with very lengthy washing. The following formula was used:

Nuclear fast red	0.1 g
Aluminium sulphate	5 g
Thymol	1 crystal
Water	100 ml

Slides were stained for 3 to 8 min and then mounted in Gray and Wess's Medium (Gray, 1958). The formula is shown below:

Gray and Wess's Medium

Polyvinyl alcohol	2 g
70% acetone	7 ml
Glycerin	5 ml
Lactic Acid	5 ml
Water	10 ml

The sections stained by this method show succinate dehydrogenase stained dark blue with nuclei magenta and cytoplasm stained varying shades of pink. Connective tissue remains unstained. Sections can be preserved for at least 5 years. Drying out of the mounting medium was prevented by sealing the edge of the coverslip with clear nail varnish.

(b) Lipids

Two methods were used to stain lipid: Oil red O in isopropanol (Culling, 1963) and Gelatine-Sudan (Govan, 1944). Frozen sections were fixed before staining. A saturated solution of oil red O (0.25 to 0.5%) in isopropanol (30 ml) was diluted with 20 ml of distilled water and then kept in a tightly closed container. This solution only keeps for 1-2 h.

The schedule was as follows:

(1)   Place slides in stain in closed container for 10-15 min.

(2)   Differentiate in 60% alcohol to clear background.

(3)   Wash in water.

(4)   Counterstain nuclei lightly in Mayer's hæmotoxylin.

(5)   Blue in tap water.

(6)   Mount in Gray and Wess's Medium.

Lipids were stained bright red by this method.

Sudan III and Sudan IV, as a saturated solution in acetone, was added drop by drop to 1% gelatin in 1% acetic acid, with constant stirring until a brick-red milky fluid was obtained. This

fluid was placed in a 37°C incubator for 2 h to evaporate off the acetone. Before use the stain was filtered through a coarse paper. The schedule was as follows:

(1)   Place slides in 1% gelatin for 3 min.

(2)   Stain for 30 min in Sudan Suspension.

(3)   Wash in 1% Gelatin for 3 min.

(4)   Counterstain nuclei with Mayer's hamatoxylin for 4-6 min.

(5)   Blue in tap water.

(6)   Mount in Gray and Wess's Medium.

Lipids were stained an orange red.

A N A L Y T I C A L   T E C H N I Q U E S

A common approach for describing the motions of a fishes body during swimming, and to find the wavelength, speed, amplitude and frequency of the propulsive wave, is to examine the excursions of a few fixed points on the body. This approach has been used by Bainbridge (1963), Grillner and Kashin (1976) and Videler and Wardle (1978). These workers were all able to pick out at least five separate points such as the base and tip of a dorsal fin or, in the case of Grillner and Kashin use reflective beads sewn onto the dorsal surface of the fish.

Neither of these approaches could be used here with fish larvae since it is difficult, due to their near transparency, to pick out the edges of structure from photographs and it would be

most difficult to attach suitably sized reflective beads to a
fish larva, even if they were hardy enough to allow it.

An alternative method was used here which depends on the
use of a computer to find fixed points on the notochord given
only an outline of the larva. The points found by the computer
were then used to calculate the parameters of the propulsive
wave illustrated in Fig. 7.

Data Aquisition

A computer-aided method was used to analyse the films and
television recordings. Before analysis, interesting sections of
television recordings were copied 'frame by frame' onto 35 mm
film. This was done using a single lens reflex camera, fitted
with a 90 mm focal length lens, and firmly mounted in front of
the television monitor. Since the television's tube takes 20 ms
to scan one field a shutter speed of more than $^1/_{50}$ s must be
used. In order to get even exposures of the whole field it was
best to use a slower shutter speed of $^1/_4$ s and an aperture of
f/11 with 125 ASA film.

Negative copies of the television recordings were back-
projected onto a digitizing table which had been built
specifically for this work. A full description is included in
Appendix 1. A slightly different method was used with the 70 mm
silhouette films. In this case it was found better to project
individual frames onto sheets of paper and trace the outlines

Fig. 7. Diagrams demonstrating body wave parameters. A) shows λ_b, λ_s, and θ (the angle between any part of the body and the direction of motion. (B) and (C) define swimming speed u and wave speed v from the passage of wave crests down the body. In (B) the two consecutive notochord lines are in their real positions and in (C) they are moved so that the heads are superimposed.

A — notochord, tail tip path, θ, $\frac{1}{2}\lambda_b$, $\frac{1}{2}\lambda_s$

B — $\partial x/\partial t = u$, $\partial x/\partial t = v - u$

C — $\partial x/\partial t = v$
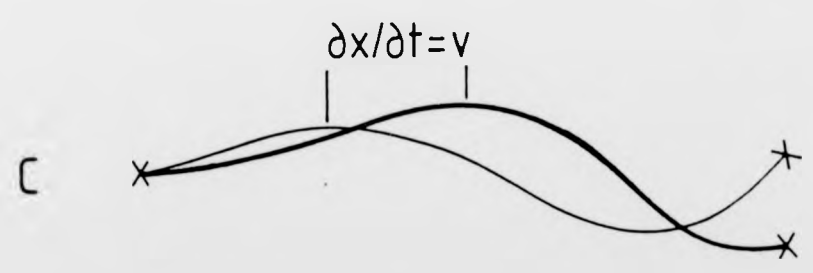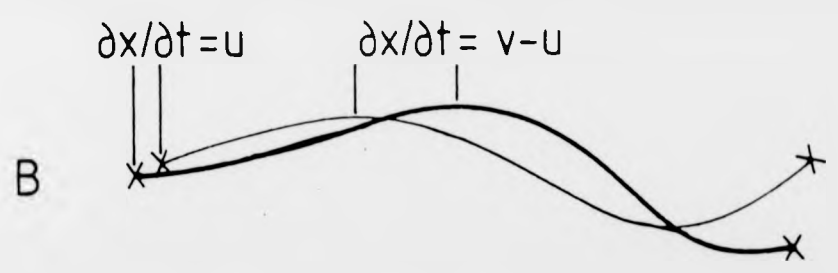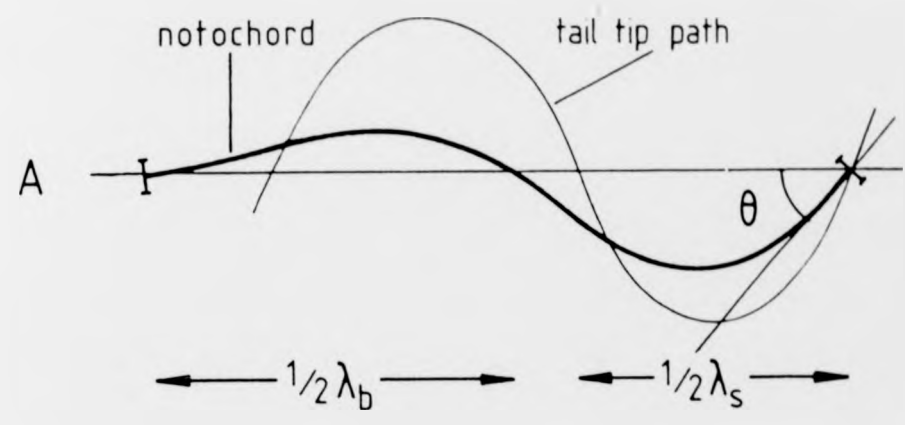
← Direction

of a larva. The sheets were then fixed to the digitizing table where whole outlines of the body and pectoral fins were traced with the cursor. Two reference points were also recorded in every frame.

The digitizer was linked to, and controlled by, a Hewlett Packard 9825 desktop computer. The computer converted the data from the digitizer into x and y coordinates and transformed the coordinates from the recorded outlines to a unified coordinate system based on the reference points, which were two fixed positions within the camera's field of view. The data for the outlines were then recorded on magnetic tape for subsequent analysis.

The computer programmes used, both in recording data from the digitizer and in analysis of the data, are described in Appendix 2.

Body Waves

The data collected by the digitizer and computer consist of two series of (more than 100) x y coordinates, one for each side of the fish. It would be difficult to analyse the data in this form, because of their complexity and bulk. The analysis is to find velocity, wavelength and frequency of the body waves and,as already mentioned,this can be most conveniently done by considering the movements of fixed points at intervals along the notochord.

Here a method is used to find a set of fixed points
centred on the notochord along a length coordinate a. This
coordinate system is illustrated in Fig. 8. This data reduction
was achieved in two stages. First, a series of points making up
a line, midway between the two sides of the larvae, was found. Then
having defined the coordinate a as the line joining these points;
the x and z coordinates for 11 points at 0.1 a increments along a
from head = 0 to tail = 1 were found by interpolation.

A simple method was used to compute the centre line which
therefore cut down the running time of the programme. The
digitizing sub-routines shown in Appendix 2 allowed for a fixed
resolution (i.e. the minimum distance between successive points
recorded by the routine 'line'), and so, if a certain speed was
not exceeded when tracing with the digitizer cursor, the points
recorded would be reasonably evenly spaced. The number of points
on each side was then reduced to 50 by removing points at
appropriate intervals.

There were now 50 pairs of points on the left and right sides
of the larva. The x, z coordinates of a mid-point between each
of these pairs was computed so that they made up a line
approximating to the centre line or notochord. These points were
then filtered or smoothed in two stages by applying the following
two pairs of equations in succession.
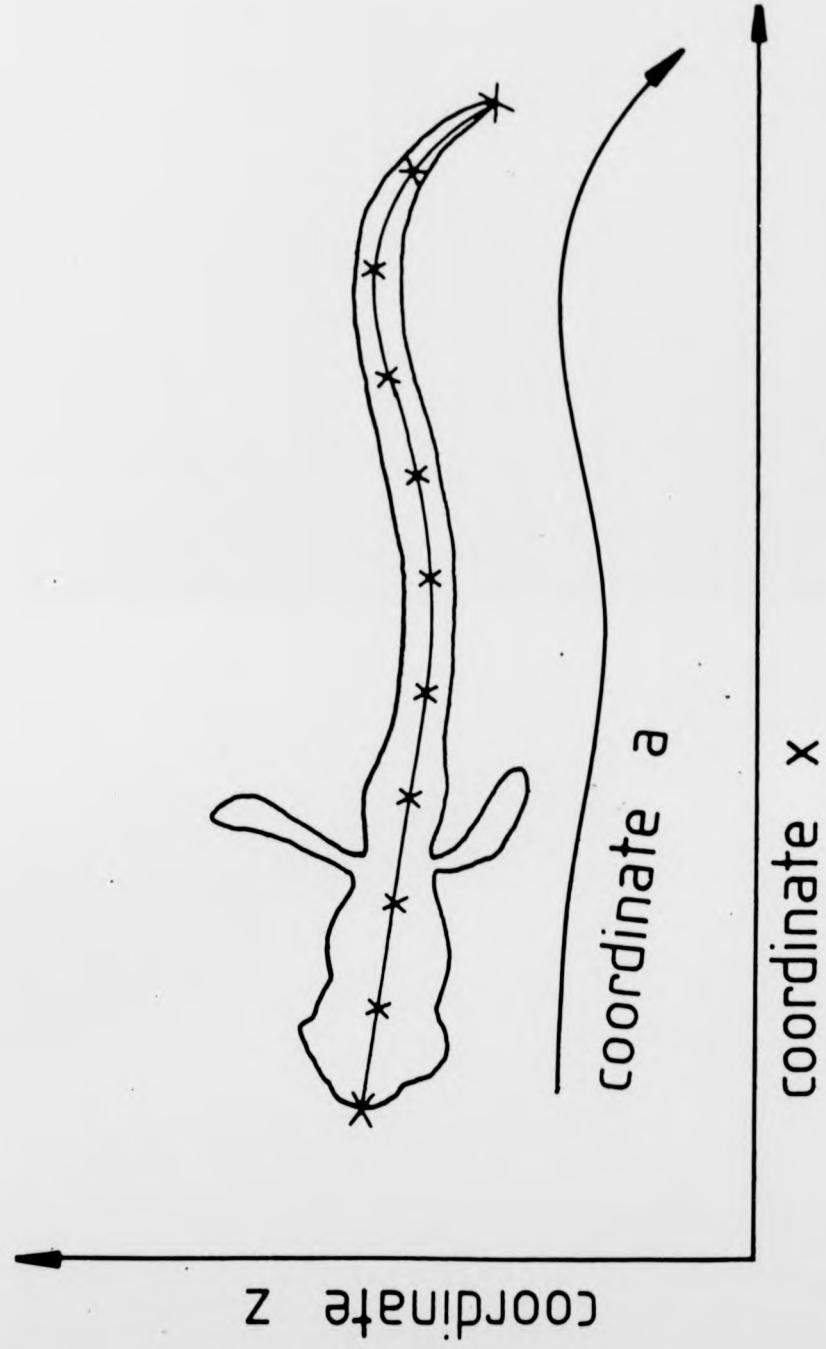
Fig. 8. A diagram showing the coordinate system and the eleven points on the coordinate a at fixed 0.1 a increments from the head (a = 0) to the tail (a = 1).

coordinate a

coordinate x

coordinate z

$$x_n = (x_{n-1} + 2x_n + x_{n+1})/4$$

$$z_n = z_{n-1} + 2z_n + z_{n+1})/4$$

$$x_n = (x_{n-2} + 2x_{n-1} + 3x_n + 2x_{n+1} + x_{n+2})/9$$

$$z_n = (z_{n-2} + 2z_{n-1} + 3z_n + 2z_{n+1} + z_{n+2})/9$$

Length coordinates a in units of L the length of the larvae were then computed for this filtered data using this equation:

$$a_n = \sum_{a=2}^{a=n} \sqrt{((x_n - x_{n-1})^2 + (z_n - z_{n-1})^2)} .$$

All these values of a were adjusted to make them vary from 0 to 1 (i.e. head = 0, tail = 1) by dividing each value by L.

The second stage of data reduction, finding a set of 11 fixed points on a at $0.1a$ intervals from head to tail, could be done by interpolation. A simple method was used where the x and z coordinates were found in the interval in which they occurred by assuming that adjacent points were joined by a straight line.

Now that the data were reduced to x and z coordinates for fixed positions on a it was a simple task to transform them to a coordinate system based on the direction of motion. The direction of motion was found by using a geometric regression

(Teissier, 1948), in which neither variable is independent, on all
the x and z values for all the points on a and for all the frames
of a sequence. The full set of coordinates could then be rotated
to fit on a new x axis which ran through the direction of motion.

It was now possible to find the various parameters of the
body waves (summarized by Fig. 7) which have already been discussed
in the introduction to this section.

Videler and Wardle (1978) used linear regression analysis to
find the velocity of the propulsive wave v. They plotted the
positions of wave crests, on the a coordinate, against time so that
the regression coefficient was an estimate of da/dt. In actual
fact v is equal to dx/dt. Videler and Wardle were able to
calculate v by multiplying da/dt by the ratio F the distance on
the x axis spanned by the body divided by the body length (L).

$$F = L/{(x_n - x_o)}$$

This should compensate for bending of the body during swimming,
but in the analysis of larval swimming, body angles (Fig. 11)
are much larger than in adult fish which would make the ratio
F larger. This adjustment might still be applied but any change
in wave speed v during the passage of one wave could not be
detected, because only mean speed could be calculated. Videler
and Wardle used a weighted regression, adding extra weight to
points with greater amplitude (i.e. nearer the tail) assuming that

the errors would be less significant. But as amplitude increases towards the tail the compression of the coordinate a on the x coordinate also increases. This could lead to a large error in computing v in this case. It was considered better to measure actual wave crest dx/dt.

The z displacements of each point against time were plotted on one page (see Fig. 9 as an example). The time at which a wave crest passed through each point was noted and then instead of regressing this against time the corresponding x coordinate was used.

Fig. 10 A, B shows plots of a against time; the fitted regression lines give da/dt and it appears that da/dt is reasonably constant and independent of a. But plots of x against time for the same sequence, shown in Fig. 10 C, D, demonstrate that dx/dt does sometimes vary along the length of the larva. This value of dx/dt is equal to $v - u$ and v may be calculated simply by adding the value of u the forward speed (see Fig. 7). Two values for v were calculated from each wave, using either all the points on a or the last 6; in other words a mean or posterior v (v_m; v_p).

Pectoral Fin Movements

A simple analysis of the pectoral fin movements of plaice larvae was made in order to describe their nature and to relate them to simultaneous body movements. It was not possible to

Fig. 9.   An example of a plot of z displacement of a larval
herring against time for each of the eleven points
on a (from $a = 0$ at the top (head) to $a = 1$ at the
bottom) (tail)).

head

tail
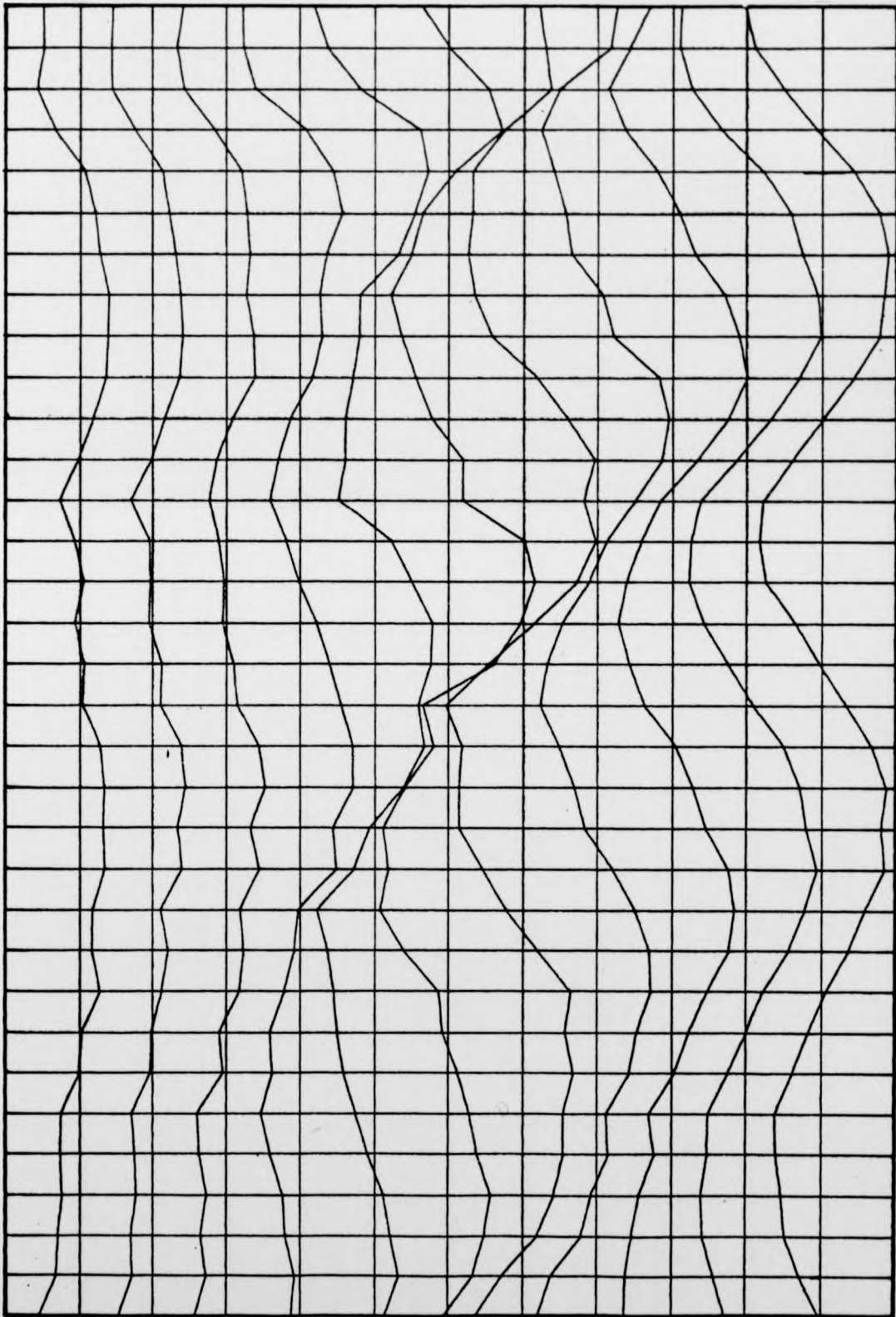
30

Frame no.

1

Fig. 10.   Wave crest positions against time for an 11 mm herring
            larva (A and B) and a 22 mm herring larva (C and D).
            Position is shown on the body co-ordinate a (A and C)
            and on the x co-ordinate, i.e. direction of motion (B
            and D).
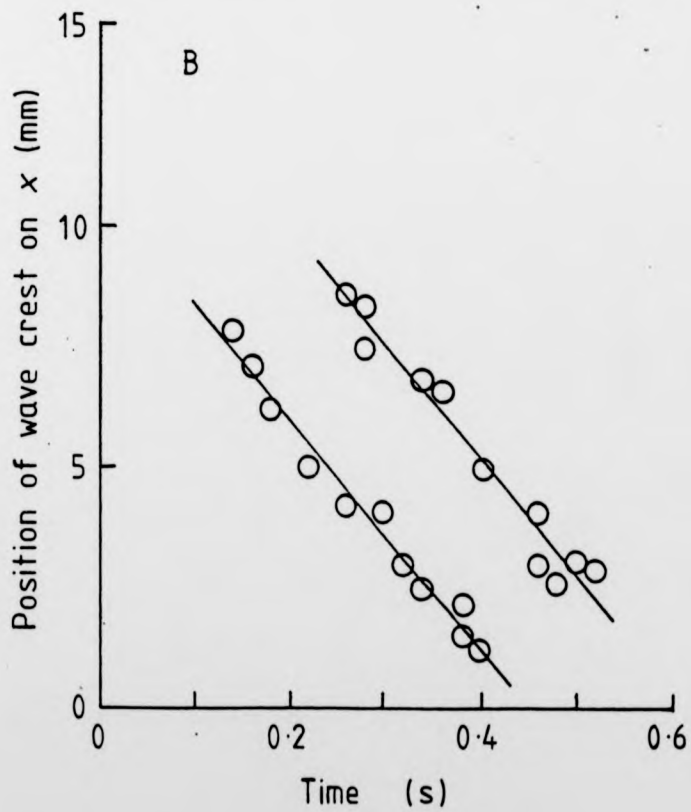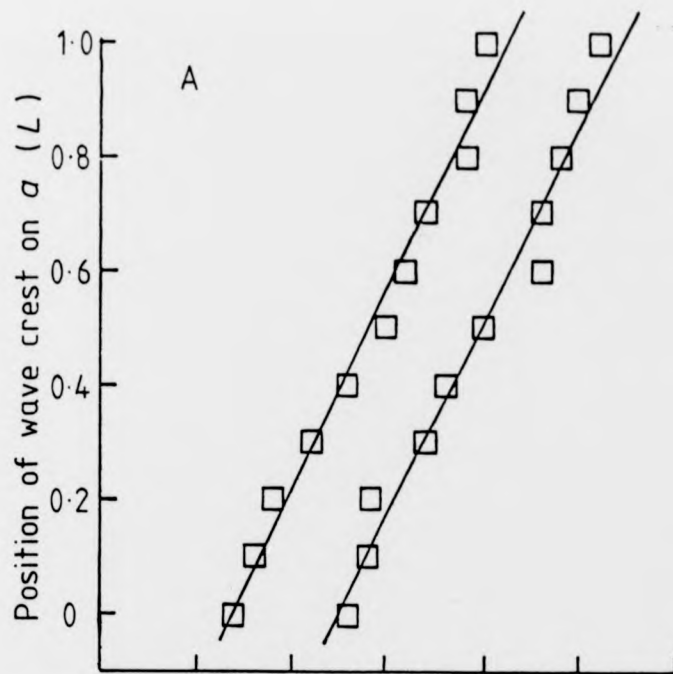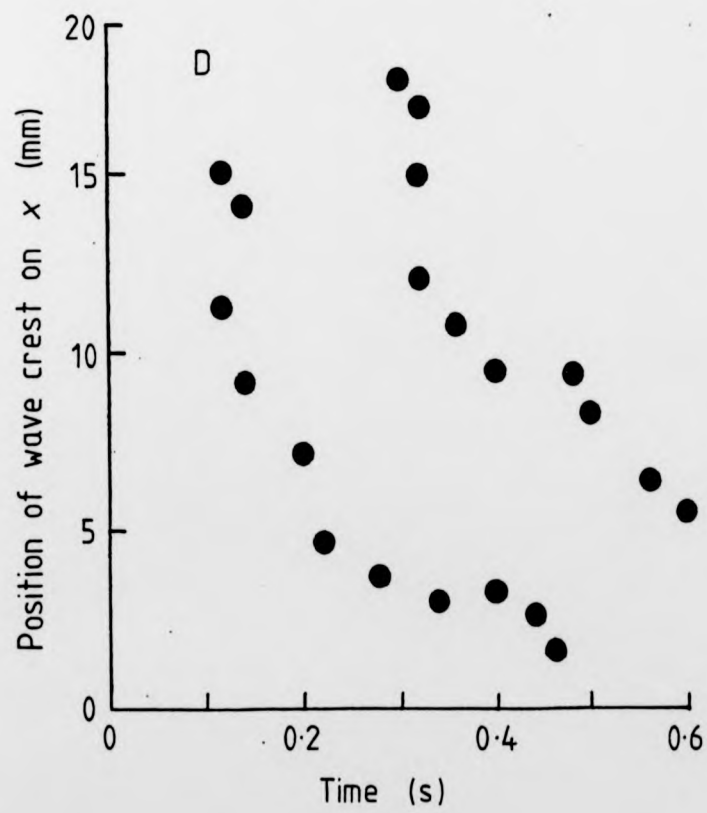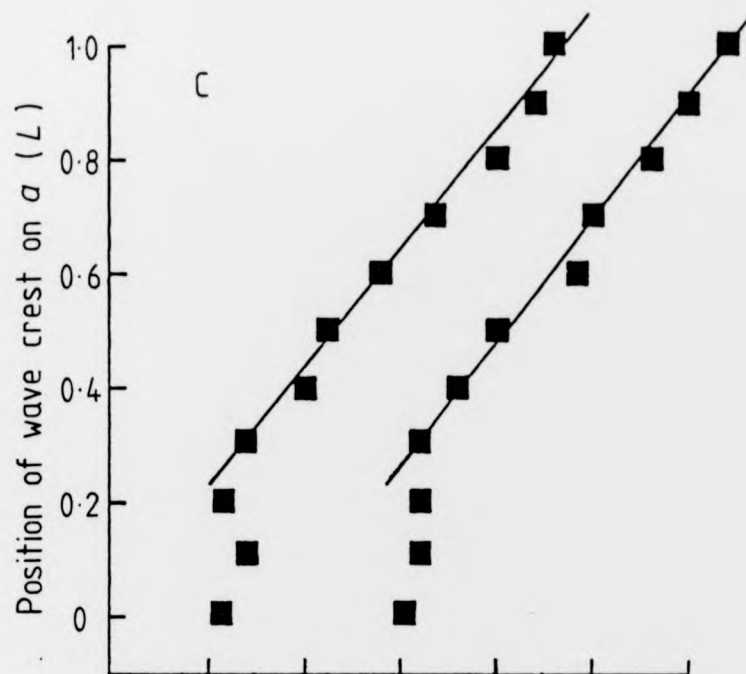
distinguish and follow individual fin rays through a fin stroke cycle as Blake (1979) did in the angelfish (*Pherophyllum eimekei*). Left and right fin-tip coordinates were defined for each frame as the point on the fin outline farthest from the base of the fin. Having found the fin-tip, the fin angle was defined as the angle between the tip of the snout, the fin base and the fin tip. The phase and frequency of fin movements and body movements could now be compared by plotting fin tip angles and tail tip z displacement against time on the same graph.

Since it was not possible to find the positions of individual fin rays the three dimensional shapes of the fins were not known, and for this reason a measurement of angle of attack, to the water flow, could not be made. An estimation of this angle of attack was taken as the projected area of the fin seen from above. When this projected fin area was low, angle of attack with the water flow was high and vice versa.

RESULTS

Swimming movements

Herring

Swimming speeds of 5 to 20 mm.s^{-1} were observed in first feeding larvae about 10 mm long. Swimming speed increased with length, larvae 22 mm long having swimming speeds in the range 5 to 60 mm.s^{-1}. Two examples of herring larvae swimming are shown in Fig. 11. The figure shows the outlines of two larvae, of 11 mm and 22 mm length, from successive 20 ms frames of the TV recording. Top views are shown drawn to different scales in order to compare the details of movement. This figure clearly shows apparent similarities between the two larvae. For example there is slightly more than one wavelength on the body at any time, the wave moving along the body with increasing amplitude towards the tail.

Further analysis shows differences in detail between the two sizes of larva. In Fig. 12 amplitude versus length curves are shown for the 11 mm and 22 mm larva and also for a 60 mm juvenile herring. The amplitudes of both lateral movements z and of the angle θ between the body and the direction of motion, which in this case is the x axis, are plotted. The shape of both curves is different in the two sizes of larvae. For the 11 mm larva the amplitude of lateral movement and the angle θ increase linearly from head to tail. In contrast the

Fig. 11.   Outlines of herring larvae swimming, A, and 11 mm

larva; B, a 22 mm larva; note difference in

scale.   Frames are at 20 ms intervals.
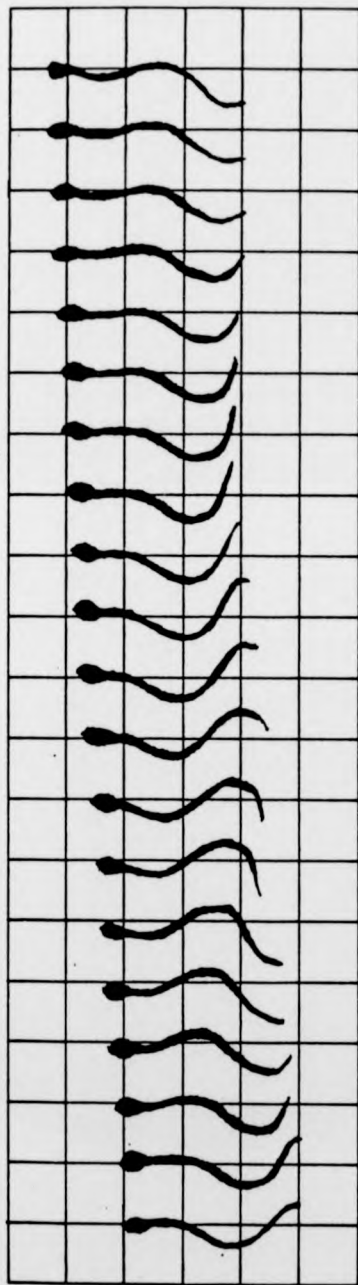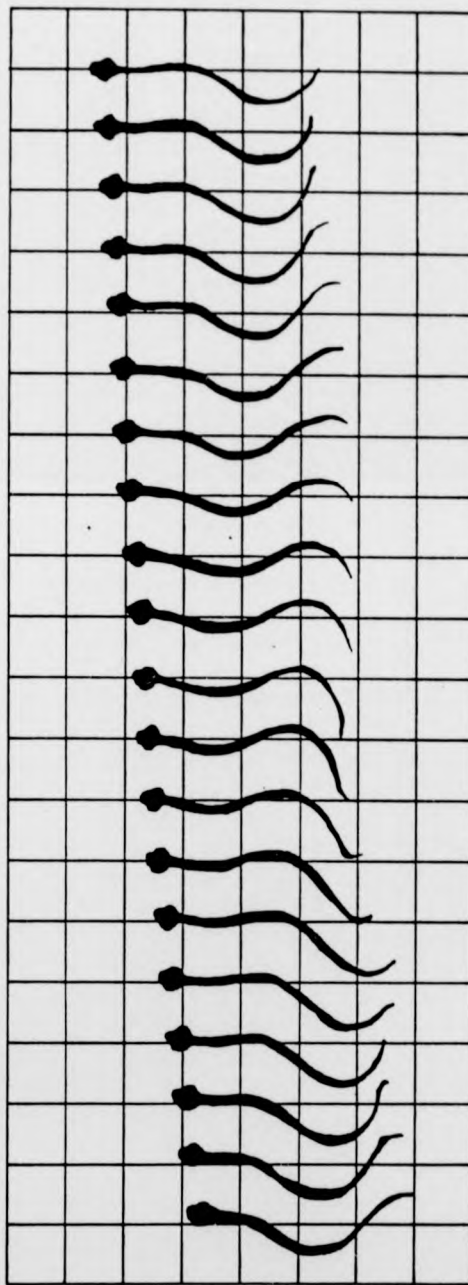
Fig. 12.   Maximum relative amplitudes X for each length

co-ordinate a, and maximum angle θ of each

interval between the points, shown by the

symbol $\bigcirc$, (A) for an 11 mm herring larva; (B)

for a 22 mm herring larva; (C) for a 60 mm

herring juvenile (with the adult form).

Distance along body a   (L)
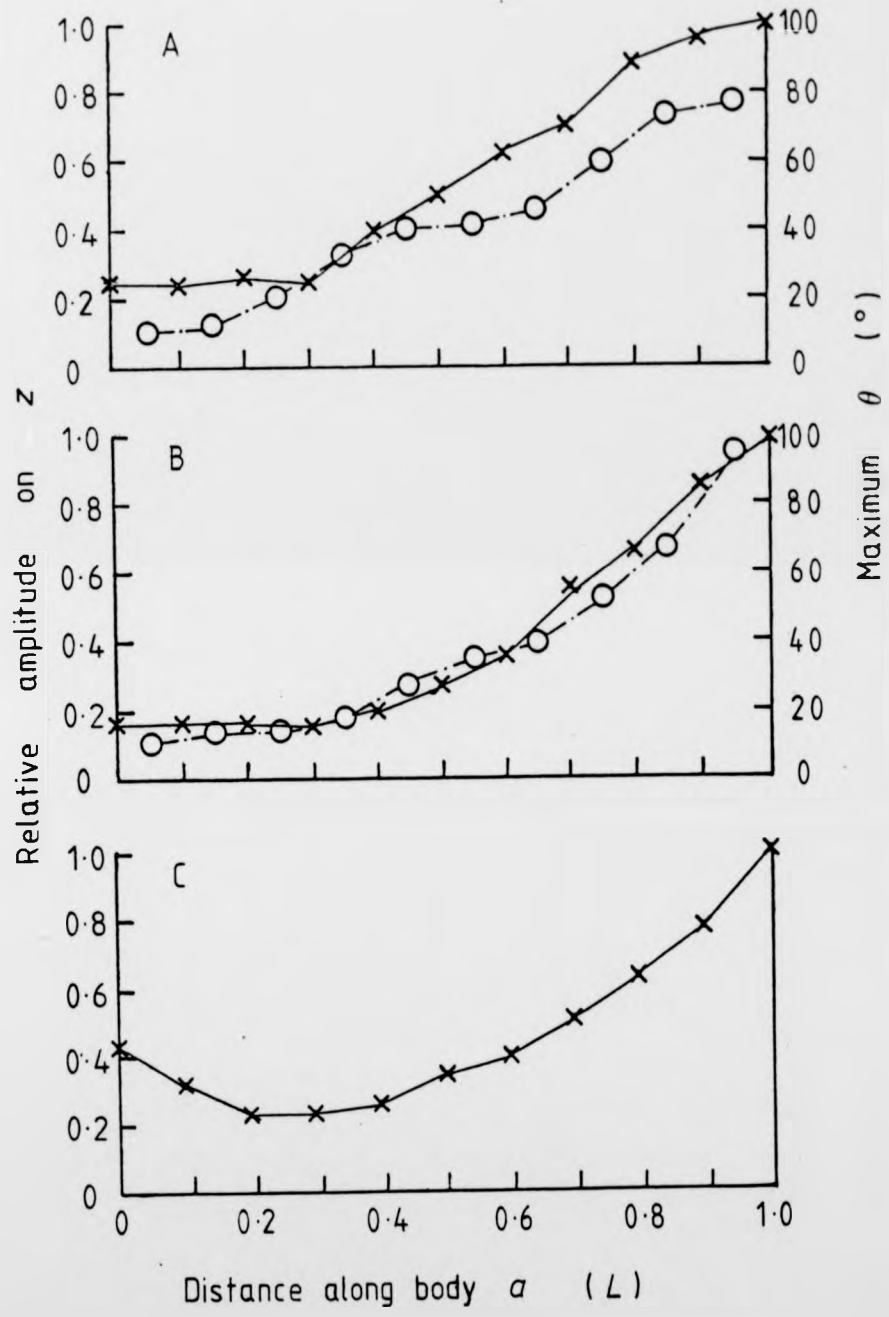
lateral movement and θ in the 22 mm larva increase at a steadily

increasing rate from head to tail and are lower at the head

and in the anterior part of the body compared with the 11 mm

larvae. Note that the angle θ at the tail is less than 90° for

the 11 mm larvae but reaches 100° for the 22 mm larva. In the

11 mm larva the whole body is involved in thrust production as

shown by the linearity of the amplitude of lateral movement. In

the 22 mm larva the situation is quite different; here the

anterior part of the body, for about one-third of its length, is

almost rigid.

The movement of wave crests of the propulsive wave on the

bodies of 11 mm and 22 mm larvae swimming at 13 mm.s^{-1} are

shown in Fig. 10. Wave crest position is plotted both along a

(the body co-ordinate) and along x (the direction of motion).

Note that the wave speed is constant along the body of the 11 mm

larva (Fig. 10A) and along its direction of motion (Fig. 10B).

In the 22 mm larva, the anterior part of the body is rigid but

the wave continues along the rest of the body at a constant speed

(Fig. 10C). The speed of the wave along the direction of motion

decreases towards the tail (Fig. 10D) due to the large values of

θ nearer the tail. The speed of the body wave can be expressed

as v for all the body or v_p for the posterior part only. It is

lateral movements that are important in propulsion and since

amplitude increased rapidly over the posterior part of the body

only v_p is important.

The ratio of swimming speed to wave speed u/v_p is a measure of the slippage of the wave speed in relation to the water. The ratio lies between 0.2 and 0.4 (Fig. 13) which is much lower than found in adult fish. There is apparently a slightly higher efficiency at faster swimming speeds.

Plaice

Cruising swimming of plaice larvae is characterized by the simultaneous use of pectoral fins and body waves, Fig. 14A, B. On the only recorded occasion when pectoral fins were used alone no forward progress was made. Body waves without the use of pectoral fins were only used at burst speeds, Fig. 14C.

a) Body waves.

Wave characteristics were analysed for two sizes of larvae, 7 mm and 11 mm. Two examples of amplitude of z displacement along the body are shown in Fig. 15, together with angle θ for the intervals between each a increment. Fig. 15A is for a 7 mm larva and Fig. 15B for a 11 mm larva. These amplitude curves are very similar to those for adult fish swimming in the subcarangiform mode (Grillner and Kashin, 1976). There is a major difference between larval and adult fish in the body angle θ curve. As with herring larvae a much larger tail θ occurs at the moderate cruising speed employed here than has been found in similar analyses of adult fish cruising. Indeed in larvae, tail angles of greater than
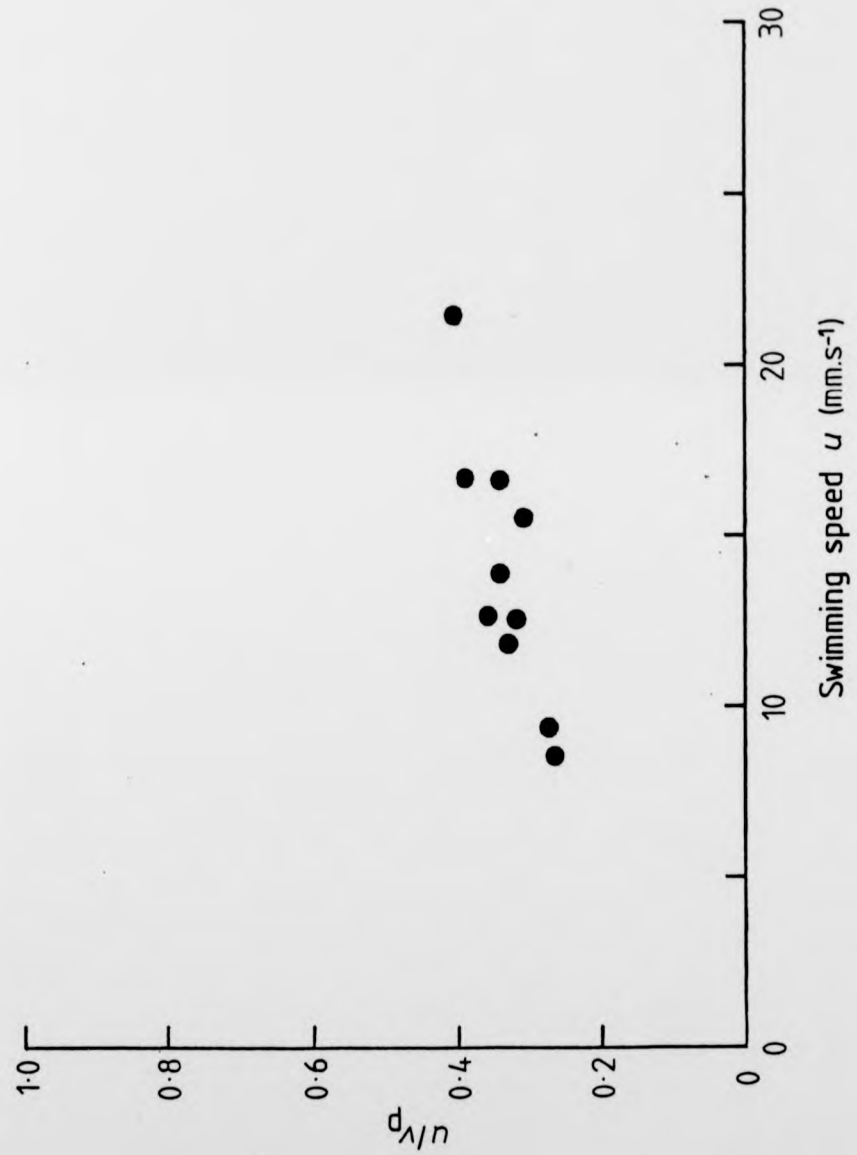
Fig. 13. u/v_p against swimming speed u for a 22 mm herring larva.
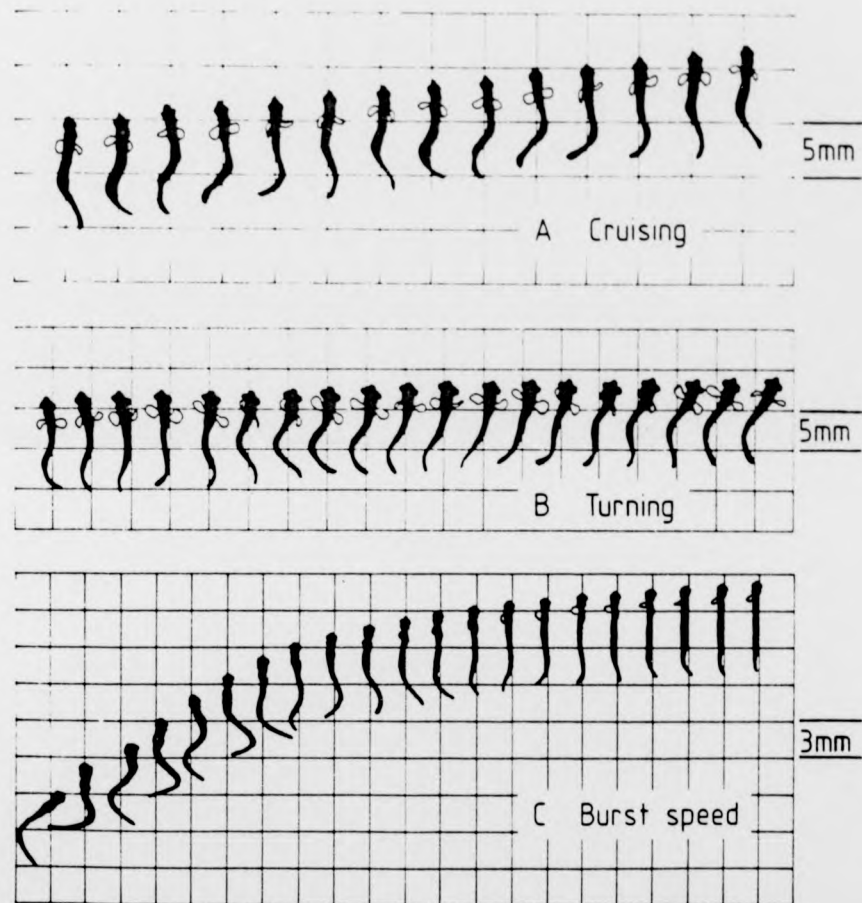
Fig. 14.   Computer plotted outlines of plaice larvae
swimming, derived from silhouette photographs.
a)   an example of cruising swimming.   b)
turning.   c) burst speed swimming.   14 ms
between frames.

Fig. 15.   Maximum relative amplitudes for each length

co-ordinate a point●,and maximum angle θ of

each interval between the points■,A for a

7 mm plaice larva and B for an 11 mm plaice
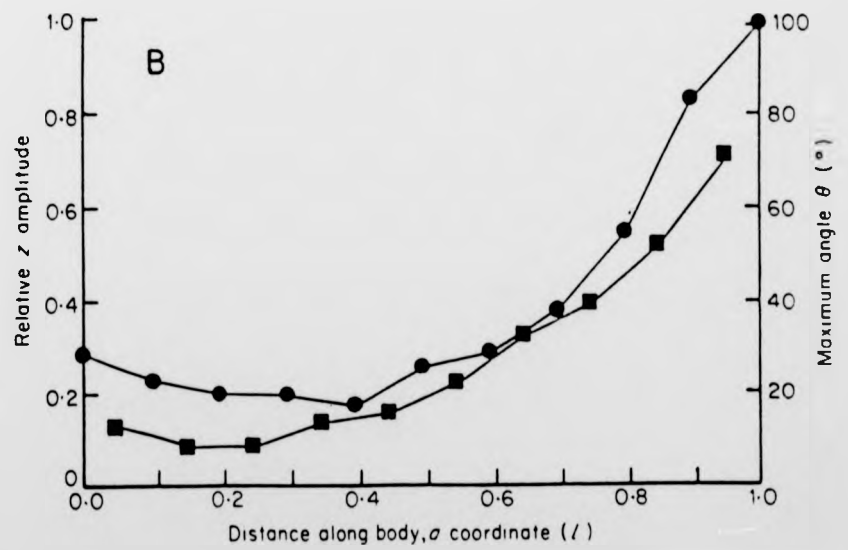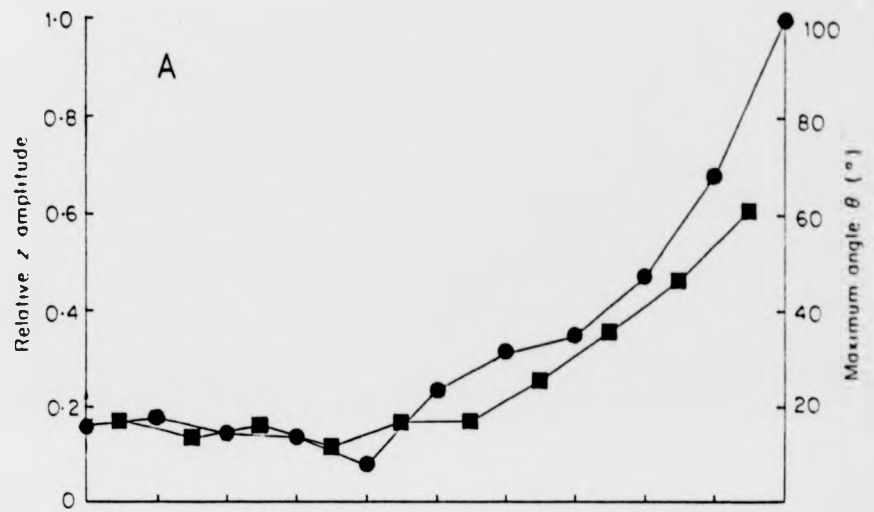
larva.

90° have been observed at higher cruising speeds and during acceleration.

The movement of plaice body waves along the body is shown in Fig. 16. The head and body up to 0.2 L of both 7 mm and 11 mm plaice larvae act as one stiff element as in the 22 mm herring larva; Fig. 16A, C. When the position of wave crests on the x axis are plotted Fig. 16B,D it is clear that wave speed is almost constant along the body of the 7 mm larva (Fig. 16B) but that wave speed slows down towards the tail of the 11 mm larva (Fig. 16D). It is notable that the measured wave speeds v show no positive correlation with forward swimming speed u (Fig. 17). In adult fish u/v is relatively constant (Videler and Wardle, 1978). The technique used to find v has some bearing on the result since for an 11 mm plaice larva v varies with position on the body (Fig. 16D), decreasing from head to tail, when u was above 30 mm/sec. For this reason both v_m and v_p are plotted in Fig. 17 which shows the changing swimming style at higher cruising speeds. Fig. 18, a plot of u/v against speed u, shows a clear increase in u/v with swimming speed and the change in style.

If v does vary along the body then so must wave length λ_b, otherwise the larvae would be ripped apart if frequency changed. Since frequency is equal to v/λ_b, when speed v decreases the wavelength λ_b must get shorter.

Tail-tip amplitude varies little with speed; therefore maximum tail θ must increase with swimming speed as the

Fig. 16.   Wave crest positions against time for a 7 mm plaice

larva (A and B) and an 11 mm plaice larva (C and D).

Position is shown on the body coordinate a (A and C)

and on the x coordinate, i.e. direction of motion

(B and D).

C

Position of wave crest on coordinate a (l)

D

Position of wave crest on coordinate x (mm)

m

p

Time (ms)
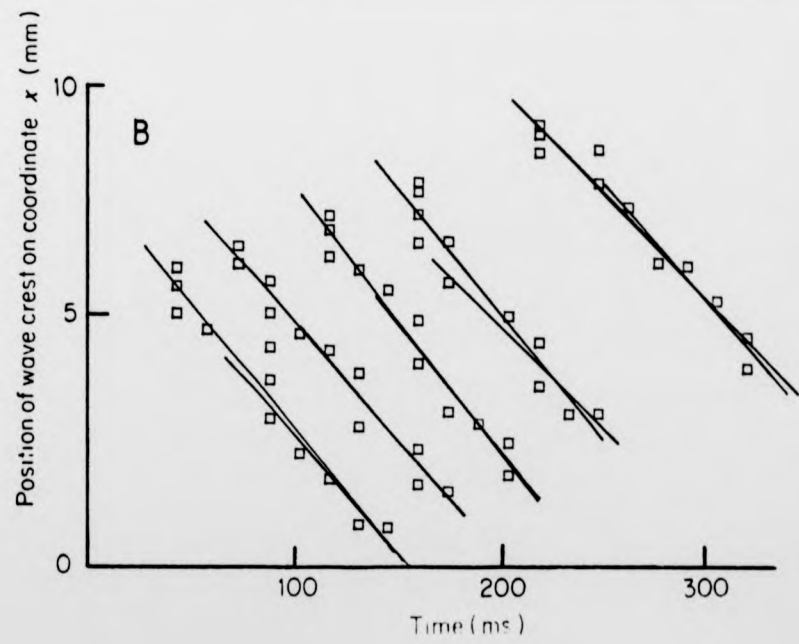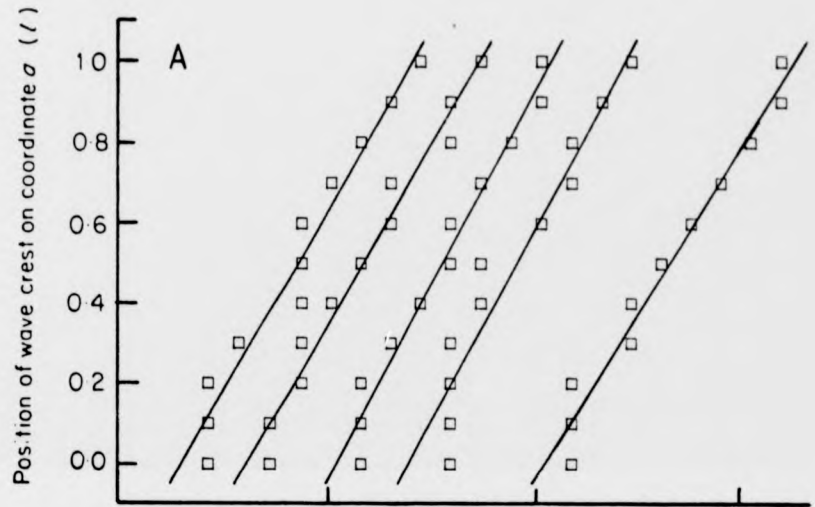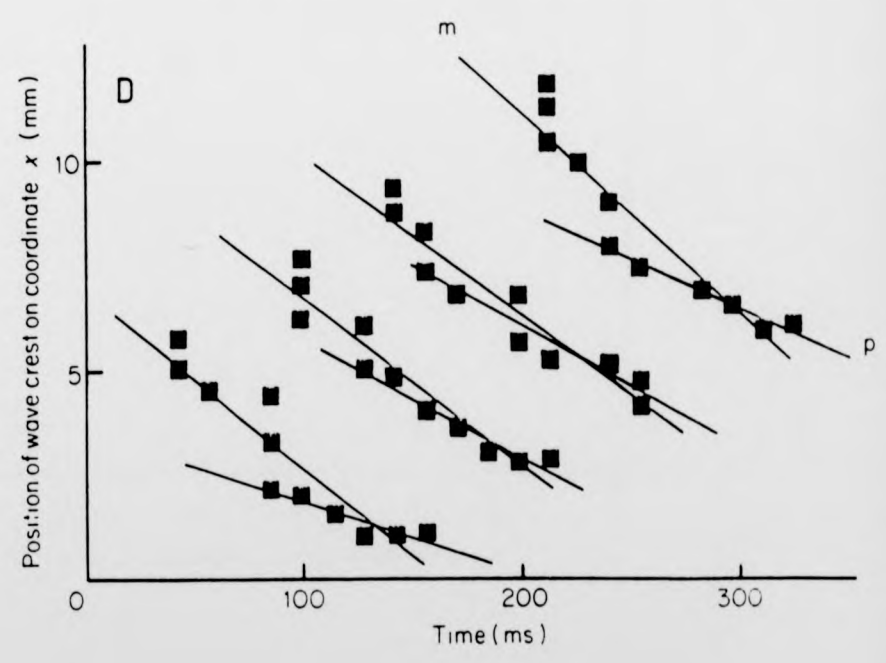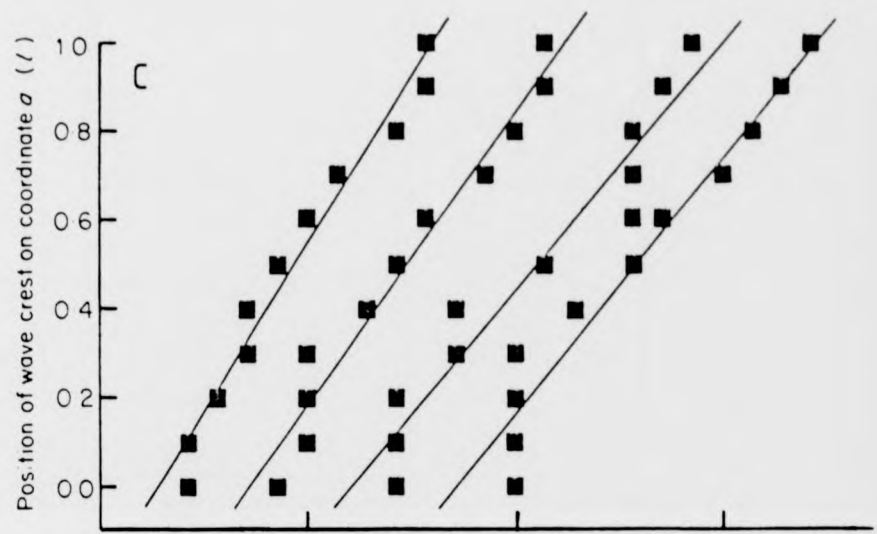
Fig. 17.   Plots of v_m O , and v_p □ ,   for plaice larvae against

u with fitted regression lines.

Swimming speed u (mm s^{-1})

Propulsive wave speed v (mm s^{-1})
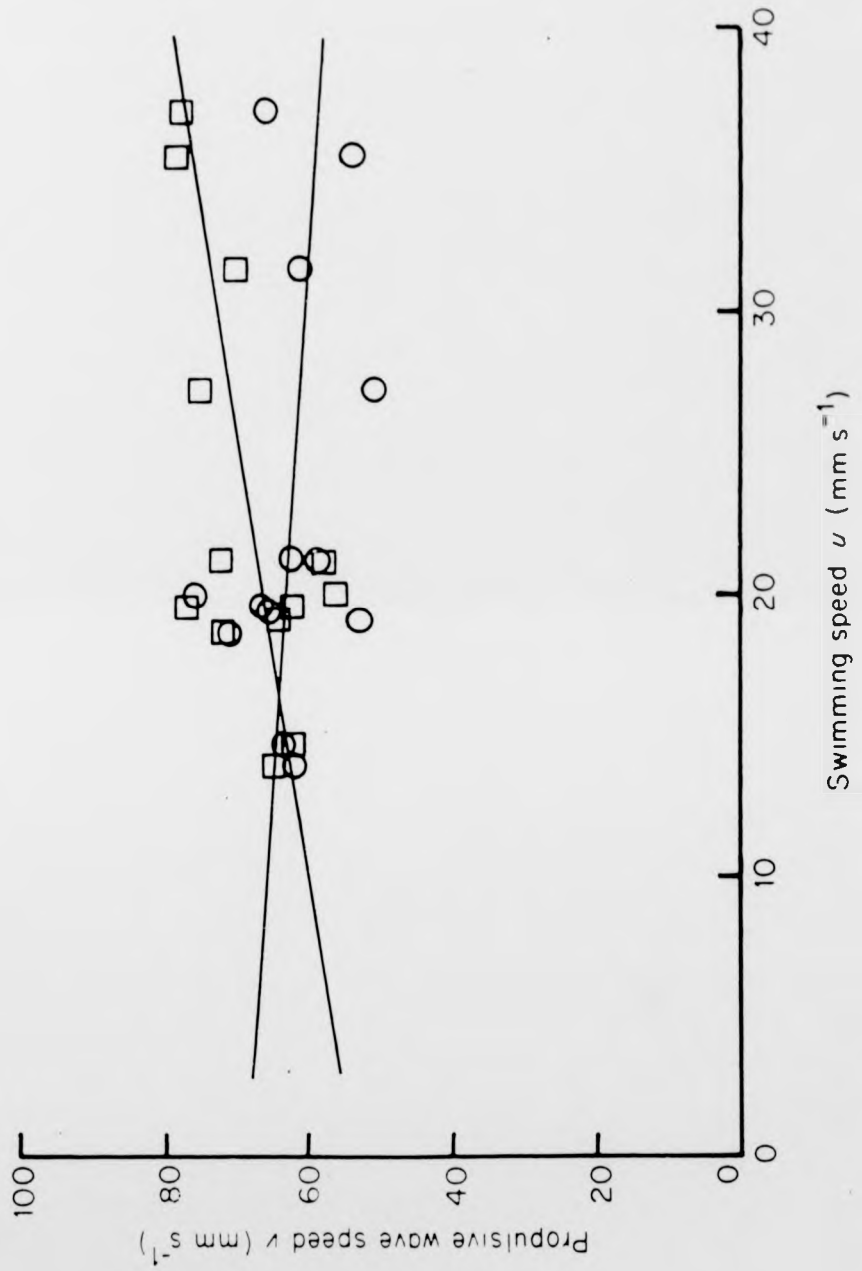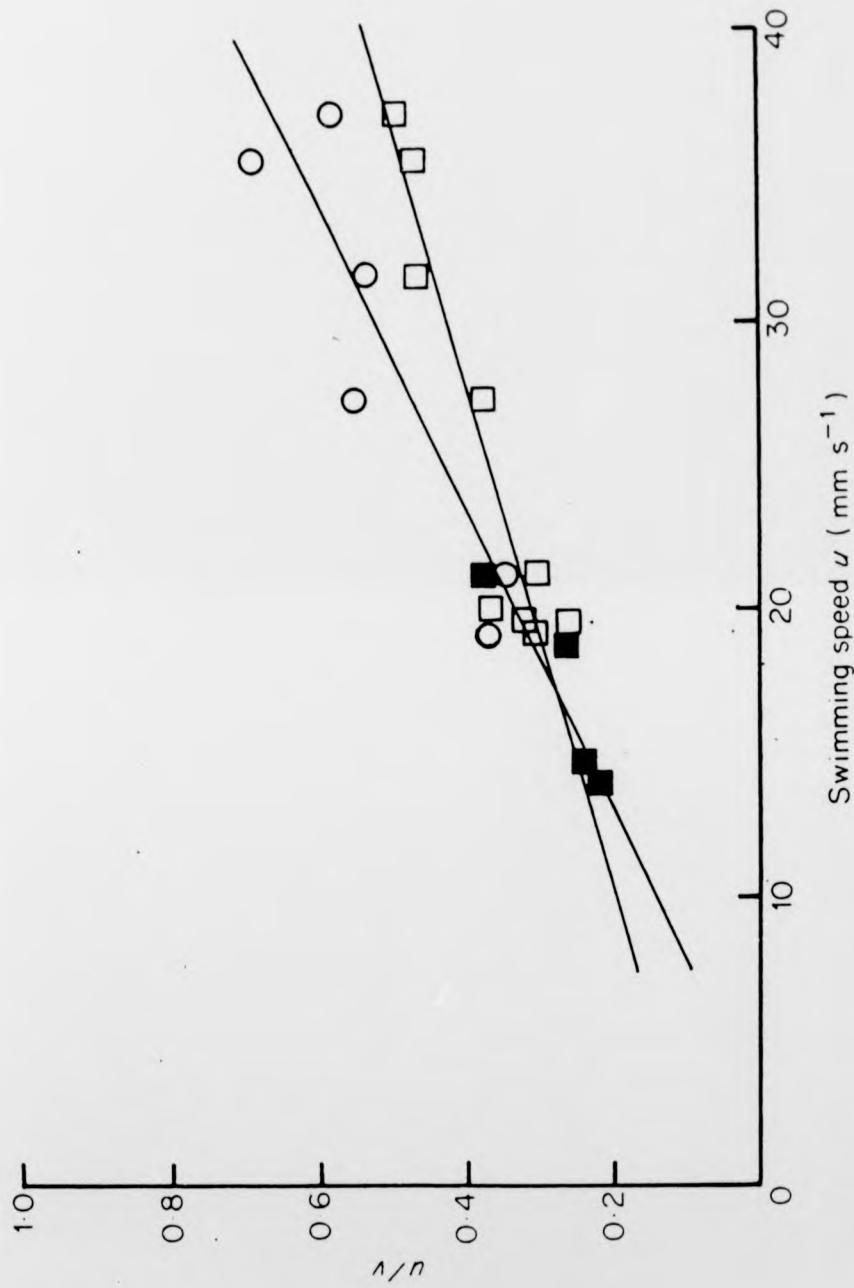
Fig. 18.   Plaice larvae, u/v_m □ and u/v_p O, against swimming speed u with fitted regression lines. ■ indicates where values for u/v_m and u/v_p coincide.

tailwards decrease in *v* becomes more pronounced. This may be the means of increasing thrust force with speed. Unfortunately, maximum measured values for θ at the tail are not very close to the true maximum value since the technique did not provide sufficient frames per second. Films at a higher frame rate would be necessary to confirm this conclusion.

Mean values of λ_b / L (body wavelength in units of body length), the number of waves included on the body and amplitude (A) are shown in Table I, for two body lengths, 7.2 mm and 10.0 mm. There is little difference between the two sizes of larva and both include slightly more than one wave on their body when swimming at cruising speeds.

b)   Pectoral fin movements

An example of an analysis of pectoral fin movements during steady forward swimming is shown in Fig. 19. This diagram clearly shows the synchronisation of pectoral fins with body waves. Their movements are of the same frequency but there is a 180° phase difference between the left and the right pectoral fin. Projected fin areas are plotted on the same axis as fin angle in Fig. 19 and give an indication of angle of attack. The projected fin area (an indication of angle of attack) varies at twice the frequency of fin beating, showing that lift or negative lift may be produced on both strokes.

Tailward strokes of the pectoral fins may have little

Table I.

Mean values of body wave parameters from two plaice larvae swimming at cruising speeds.

Length on a mm	Length on x mm	λ_b/L L	Waves on Body	A/L L
7.2	6.7	.84	1.1	.32
10.0	9.2	.82	1.1	.35
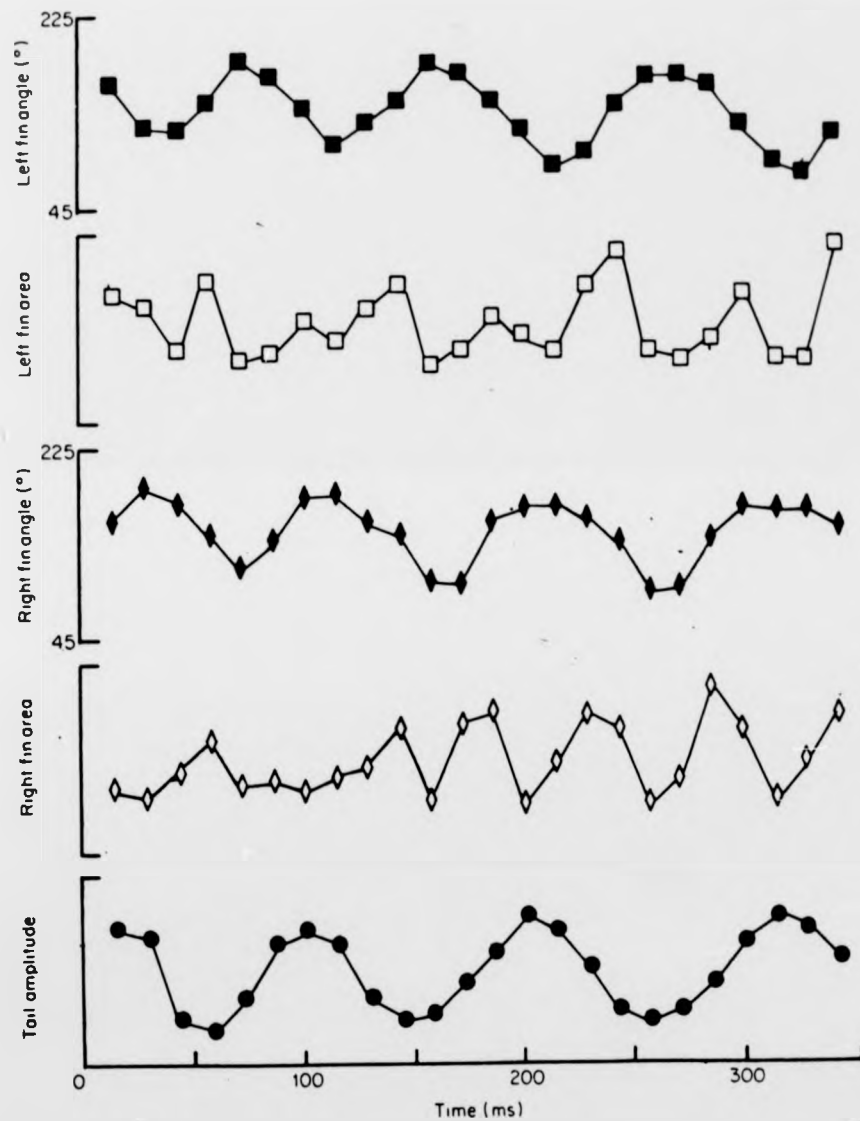
Fig. 19.   Pectoral fin movements during straight swimming
of a 10 mm plaice larvae. ■ left fin angle,
□ left fin area, ◆ right fin angle,
◊ right fin area, ● tail tip lateral displacement.

propulsive effect. Figure 20, a graph of fin-tip x coordinate against time, demonstrates the low or zero effect on the water of tail strokes, but the synchronisation of pectoral fin strokes with propulsive waves will tend to reduce head yaw by counteracting the recoil effect produced by the tail fin strokes. The pectoral fin strokes are perfectly timed to do this and improve efficiency by reducing drag induced by swimming movements.

c)   Turning

Pectoral fin movements change during turning. In the example shown in Fig. 14(B) the larva is turning to the right. The right fin moves between a point perpendicular to the body and a point 180° from the head, as in straight swimming, but the left fin moves between 0 and 90° from the head; this situation is reversed in left turns. An analysis of this turn (Fig. 21) shows a movement similar to straight swimming except for this change in the stroke of the left fin to move in the range 0 to 90° from the head.

The part played by the pectoral fins during turning is not clear, especially since the turning couple on the head would tend to rotate the head against the desired direction.

d)   Burst Speeds

At burst speeds only body waves are used (Fig. 14C) and are apparently of a different form to cruising speed swimming.
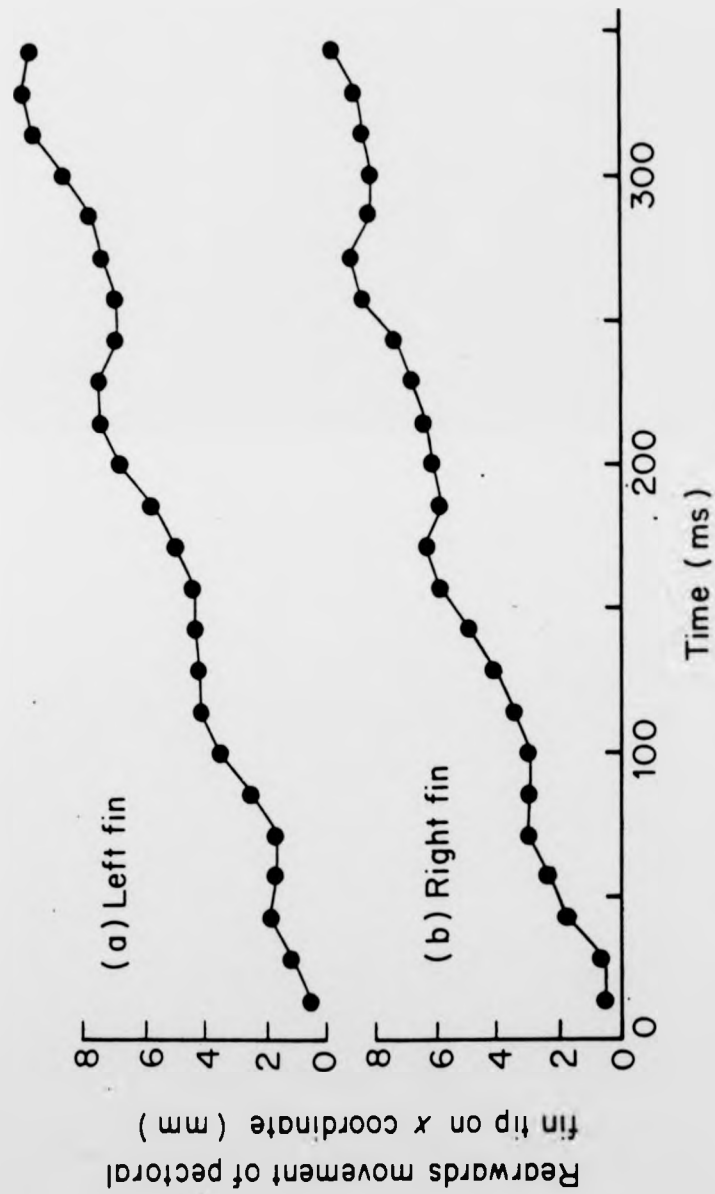
Fig. 20. Pectoral fin tip x coordinate position against time for the same sequence shown in Fig. 19.
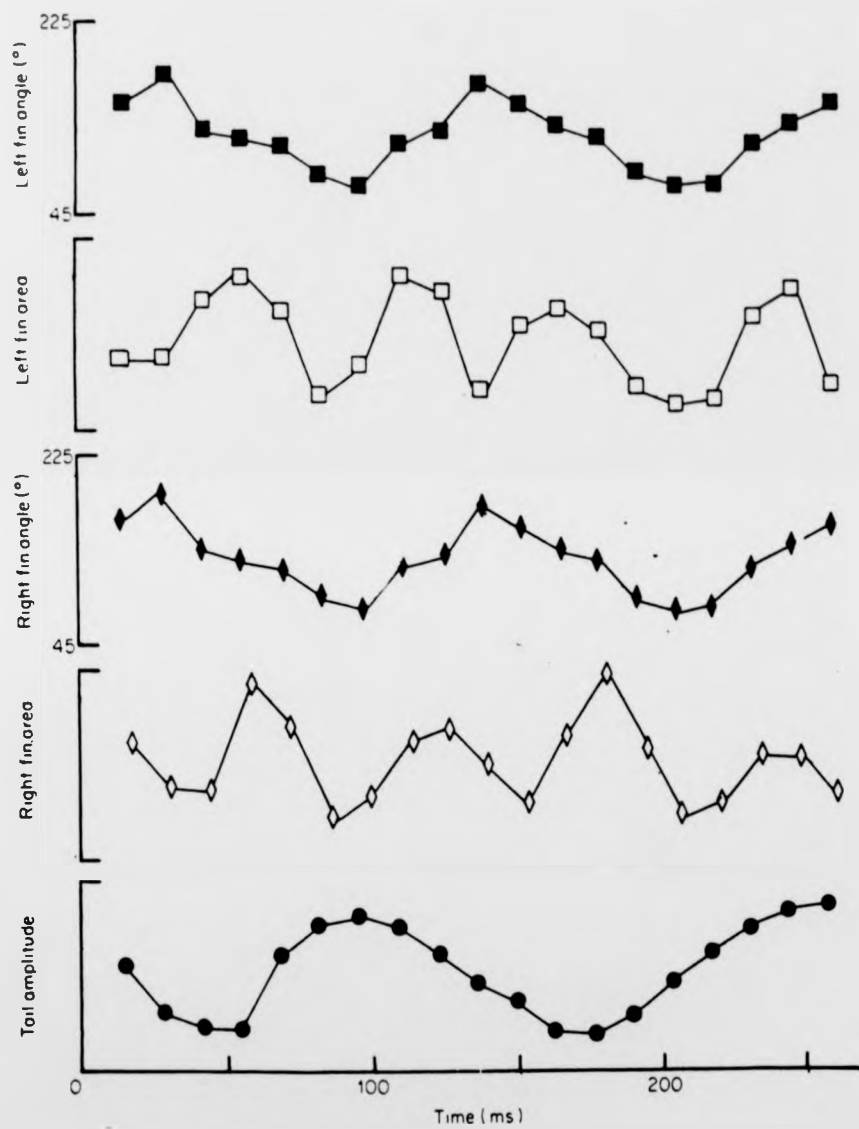
Fig. 21.   Pectoral fin movements during a right turn.

Labelled as in Fig. 19.

Unfortunately the photographic method used has limited the number of frames per tail beat to 2, at this speed, so that a proper analysis of the propulsive waves cannot be made. An examination of the outlines of a 7 mm larva shown in Fig. 14C indicates that wavelength λ_b is longer than one body length and that amplitude is much greater than during cruising. These two changes cause less than one complete wave to be included on the body. It seems that the larva has "changed gear" in order to swim at this higher speed of 140 mm s^{-1} (20 L s^{-1}) whilst using a very high tail beat frequency of 35 Hz. A considerable yaw of the head is seen in this sequence, compared with cruising swimming (Fig. 14A) when pectoral fin movements are used. Measurements of maximum tail beat frequencies of the plaice larvae are plotted in Fig. 22 together with similar data obtained by Bainbridge (1958) for adult fish and by Hunter (1972) for anchovy larvae.

The graph demonstrates that maximum tailbeat frequency is strongly dependent on size, increasing as size decreases. This observation is confirmed by the findings of Wardle (1975) on the contraction time of adult muscle which shows the same type of size effect.

Body dimensions

Herring

Measurements were made from tracings of the projected silhouette photographs. The fin positions and body and tail

Fig. 22.   Maximum tail beat frequencies of different sizes

of fish.   O   plaice larvae,   ●   anchovy larvae

(Hunter, 1972),   ■   adult fish (Bainbridge, 1958).
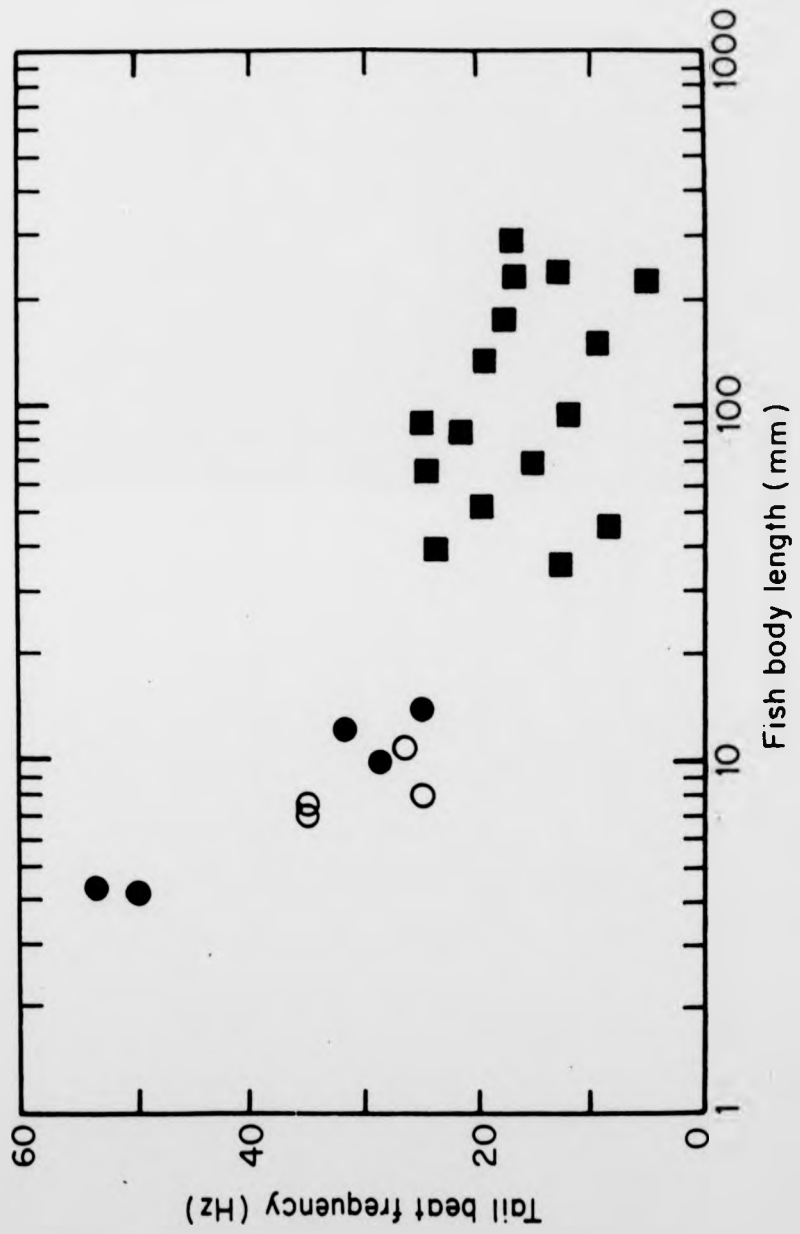
blade depth were measured at stages throughout development. Fig. 23 shows outlines of herring larvae at different stages, together with the parameters measured.

The position of the pectoral fins is very important for stability in the vertical plane. They produce lift or a downward force as a means of altering body orientation and maintaining position within the water column. Fig. 24D is a plot of the position of the pectoral fins in units of body length from the head. This graph clearly shows that the pectoral fins are very far forward throughout larval life but do move tailwards during this time. The position of the centre of mass is not known since it is difficult to measure in a fish larva, but due to the uniformity of the cross section of the body it is probably close to, but less than, half the body length from the head. It appears that the centre of lift is always well ahead of the centre of mass. This accounts for the observation that young larvae, particularly, swim with the body inclined to the horizontal with the head uppermost. This attitude allows some thrust force produced by the tail to act as lift and so augment the lift produced by the pectoral fins shifting the centre of lift backwards. The position of the trailing edge of the dorsal fin in units of L is plotted in Fig. 24C. The edge of this fin remains in the region 0.74 to 0.75 L until late in development. At lengths greater than 30 mm it moves forward to about 0.68 L at metamorphosis (40 mm length). This fin is developed unusually

Fig. 23.   Outline profiles of herring during growth, drawn

to the same size but not the same scale. The

length in mm is shown on the left of each drawing.

The dorsal fin of the 102 mm juvenile is drawn as

a broken line since it can be folded against the

body.
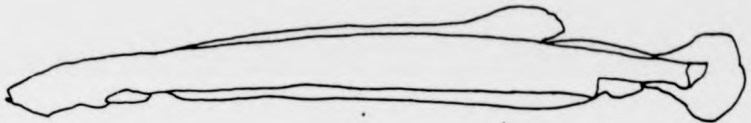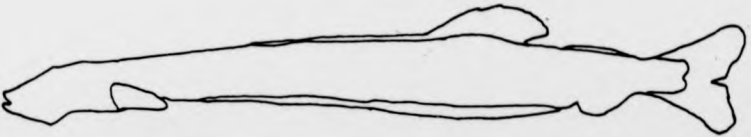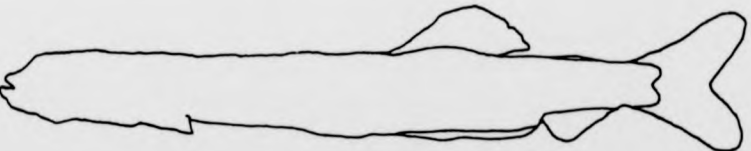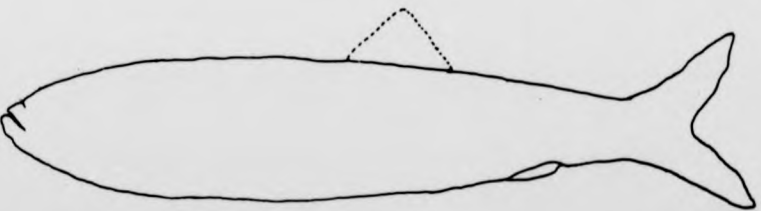
Fig. 24.   Changes of important dimensions of herring larvae during growth in length L.   (A) maximum body depth/L;   (B) tail depth/L;   (C) tip of dorsal fin/L;   (D) position of pectoral fins/L.
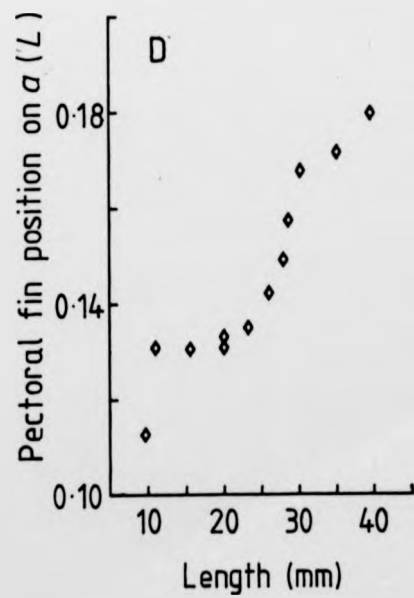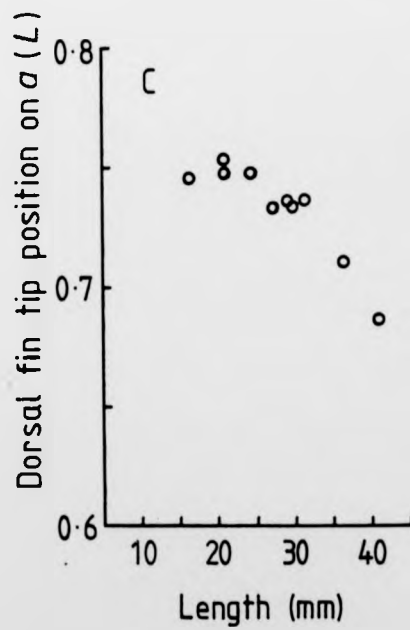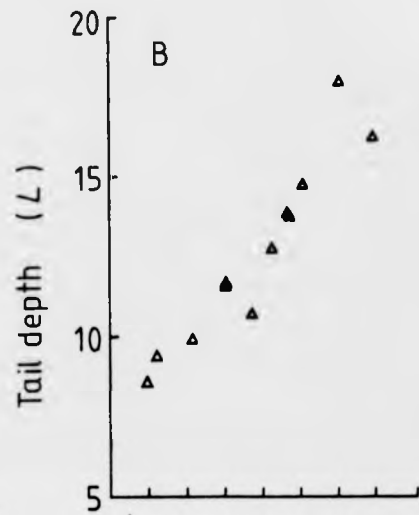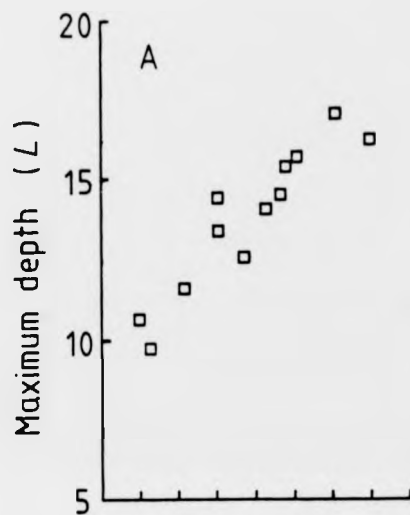
early in the clupeoids and is very large in the larval stages.
Its position well back on the body is also unusual; in fact
it migrates considerably further forward after metamorphosis
to 0.58 L at a length of 17.5 cm. Another interesting feature
of the herring larva's body shape is the position of maximum
body height. Once the dorsal fin has been developed, at around
15 mm long, the maximum body height is within the base of this
fin and would be even if the height of the fin were excluded.
The body is very deep at this point due to position of the gut,
the largest part of which is situated at this part of the body
(see Fig. 23).

In examining body height (Fig. 24A) the fullness of the gut
has not been considered. Disregarding relative fullness of the
gut, body height increases from 0.1 to 0.17 as a proportion of
length during development. Observations have shown that a full
gut causes a slight increase in body height. It has also been
observed that the gut is always filled from the rear (i.e. food
is quickly packed down to the end of the gut). The significance
of this concentration of body height and large mass (due to a full
gut) in this region and its effects on the dynamics of swimming
are discussed later. The height of the tail blade is plotted
in Fig. 24B. It is shown that tail height increases steadily with
length and is generally slightly less than maximum body height.

Plaice

In a similar manner to the herring the pectoral fins of plaice
larvae move tailwards during development, from about 0.13 to 0.25 L
(Fig. 25A). This movement is more dramatic than in the herring and
is particularly interesting since the pectoral fins are very important
for the plaice larva in counteracting head yaw (see page 54). The
position of attachment of these fins is very important in this respect
and their movements may have to be modified to cope with it.

Plaice larvae differ greatly from the herring in their body height,
plaice having very deep bodies. Maximum body depth and tail blade height
are plotted together in Fig. 25B. Tail heights of plaice are very
similar to those of herring but body height is much greater than tail
height throughout development. The ratio of body to tail height
increasing from slightly less than 2 to about 3.

The position of maximum body height varies. It can be within the
length of the gut or behind it, but is always less than 0.5 L (Table II).

Muscle Histology

SDHase staining

Photomicrographs of stained sections of herring larvae are
shown in Fig. 26. These transverse sections show two distinct
areas in the body muscle, one unstained area and the other of
red muscle staining strongly for SDHase. In the yolk-sac larva
of 10 mm length (see Fig. 26A) red muscle appears as a band of
fibres one fibre thick, surrounding the myotome. This arrangement

Fig. 25.   Changes of important dimensions of plaice larvae
during growth in length.   (A) position of pectoral
fins/L;   (B) maximum body depth/L □ and tail
depth/L ● .
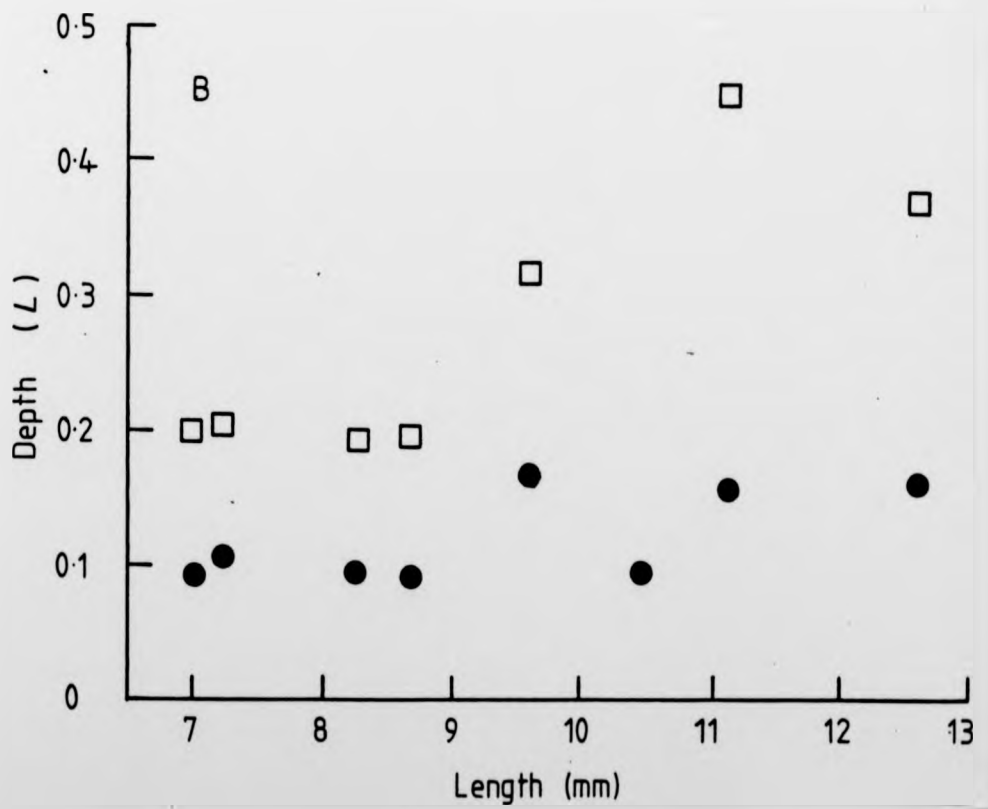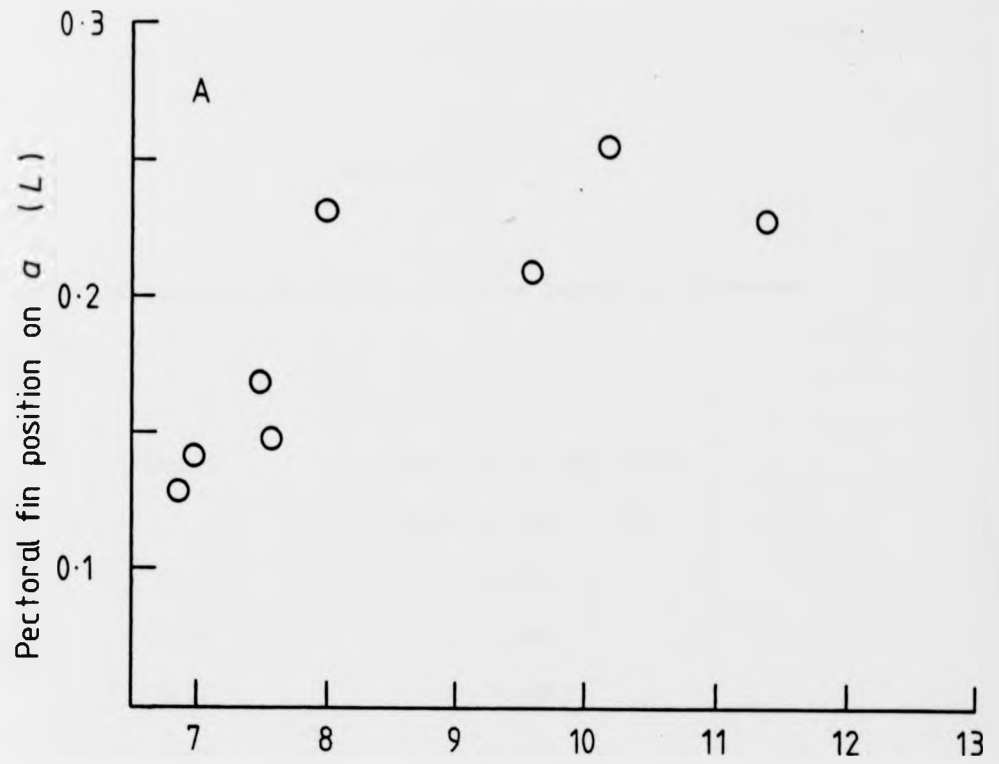
Table II

Position of maximum body depth of plaice larvae of different lengths.

Length	Position of max. body depth on body (L)
7.02	0.513
7.26	0.460
8.25	0.508
8.68	0.518
9.63	0.262
10.50	0.532
11.14	0.496

Fig. 26.   Photomicrographs of transverse sections of herring

larvae stained for SDHase.   Dark areas indicate a

positive reaction.   A, 10 mm yolk-sac larva; B,

11.5 mm larva; C, 25 mm larva; D, 27 mm larva at

centre of myotome; E, 35 mm metamorphosing fish

F, 5cm juvenile fish showing red and white muscle.

Scale marks, A, B, D, F, 50 μm; C, E, 500μm.

A

50 μm

B

50 μm

C

D
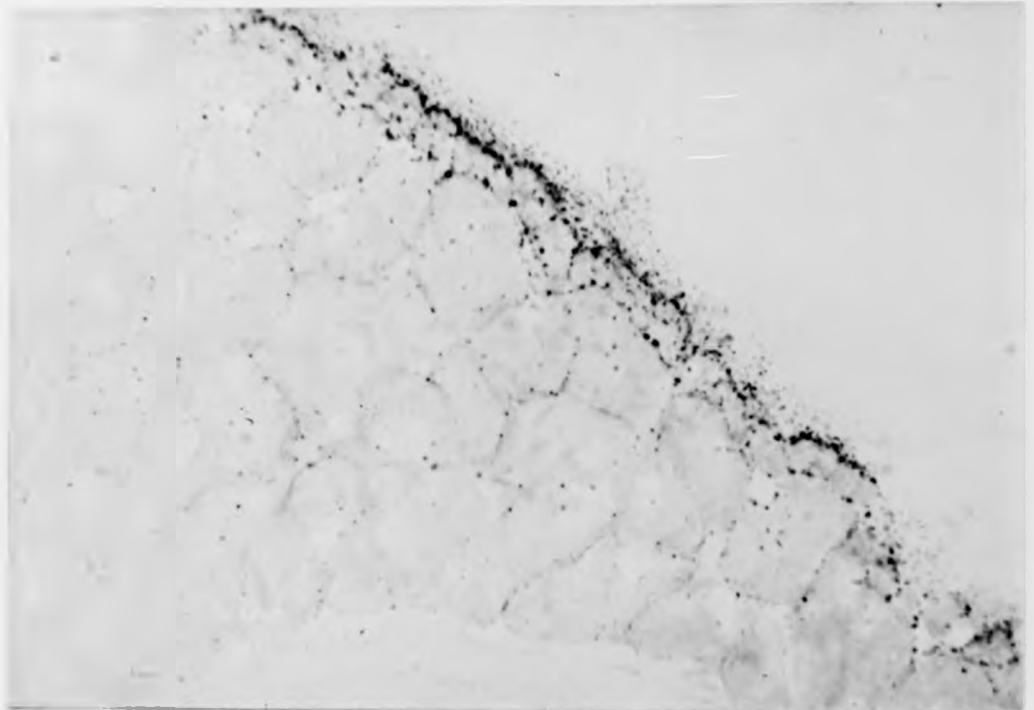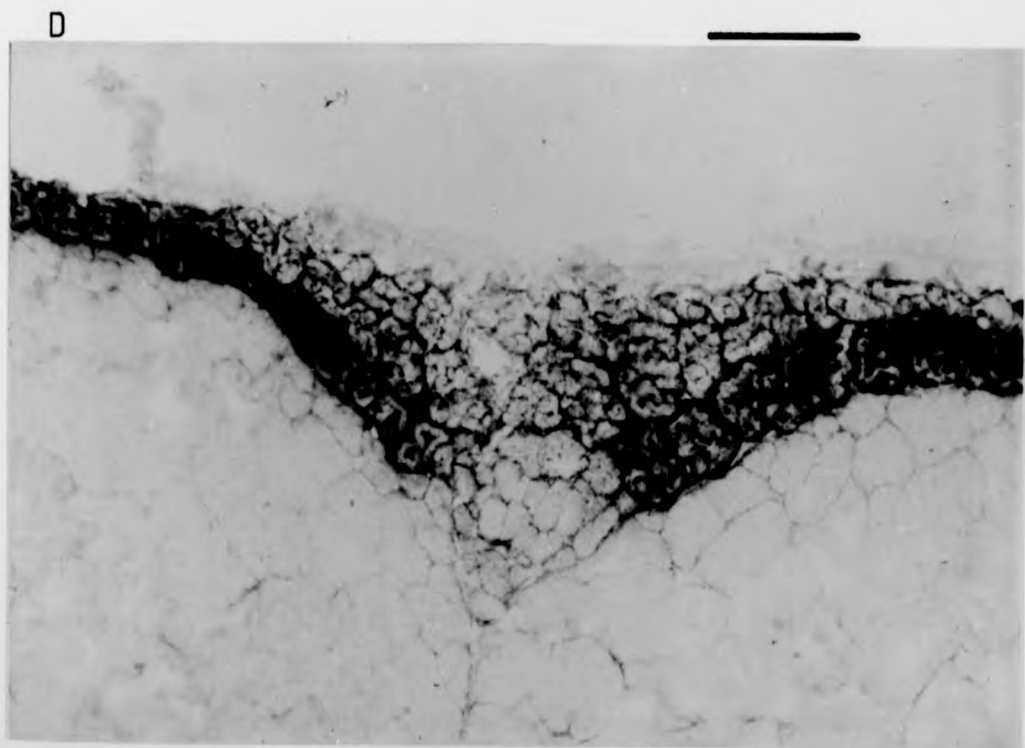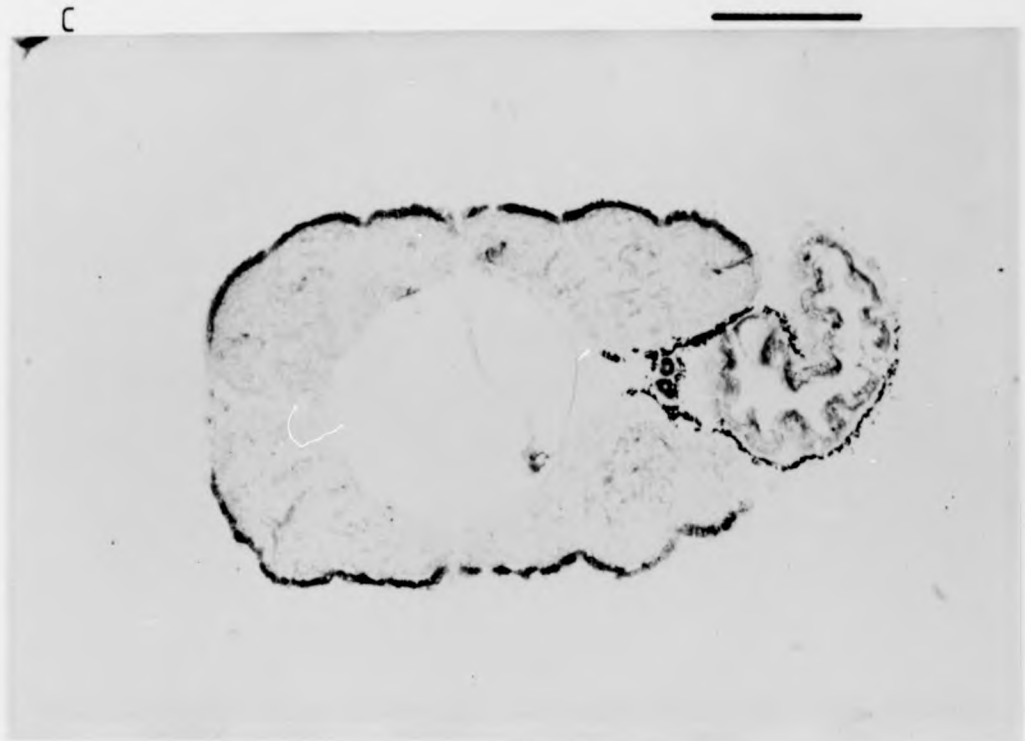
E
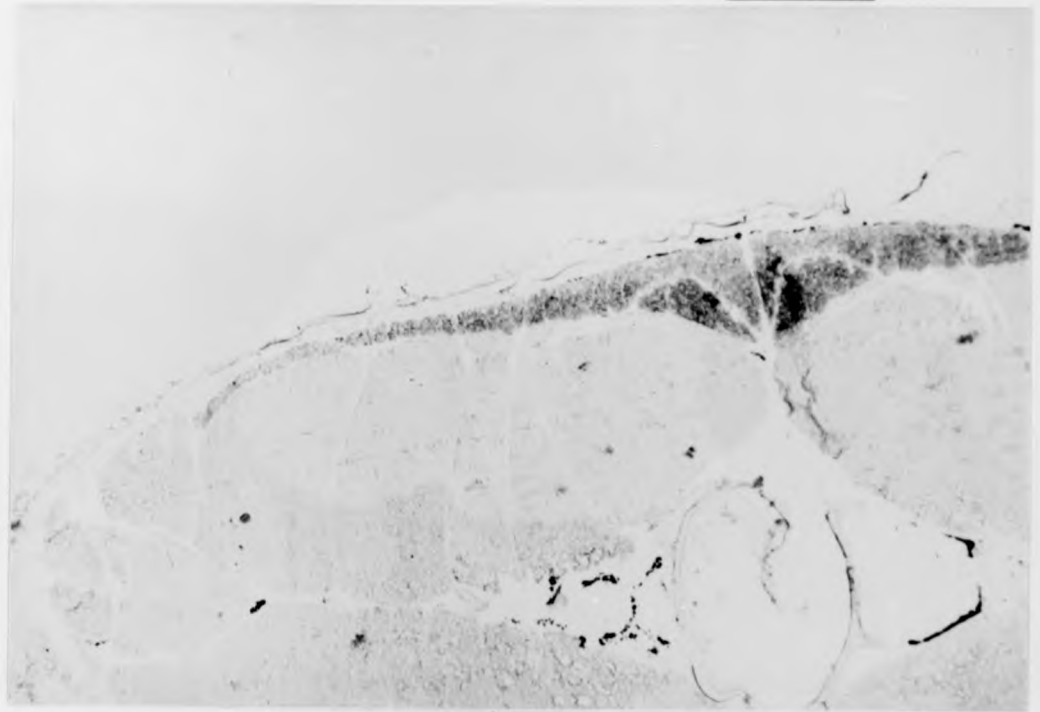
F
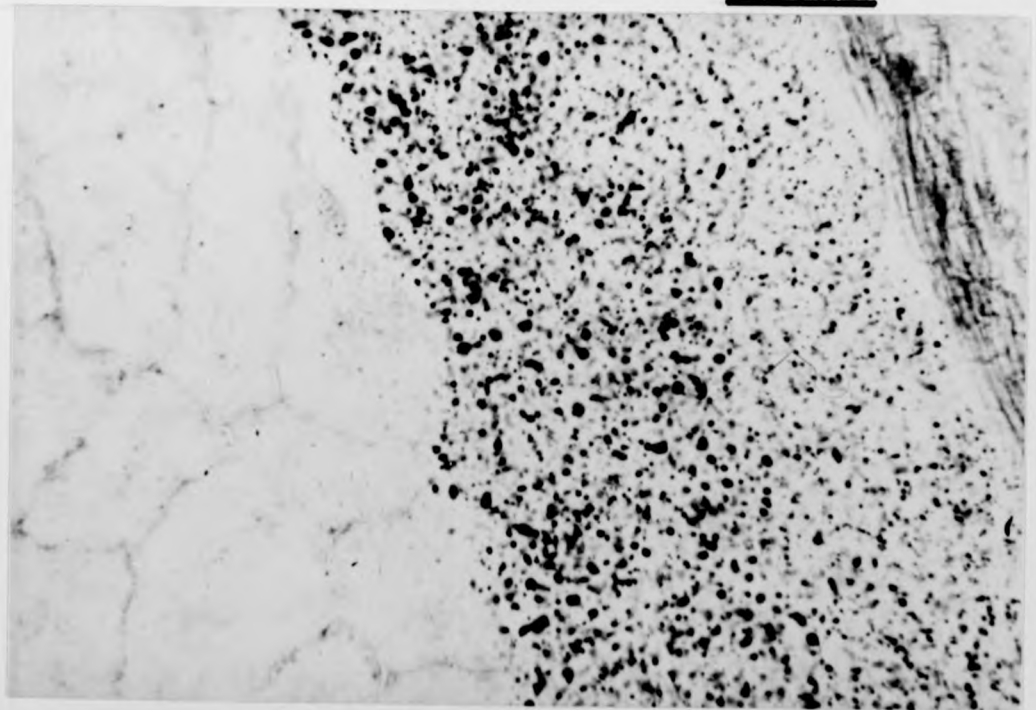
Persists through most of larval life, Fig. 26B shows an 11.5mm

post yolk-sac larva and Fig. 26C a 25 mm larva.

At a length of about 27 mm (Fig. 26D) further developments

start to take place in the red muscle. In this photograph an

inturning of the red muscle band at the horizontal axial plane

of the myotome can be seen. Between the original red muscle band

and the skin are a number of new muscle fibres which stain well for

SDHase but do not exhibit such a strong reaction as the other

red fibres. As these fibres develop and proliferate then the

staining reaction becomes uniform. Red and white muscle

distributions approaching those of adults are observed in the

35 mm larva (Fig. 26E). On the basis of SDHase staining, there

appears to be only two types of muscle fibre pure red fibres and

pure white fibres. The same is the case in the adult fish. Figure

26F shows a section through both red and white muscle in a 5 cm

long juvenile fish.

Lipid staining

Staining for lipids in the muscle using both Oil Red O

and Sudan demonstrated lipid droplets in the red muscle of juvenile

5 cm long fish some weeks after metamorphosis. Lipid droplets

were not observed in any larval fish neither in red or white muscle.

It is possible that very small lipid droplets in larval fish could be

more easily dissolved and washed away by the stain. This effect

would be exacerbated by the very small size of these sections. In

general this is thought to be unlikely. Since the triglyceride
content of whole herring larvae is quite low (less than 8% of the
dry weight(Ehrlich, 1974)it seems probable that red muscle has no
lipid energy store in herring larvae.

Proportions of red and white muscle

The relative proportions of red and white muscle during
development of herring larvae were measured by finding their
relative areas in camera lucida drawings of transverse sections.
All the sections used were taken from a point one third of the
length along the body from the tail. This is the same point
used by Walker and Pull (1975) in a survey of red and white muscle
in marine fish, and was used so that comparisons could be made with
their results.

The results are shown in Fig. 27A indicating a decline in the
proportions of red muscle from 13% at the end of the yolk-sac stage
to a low point of about 8% at a length of about 30 mm. In the
juvenile fish it has increased to about 16% by 7 cm length, the
same proportion found by Walker and Pull (1975).

Relationship of muscle development to respiration.

Data taken from the work of de Silva (1973) are shown in
Fig. 27. Her results for gill area (Fig. 27B) and body surface
area (Fig. 27C) per unit wet weight are plotted to allow a comparison
with percentage red muscle. The vertical pecked line indicates

Fig. 27. Herring larvae, (A) changes in the proportion of red

muscle, at a = 0.67; (B) body surface area to body

mass ratio, all plotted against length. Parts B and

C use data taken from de Silva (1973). The vertical

dashed line at 27 mm shows the length at which red

muscle distribution starts to change to the adult

form.
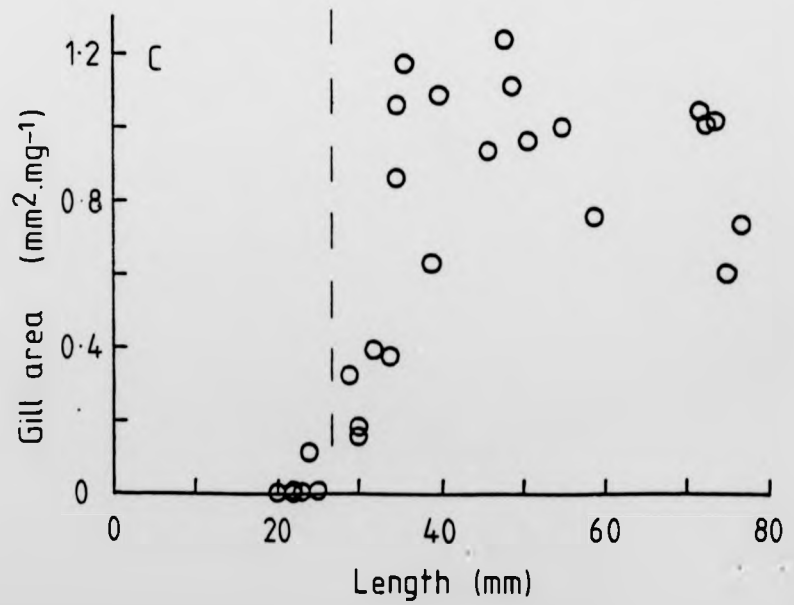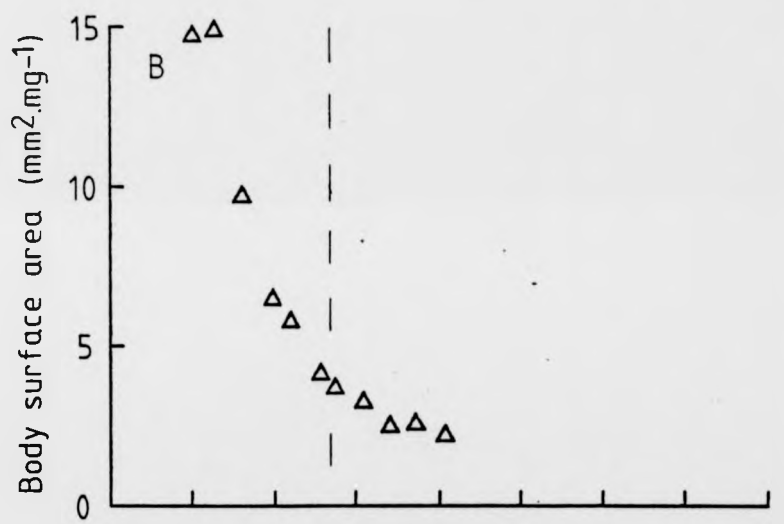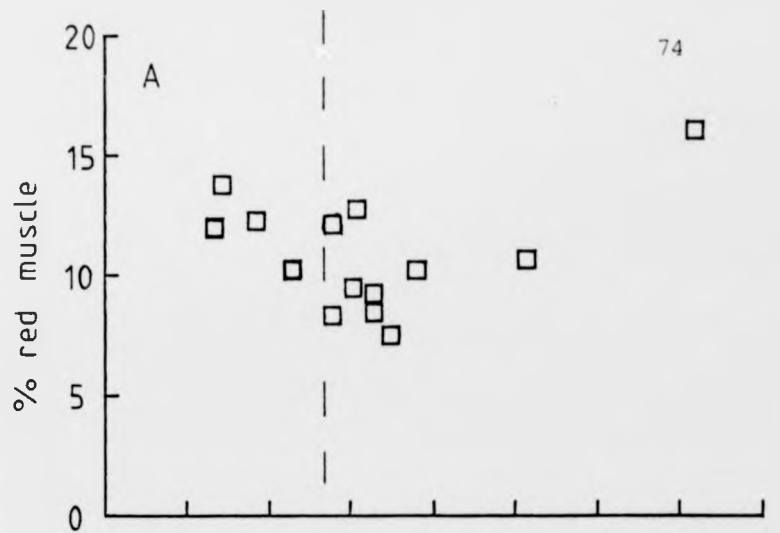
the body length at which the adult distribution of red muscle
fibres starts to develop.

The gills develop very rapidly from a length of 22 mm
onwards, the most rapid development occurring at around 30 mm
long. The maximum gill area to body weight ratio, of $1.2 \text{ mm}^2.\text{mg}^{-1}$
metamorphosis at 40 mm, is much less than the body surface area
at this time, $2.5 \text{ mm}^2.\text{mg}^{-1}$ body weight. It appears the cutaneous
respiration is more important than gill respiration during most of
the larval stage. Gill respiration becomes of importance when
the gill area increases at around 25 mm, coinciding closely with the
development of red muscle which until then is restricted by its
dependence on cutaneous respiration. Up to this size all red muscle
fibres are in contact with the skin but subsequently their
proportion relative to white muscle declines until the point is
reached when new red muscle fibres can develop which no
longer need to be in contact with the skin. Improvement in the
oxygen supply, as a result of gill development, allows these
more internal red muscle fibres to be serviced.

A MODEL FOR LARVAL FISH SWIMMING

Introduction

The two-wave model of fish swimming of Gray, 1933 which has been applied recently by Videler and Wardle (1978) and Wardle and Videler (1980) assumes that sinusoidal curves flow down the body of the fish towards the tail and that each part of the body follows a similar track in space. The waves observed in some species of adult fish do appear to conform to this model at small tail beat amplitudes. This model can be only loosely applied to fish larvae, as has been shown in the previous chapter. The very large θ angles found at the tail tip (sometimes exceeding 90°) cannot be modelled as a sine function of x.

The 'two-wave model' does not allow for the body shape of a swimming fish larva. A more general model, applicable to both larval and adult fish, is therefore developed here. This model follows the bending of the fish's body rather than its amplitude on the z coordinate. Using bending has a number of advantages. Since we are dealing with the angles between parts of the body and the x coordinate, then the x coordinate need not be the direction of motion, but a constant can be introduced to define it. The model is based on a spine ordinate a and therefore only one equation is needed to define the value of θ: x and z coordinates are derived from the angle θ as integrals. A model based on x is rather awkward because of the limiting value of x which will vary

with time, i.e. depending on the position within the tail beat cycle. An alternative model based on the amplitude of z versus a has problems too. Like the x, z model it cannot cope with negative-going x at the tail (when θ is greater than 90°) unless a second equation for x against a (with parameters) is introduced into the model.

The Model

In this model the angle θ' is defined as the angle between a tangent to any position on the body, a, and the 'instantaneous direction of motion' which is the tangent to the direction of motion at that instant.

Bending is defined as the rate of change of θ' at any point in length (i.e. coordinate). Thus:

$$\frac{d\theta'}{da} = c \cos a \qquad (1)$$

It would be simpler to use θ the angle between the body and direction of motion and so integrating equation 1 we get:

$$\theta' = \int c \cos a \, da \qquad (2)$$

Therefore:

$$\theta' = \int c.\sin a \, da \qquad (3)$$

The following standing wave equation is used as the model:

$$\theta'_{(a,t)} = ka^g . \sin (2\pi a / \lambda_{at} - 2\pi b_t) \qquad (4)$$

where b_t is the phase of the wave at time t, amplitude is given by the power curve ka^g which defines the relationship between amplitude and length along the body.

If the model is to be fitted using a frame of reference or coordinate system fixed through a sequance, the relationship between the coordinate system, which moves with the fish and has the x axis aligned along the instantaneous direction of motion, and a fixed coordinate system muste be defined. These coordinates x', z' are related to x, z by the angle ψ (see Fig. 28). Using this method yaw of the body while swimming can be observed and curved swimming paths can be analysed.

In place of λ_b , a parameter λ_a which is the wavelength along the body coordinate a is used. Wavelength λ_b is not constant along the x axis but λ_a is constant along a, since wave speed is constant along a rather than x (See Fig. 12 C, D). Also $1/\lambda_a$ gives the number of waves on the body. λ_a is related to λ_b:

$$\lambda_b = \lambda_a . \int_{a = 0}^{a = 1} \cos \theta' . da \qquad (5)$$

Fig. 28.   Parameters used in the model. The mid-dorsal line

of a larva is shown as the heavy black line. H is

the head and T the tail. The two sets of coordinates

x, z and x', z' are related by the angle ψ. The data

are expressed in the co-ordinates x,z,a. In fitting

the model the angle ψ is found which defines the

instantaneous heading of the larva. Other parameters

wavelength λ_a etc, are fitted using θ' (the angle of

a point on the body a) relative to the x', z'

co-ordinates.
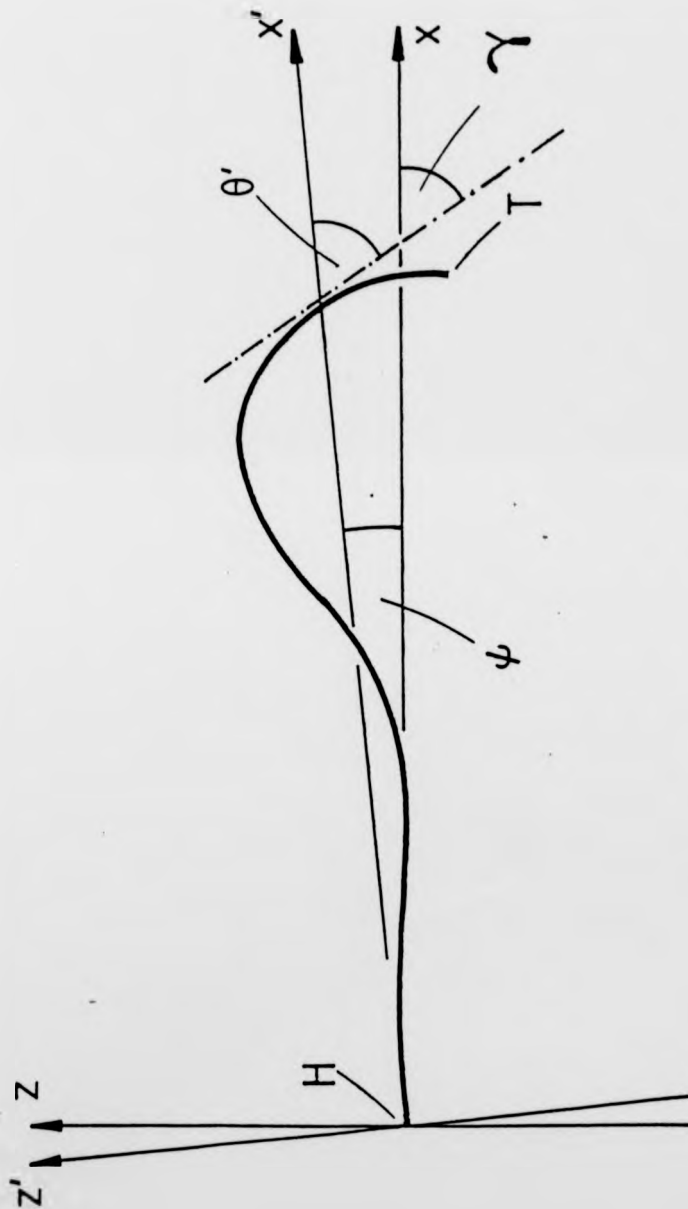
To simplify fitting of the model to the fixed coodinates x, z
the model is fitted to an angle γ (see Fig. 28).

$$\gamma = \theta + \psi \tag{6}$$

γ is the angle between a part of the body and the x axis.
x and z for any point i on the centreline can be found by integration:-

$$x'_{(i,t)} \int_{a=o}^{a=i} \cos \gamma_{(a,t)} \, da \tag{7}$$

$$z'_{(i,t)} = \int_{a=0}^{a=i} \sin \gamma_{(a,t)} \, da \tag{8}$$

The model can be fitted on this basis to single frames of a
swimming larva.

To include time and therefore a time series in this model
requires a suitable modification. Obviously $b = f(t)$ but ψ
may also be related to time, oscillating with yaw. Other
parameters may also vary with time and, if swimming is not steady,
may vary during a series. g is particularly prone to variation
in non-steady swimming where amplitude may vary, thus altering

the shape of the θ' maximum curve considerably.

Fitting the model to experimental data.

There are two possible approaches to this problem, but both require a number of points along the spine coordinate a to be defined. One method would find the angle γ at each point and then fit the model to pairs of a, γ coordinates. Another method would fit curves to (x, z) coordinates scaled in body lengths (i.e. with $a = 1$ at the tail). This coordinate must have its origin at the tip of the head in each frame, but the body may have any orientation to the coordinate system (i.e the coordinate system is independent of the direction of motion).

The second method will be used here since errors are likely in calculation of γ near the head and although the model may fit γ well, error in γ near the head may throw the curve off the (x, z) coordinates of the body as the tail is approached, since x, z are calculated from integrals of γ.

The same technique that is described on pages was used to reduce the data from a herring outline to a line centred on the spine. Then, after centring the origin of the (x, z) coordinate system on the head, coordinates of each data point were calculated and scaled (by dividing by L) to have values between O and 1. The (x, z) coordinates were also divided by L to the same scale as a.

The model could be fitted by a search method (searching for

nearest point on the curve to the data point) but since there are a large amount of data (100 points between $a = 0$ and $a = 1$) the method can be simplified. The modelled (x, z) coordinates of each data point i are calculated by computing the value of γ at each data point j up to i and finding x_i and z_i from the sums of the increments of x_j and z_j:-

$$x = \sum_{j = 1}^{j = i} \cos \gamma \; (a_j - a_{j-1})$$

$$z = \sum_{j = 1}^{j = i} \sin \gamma \; (a_j - a_{j-1})$$

In order to converge on the ideal fitted model the sum of squares of the geometric deviations of (x, z) from the fitted curve is minimised:

$$dx^2 . z^2 = \sum_{j = 1}^{j = 100} (x_j - x_j)^2 + (z_j - z_j)^2$$

This method was followed, using the 2980 computer at the Edinburgh Regional Computing Centre. The Nag library FORTRAN

routine EO4 JAF (NAGLIB Mk6 : May 77) was used to minimize the
sum of squares. The Fortran main programme used with this
NAG routine is described in Appendix II.

Results

Curves fitted by the above method are plotted in Fig. 29
together with the original data. There is close agreement
between the model curves and the data except in some cases at
the tail. It appears that the tail must have a lesser flexibility
than the part of the body preceeding it since it is always lagging
behind the modelled curve. This indicates that the model should be
modified to include a decreased flexibility within the length of
the caudal fin.

Table III lists the parameters of the model for each frame
plotted in Fig. 29. As would be expected variation of ψ, the
orientation of the body to the x axis varies little. The
amplitude at the head is small and θ_{max} is small at the head of
the herring larva (Fig. 11).

The other parameters vary more than might be expected if
simple sine waves were involved. Wave length may be expected
to vary and so make subtle changes to the shape of the waves
but it is surprising that k, the θ maximum at the tail-tip, and
the 'shape' of the amplitude curve vary so much. These
variations may be artefacts due to the poor fit at the tail. A
further problem is that the tail is not just less flexible than

Table III

Parameters fitted by the model when the tail was included.

Frame No.	ψ	k	g	b	λ
1	-0.93630	0.98102	1.07575	0.59087	0.80825
2	-0.91987	1.05329	1.08367	0.66093	0.81176
3	-0.91482	1.21780	1.22597	0.71250	0.81269
4	-0.92590	1.35310	1.44336	0.74733	0.81924
5	-0.91925	1.39700	1.48349	0.78525	0.82938
6	-0.89540	1.42037	1.42588	0.79733	0.84814
7	-0.93075	1.30444	1.37983	0.94596	0.74292
8	-0.94869	1.10529	1.36714	0.03057	0.71441
9	-0.96079	0.95450	1.10845	0.11164	0.68943
10	-0.99361	0.87266	0.93031	0.20384	0.67837
11	-0.98247	0.92114	1.01420	0.23262	0.72113
12	-0.99711	0.93963	0.98752	0.29783	0.74697
13	-0.97686	1.16491	1.30250	0.38867	0.73160
14	-1.02965	1.21183	1.07127	0.34650	0.81931
15	-1.01386	1.17563	1.03933	0.43123	0.78861
16	-0.98382	0.99436	0.84556	0.50549	0.78239
17	-0.96794	0.89286	0.66994	0.55547	0.81605
18	-0.97634	1.06911	0.77810	0.58092	0.86266
19	-0.96622	1.26289	0.93120	0.62940	0.90263
20	-1.01583	1.64650	1.47027	0.70590	0.88100
21	-1.01806	1.75181	1.43192	0.79823	0.83465
22	-1.04649	1.51600	1.52070	0.91144	0.78366
23	-1.07535	1.14210	1.27463	0.00445	0.74949
24	-1.11893	0.88655	0.80887	0.13044	0.71813
25	-1.12430	0.97925	0.87928	0.18045	0.77528
26	-1.08680	1.35400	1.36431	0.27185	0.76600
27	-1.15130	1.27682	1.11584	0.29272	0.82509
28	-1.16738	1.42925	1.33137	0.36443	0.81925
29	-1.14238	1.11148	0.95541	0.45372	0.80660
30	-1.14259	1.06540	0.84931	0.50169	0.85861
31	-1.14253	1.17112	0.94330	0.55492	0.88701
32	-1.13226	1.31205	1.08861	0.58900	0.93904
33	-1.15890	1.63035	1.77070	0.66205	0.93934

Fig. 29. Computer plots of mid-dorsal lines of a 22 mm herring larva. The first 17 frames of the series to which the model was fitted. The interval between each line is 20 ms. Dotted lines are data and continuous lines the curves fitted by the model when the tail was included.
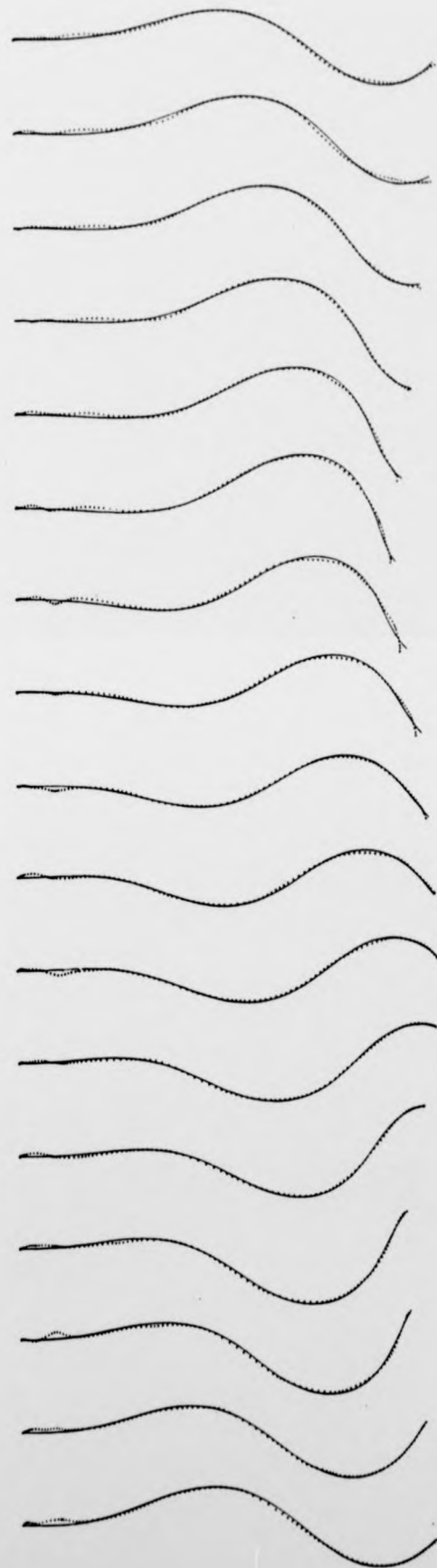
the end of the trunk but its deformation,rather then being

caused by muscular contraction, is caused by water it acts on.

For this reason the tail cannot follow the same sine function

as the rest of the body. The tail would be better modelled as

an arc of the same radius as the curve at the caudal peduncle.

The model was fitted again but an arc of constant radius c

applied to the body from $a = 0.75$ (i.e. along the length of

caudal fin). In Fig. 30 these fitted curves are plotted over

the data points and demonstrate the very good correlation between

data and model. (See Table IV for a list of fitted parameters).

The important parameters λ_a, b and ψ are shown in Table IV

and plotted against time in Fig. 31 together with tail amplitude.

Orientation of the body (ψ) varies (Fig. 31 C); there is an overall

change in this angle indicating that this larva is following a

slightly curved path. The cyclical variation in ψ and tail beat

frequency (Fig. 31 A) appear to have the same period. The

cyclical variation is due to yaw, i.e. lateral recoil of the head

caused by the lateral movements of the tail. In this sequence λ_a

(Fig. 31 B) increases at the same point in the tail beat (near the

beginning of a rightward sweep of the tail). These same points on

the plot of b (Fig. 31 D) show discontinuities of the slope.

These results can only be interpreted as asymmetrical swimming

in which a sudden effort is made once in every tail beat cycle when

the caudal fin reaches a very high angle θ. At this point λ_a is

reduced as the body is thrown into a much tighter wave, producing

Table IV

Parameters fitted by the model when the tail was excluded.

Frame No.	ψ	k	g	b	λ_a	c
1	-0.95335	1.15131	1.32053	0.60452	0.79007	-0.24100
2	-0.94584	1.29433	1.41450	0.72196	0.74396	0.07159
3	-0.93214	1.31308	1.36165	0.76126	0.75871	-0.20785
4	-0.93961	1.38265	1.50017	0.79372	0.76874	-0.19060
5	-0.94392	1.33565	1.44871	0.86456	0.74559	0.32139
6	-0.93058	1.29513	1.32383	0.89090	0.74739	0.58680
7	-0.96950	1.10132	1.10895	0.04067	0.66209	0.71663
8	-0.97660	0.89955	1.02682	0.09081	0.66380	0.64888
9	-0.96484	0.91999	1.04810	0.11678	0.68479	0.31952
10	-0.99405	0.87266	0.91283	0.20879	0.67326	0.29118
11	-0.98134	0.93153	1.02926	0.23634	0.71754	0.76059
12	-0.99593	0.94396	0.99373	0.30165	0.74310	0.65205
13	-0.97154	1.16238	1.29869	0.40768	0.71474	0.47153
14	-1.01382	1.55571	1.01686	0.37361	0.78859	-0.15541
15	-0.99449	1.07930	0.92588	0.45662	0.76172	-0.39419
16	-0.98908	1.02680	0.88751	0.50228	0.78562	-0.29761
17	-0.98210	0.97647	0.78655	0.55733	0.81161	-0.34864
18	-0.99031	1.14532	0.87552	0.59177	0.84486	-0.45729
19	-0.99258	1.33624	1.04381	0.66894	0.84391	-0.15505
20	-1.03983	1.63566	1.50692	0.77435	0.79792	0.21612
21	-1.07795	1.59792	1.33148	0.94306	0.69389	1.00000
22	-1.07930	1.30376	1.29244	0.98505	0.71474	0.72104
23	-1.07978	1.11288	1.23173	0.01249	0.74185	0.36659
24	-1.12027	0.87266	0.78907	0.12968	0.71866	0.61287
25	-1.12937	0.94295	0.82674	0.17152	0.78568	0.91499
26	-1.08991	1.33547	1.33799	0.26272	0.77526	1.00000
27	-1.14627	1.27050	1.11436	0.30325	0.81281	0.25997
28	-1.14889	1.32642	1.23464	0.39953	0.78140	-0.40158
29	-1.15480	1.18660	1.04127	0.44255	0.81869	-0.24638
30	-1.16837	1.22705	1.04496	0.49578	0.86114	-0.34692
31	-1.17368	1.39586	1.20791	0.58128	0.84318	-0.09260
32	-1.16285	1.43676	1.26407	0.64305	0.85433	-0.01197
33	-1.17258	1.61170	1.80455	0.72353	0.85591	0.17338

Fig. 30.   Computer plots of mid-dorsal lines. The first 17

frames of the series at 20 ms intervals fitted by

the model are plotted. Dotted lines are data and

continuous lines the curves fitted by the model

with the tail excluded. The transverse line is at

the point where a = 0.75L, corresponding to the

trailing edge of the dorsal fin.
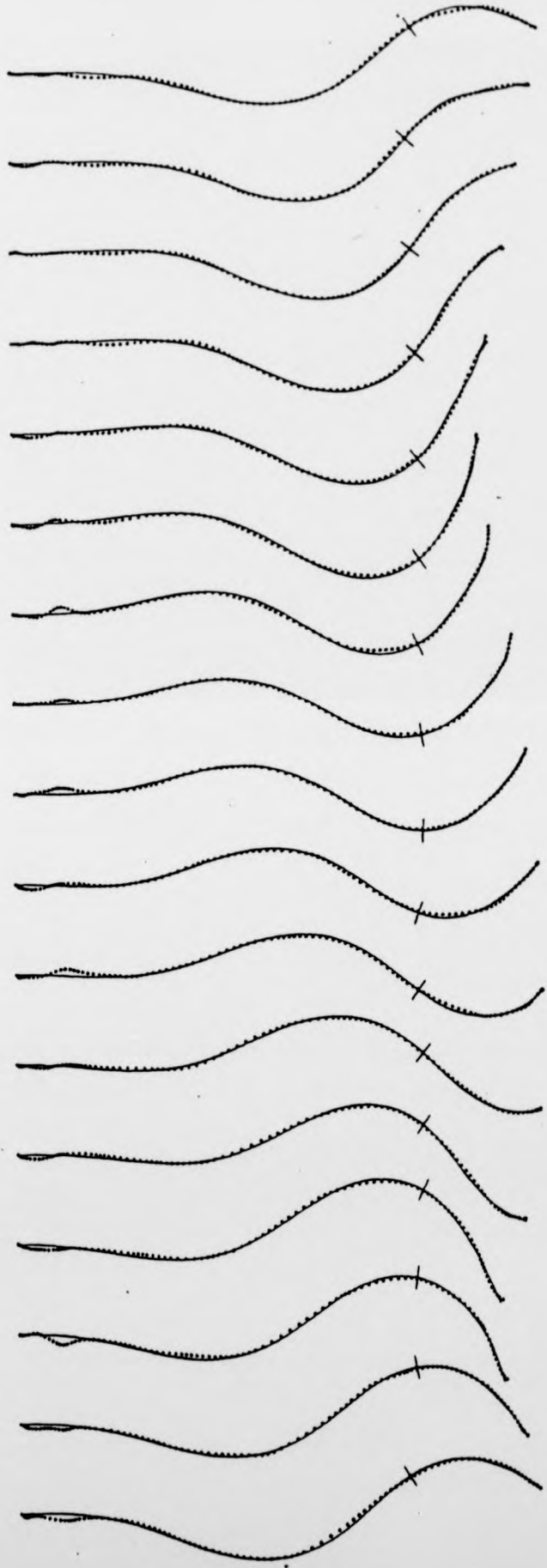
Fig. 31.   Parameters fitted by the model for a 22 mm herring

larva.   (A) Tail amplitude z.   (B) Wavelength $\lambda_a^{\cdot}$.

(C) Heading ψ.   (D) Phase b at the head i.e. where

$a = 0$.
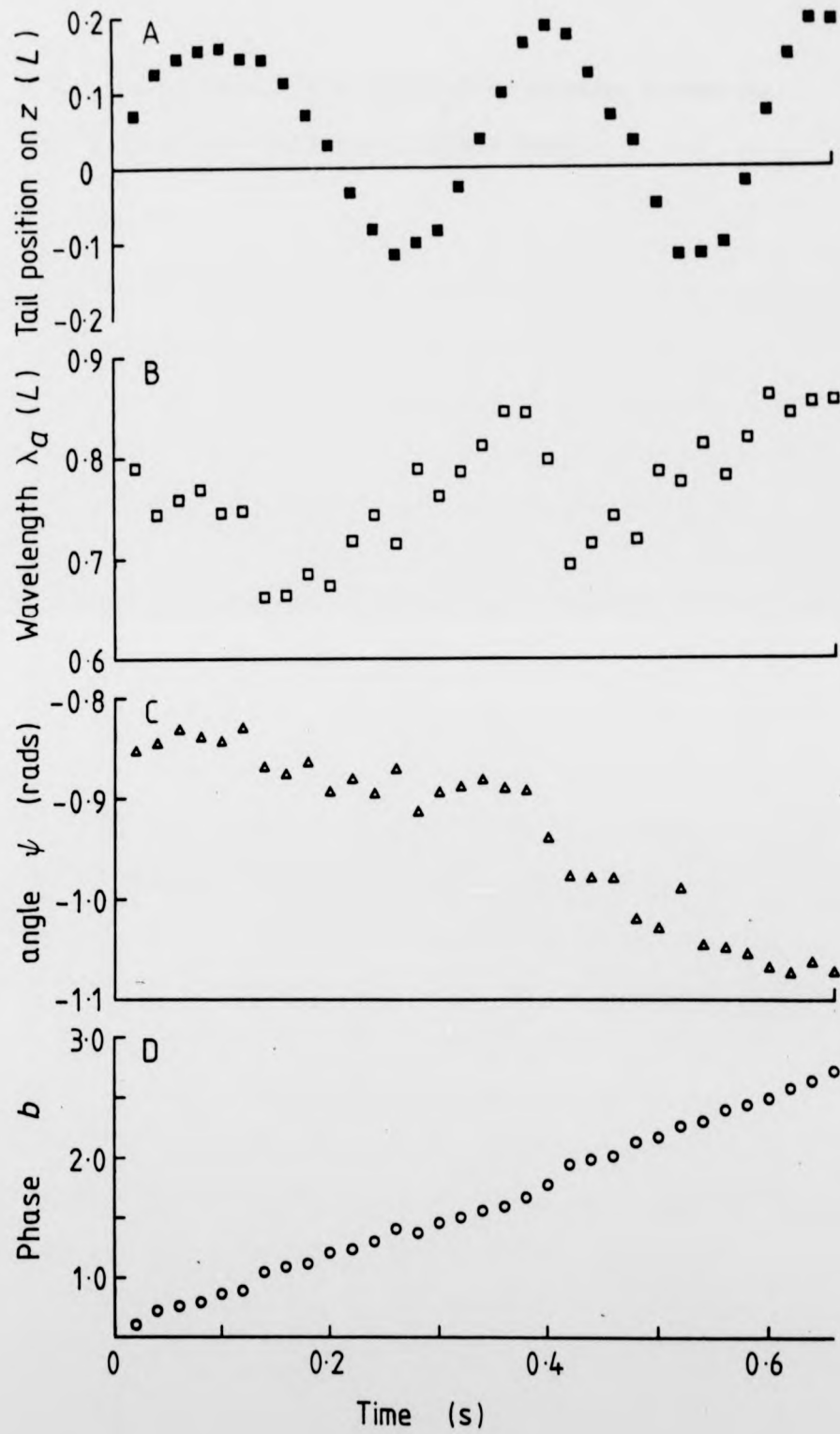
a forward acceleration. This asymmetrical swimming caused the
fish shown in Fig. 30 to swim in a slight curve.

DISCUSSION

This study has demonstrated the nature of the muscle available to propel a fish larvae, its distribution and the relationship between this and respiration during development. The shape of the body has been considered after accurate measurements made from silhouette photographs. A kinematic analysis of swimming movements has been made, using some new techniques and has shown many differences between larvae and adult fish.

Reynold's number and flow pattern.

Before considering the swimming movements of larvae it is important to discuss the type of flow around a body moving in water. Reynold's number is a measure of the hydrodynamic similarity of bodies of different sizes moving at different velocities. It can be shown that a small body moving at a high velocity may be hydrodynamically similar to a large body moving at a low velocity (i.e. the pattern of flow around them may be similar). Viscosity and density of the medium also have an effect but in the present case, unless temperature varies greatly (temperature effects viscosity), it is velocity and body length that are important. Reynold's number is defined as:

$$R_L = \frac{\rho L u}{\mu}$$

L is the length of the larva, u the velocity of swimming speed, μ is viscosity and ρ is the density of the medium. We will now consider the two extremes of Reynold's number that plaice and herring larvae may experience.

For the lower limit let us consider a 6 mm plaice larva swimming at 10 mm.s^{-1} (this speed is lower than the range of cruising speeds examined in this study) in water of temperature 10°C and 30 ppt salinity. In these conditions ρ = 1024 Kg.m^{-3} and μ = 0.0014 Pa.s, L = 0.006 m and U = 0.001 m and the Reynold's number is 4.

For the upper limit take a 40 mm herring, the length near metamorphosis, swimming at a maximum speed of 1 m.s^{-1} at 10°C and 30 ppt. This gives a Reynold's number of R_L = 3 x 10^4.

Reynold's number is a measure of the ratio of inertial to resistive forces acting on the body. Since R_L is substantially greater than zero for larvae, inertial forces are important but, as viscous forces are important in the boundary layer, they cannot be ignored. Conversely for a spermatozoan (Gray, 1955), with a Reynold's number of 1 x 10^{-5}, inertial forces can be ignored.

The maximum Reynold's number calculated for a 40 mm herring larva is considerably less than the critical Reynold's number, $(R_{L\ CRIT})$ = 1 x 10^6, when transition between laminar and turbulent flow in the boundary layer takes place (Hertel, 1966; Webb, 1975). Separation of the boundary layer is also likely at $R_{L\ CRIT}$

but could occur at lower Reynold's numbers under certain
conditions such as adverse pressure gradients (Webb, 1975).
It appears that for larvae under all conditions flow will be
laminar and the boundary layer will be attached throughout the
length of the body.

Weihs (1980a) showed theoretically that the swimming style
of anchovy larvae changes as they grow ,due to the increase of
R_L, so that intermittent swimming becomes energetically more
advantageous as viscous forces become less important. Weihs
(1980a) defined three regimes: R_L < 10 where viscosity is much more
important than inertial force effects, 10 < R_L < 200 which is a
region of transition where the flow changes from the viscous
regime to the inertial regime,where R_L > 200. In low R_L regimes,
drag coefficient is inversely related to R_L which makes swimming
at low speeds very inefficient.

The shape of the amplitude of the body waves against length
curve (Fig. 12) changes as herring larvae grow. Initially, at
11 mm length, it is linear, but once larvae have grown to 22 mm it
becomes non-linear. At this length amplitude increases more
rapidly as the wave moves tailwards. The shape of this curve is
characteristic of the type of swimming motion employed (Grillner
and Kashin, 1976; Videler, 1981). A linear increase in amplitude
along the body, giving a large amplitude over most of the body,
is characteristic of fish swimming in the anguilliform mode. In
this type of swimming lateral acceleration of water is constant

along the body, indicating that resistive forces are important. The non-linear increase in amplitude seen in a 22 mm larvae (Fig. 12B) is typical of carangiform or subcarangiform swimming; in this mode lateral acceleration of water by the fish body increases rapidly towards the tail, so that in this type of swimming reactive (inertial) forces predominate.

These changes in swimming style fit in with changes in flow pattern as R_L increases. Until the larva exceeds a length of 15 mm and the R_L at the searching speed of the larva has exceeded 200, subcarangiform swimming would be very inefficient. It is therefore advantageous for herring larvae less than 15 mm in length to use the anguilliform mode of swimming. The appearance of the caudal and dorsal fin when the larvae are between 15 mm and 20 mm in length (Fig. 23) increases the effectiveness of swimming in this mode and the change in swimming style from anguilliform to subcarangiform occurs over this length range.

Role of plaice pectoral fins.

The results have shown that the pectoral fins are not important for producing thrust to propel plaice larvae. It appears that their role is to produce lift, which is important since the larvae are negatively buoyant (Ehrlich,1972), and at the same time, to reduce head yaw.

Yawing movements of the head are caused by angular recoil forces which are generated by lateral movements of the tail

(Lighthill, 1977). The opposing forces produced by a pair of pectoral fins form a couple tending to turn the head against the recoil caused by the tail (Fig. 32). A reduction in head yaw should lead to a decrease in drag caused by swimming movements. This drag reduction is due to a decrease in effective frontal area of the fish, thereby reducing pressure drag, and a reduction of wasteful lateral movements against the water which will cause negative thrust anterior to the yaw pivot.

This reduction of drag is at the expense of drag on the fin which is moving forward at any time, but this fin is also producing lift and so this drag is of some value. If alternating fin movements were not used lift would be produced by fixed fins, resulting in drag. The alternating pectoral fin movements of plaice larvae increase swimming efficiency by using energy spent in producing lift to reduce the amount of drag that is induced by swimming movements.

The one disadvantage of this mechanism is that roll might be induced, since the centre of lift is always being laterally displaced from the centre of mass. Roll, if it exists, would be too small to be observed in the films made in this study. Roll would be expected to be very small in a plaice larva since the very deep body will dampen and stabilize a rolling tendency effectively.

The pivot for the pectoral fins is anterior to, but close to, the yaw pivot, which is the point on the body at which minimum angular displacement occurs (Fig. 15). The movements of the pectoral

Fig. 32. A diagram showing the interrelationships between
lateral recoil forces and forces produced by the
pectoral fins of plaice larvae while swimming at
cruising speeds. Q is the lateral component of the
force produced by the tail. F_1 is the recoil force
acting on the head. P is the yaw pivot and M is the
point of minimum amplitude. F_C is the force, produced by the
pectoral fins, which counteracts the recoil force F_1.
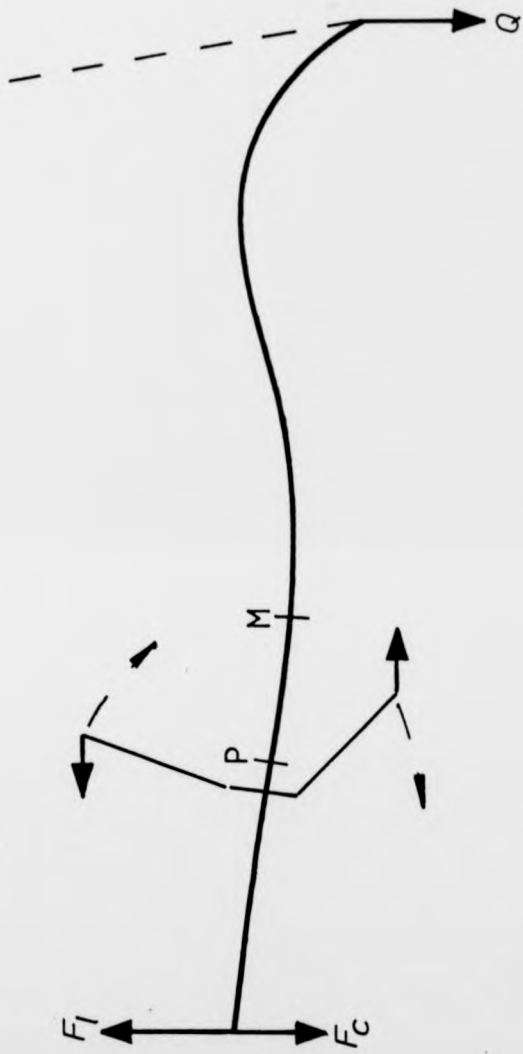
y the

fins are therefore unlikely to have any effect on the position of this pivot. It is interesting that the yaw pivot and the point of minimum lateral amplitude do not coincide, as in the case of herring larvae (Fig. 12). The point of minimum lateral amplitude is further back along the body at about $0.4\ L$ (Fig. 15) and its position can be explained by the effect of the force couple produced by the pectoral fins. This couple will tend to counteract both lateral recoil movement of the head and reduce lateral movements in the middle portion of the body,so causing the point of minimum amplitude to move back along the body.

Swimming style of plaice larvae.

If the body waves of plaice larvae are compared with adult fish they are most like adult fish swimming in the subcarangiform mode (Breder, 1926). The amplitude against length along the body curve shows a non-linear increase in amplitude, the amplitude increasing more rapidly towards the tail. This indicates that inertial forces are exploited more in swimming than resistive forces, which would be rather inefficient since, at the Reynold's numbers occurring during the cruising-swimming of plaice, resistive forces should dominate.

It was shown above that the action of the pectoral fins would reduce lateral movements in the middle section of the body and move the point of minimum amplitude of the body waves posteriorly. This is the cause of the non-linear increase in amplitude. In the analyses carried out in this work the dorsal and anal fin have been

ignored and only a computed mid-line used. In the films the

edge of the dorsal fin could often be seen clearly. The dorsal

fin appears to have a wave passing down it in phase with the

body wave, a feature which has also been observed in adult plaice

(Aleev, 1963). Thus the dorsal and anal fins will tend to increase

the effective amplitude of movements in the middle of the body.

Turbulent boundary layer - another role for pectoral fins

The nature of water flow around a fish larva has already been

discussed. Frictional drag coefficient C_f is related to Reynold's

number but in different ways depending on whether a laminar or

turbulent boundary layer exists (Webb, 1975).

$$C_{f\ lam} = 1.33\ R_L^{-1/2}$$

$$C_{f\ turb} = 0.072\ R_L^{-1/5}$$

If $C_{f\ lamb}$ and $C_{f\ turb}$ are plotted against Reynold's number

(Fig. 33) a crossover point is seen at about 2×10^4. At Reynold's

numbers higher than this laminar flow is advantageous and many fish

have devices which help to maintain laminar flow (see review by

Webb, 1975). Below this crossover point the converse may be true.

Here an early transition to turbulent flow may be of great advantage

in reducing drag. At these Reynold's numbers a laminar layer would

be relatively thick and so viscous forces very large; a transition

Fig. 33. The effect of increasing Reynold's Number on the frictional drag coefficient C_f for an infinite flat plate. The effect of turbulent boundary layer reducing C_f at low Reynold's Numbers is shown.
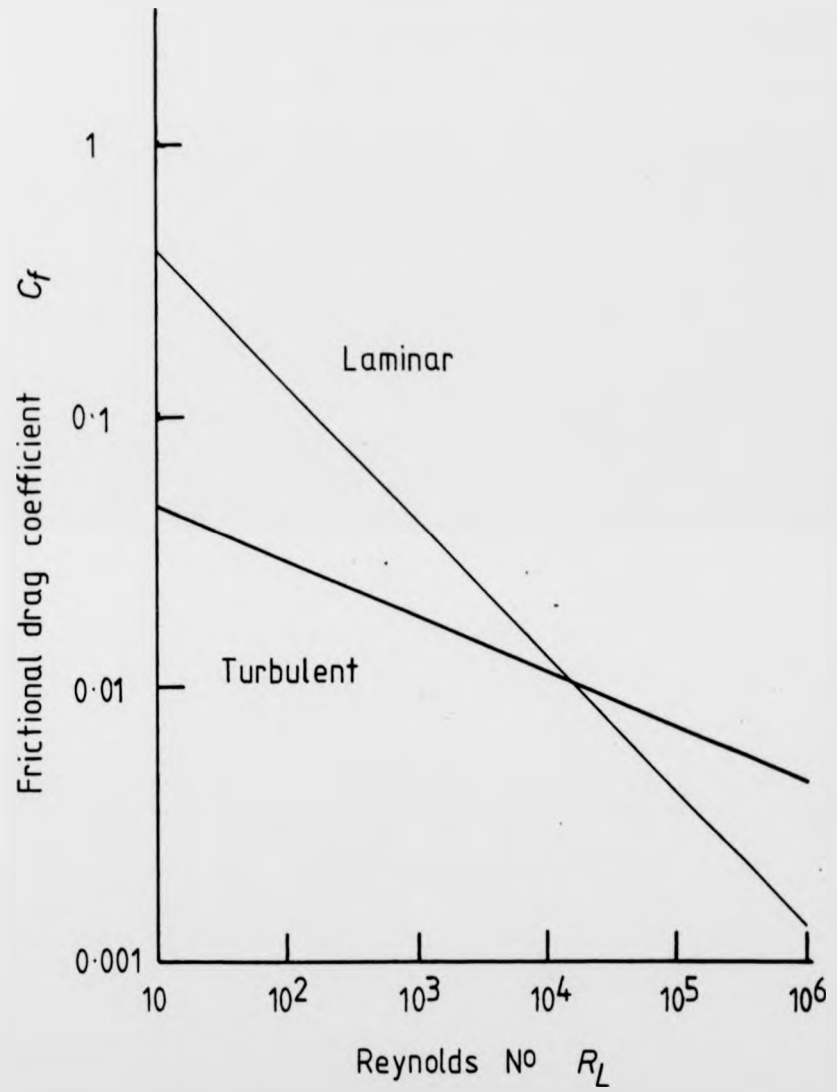
to turbulent flow would cause a reduction in the thickness of the boundary layer and so reduce viscous drag. Boundary layer thickness (δ) is given by:

$$\frac{\delta_{lam}}{a} \simeq 5.0\ R_L^{-1/2}$$

or $$\frac{\delta_{turb}}{a} \simeq 0.37\ R_L^{-1/5}$$

where a = distance along the body from the leading edge. At Reynold's numbers above $R_{L\ CRIT}$ a turbulent boundary layer would be thicker and also energy dissipation in the turbulence would add to drag.

The thickness of a plaice laminar boundary layer would be approximately 0.5 x a. Thus thickness δ at the base of the pectoral fins would be about 1 mm. The pectoral fins are about 1 mm long and hence occupy the whole of the thickness of the boundary layer. Their movements are therefore likely to disturb the boundary layer and create turbulence within it. This may cause a partial transition to turbulent boundary layer flow with a possible considerable reduction of frictional drag coefficient (Fig. 33). This reduction in drag is due to a reduction in boundary layer thickness and therefore less water will be influenced by the surface friction of the body.

Propulsive wave speed, swimming speed and propeller efficiency.

The speed of the propulsive wave *v* and tail beat frequency are not firmly linked to swimming speed *u* at cruising speeds in larvae as they are in adults. This means that u/v, found to decrease only slightly with increasing speed for adult fish (Videler and Wardle, 1978), actually increases with increasing speed in the larval plaice and herring. However u/v is much lower (0.2 to 0.4) than in adult fish where it is in the range 0.6 to 0.8.

Values of u/v may be used to calculate propeller efficiency η_p (Lighthill, 1960) provided that amplitude increases from near zero at the head to a maximum at the tail tip. Thus:

$$\eta_p = \tfrac{1}{2} (1 + u/v)$$

Using this formula η_p would be in the range 0.6 to 0.7 for plaice larvae or 0.8 to 0.9 for most adult fish. Webb (1977) used results obtained by C.C. Lindsey to make estimates of propeller efficiency for a wide range of sizes of fish. He showed that propeller efficiency was size-dependent and directly related to the length of the fish.

Prediction of ideal tail blade θ.

An earlier attempt to predict the ideal tail blade θ angle was made by Videler and Wardle (1978). They assumed that the ideal angle would be when the tail blade produced maximum thrust

directed along the x axis. Their Fig. 4 shows curves for

thrust P calculated from Lighthill's (1971) large amplitude

elongated body theory of fish locomotion.

Lighthill had derived a vector equation to predict the

propulsive forces produced by the body in two planes;

P along the x axis and Q perpendicular to P along the z axis:

$$P, Q = \left[- u_p \, m \, w \left(\frac{-\partial z}{\partial a}, \frac{\partial x}{\partial a} \right) + \frac{1}{2} \, m \, w^2 \left(\frac{\partial x}{\partial a}, \frac{\partial z}{\partial a} \right) \right]_{a = 0}$$

$$- \frac{d}{dt} \int_0^L m \, w \left(\frac{\partial z}{\partial a}, \frac{\partial x}{\partial a} \right) d \, a.$$

This equation follows the notation already used here with the

addition of w which is the velocity of the tail blade perpendicular

to its axis and u_p the velocity of the tail blade tangential to the

tail tip. m is the virtual mass of any slice of the body. In Lighthill's

notation a = 0 at the tail tip and a = L at the head; also his

coordinate system is lefthanded. Fig. 34 summarizes these terms

and their interaction.

This first term in the equation above is a force acting

perpendicular to the tail blade and the second term is a force

acting tangential to it. The third term is the integral of all the

accelerative forces produced by the wave of contraction on the whole

body. Videler and Wardle (1978) calculated P for various values of

Fig. 34.   Lighthill's model. The motion of the tail blade of

a fish is shown in A. The velocity of the tail tip

V is resolved into two components u tangential to the

tail blade and w normal to it. The angle θ between

the tail and the direction of motion and α the angle

of attack are shown. B shows the two forces produced

by the tail and the resulting force vector V which

can be resolved into two components, P thrust force

acting along the direction of motion and Q lateral

force which causes recoil (yaw) of the head. C the

special case when θ is such that T acts along the

direction of motion i.e. Q is zero.

A

Tail tip path

Tail blade

V

u

α

w

θ

Direction of motion

B

Tail tip path

½mw²

P

T

Q

umw
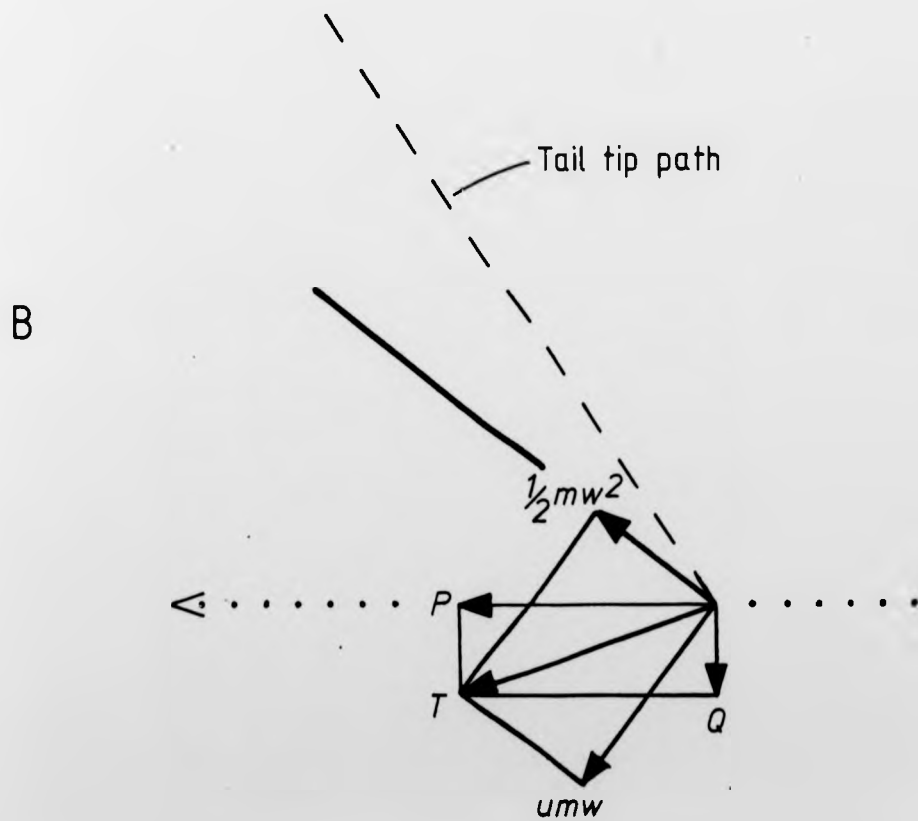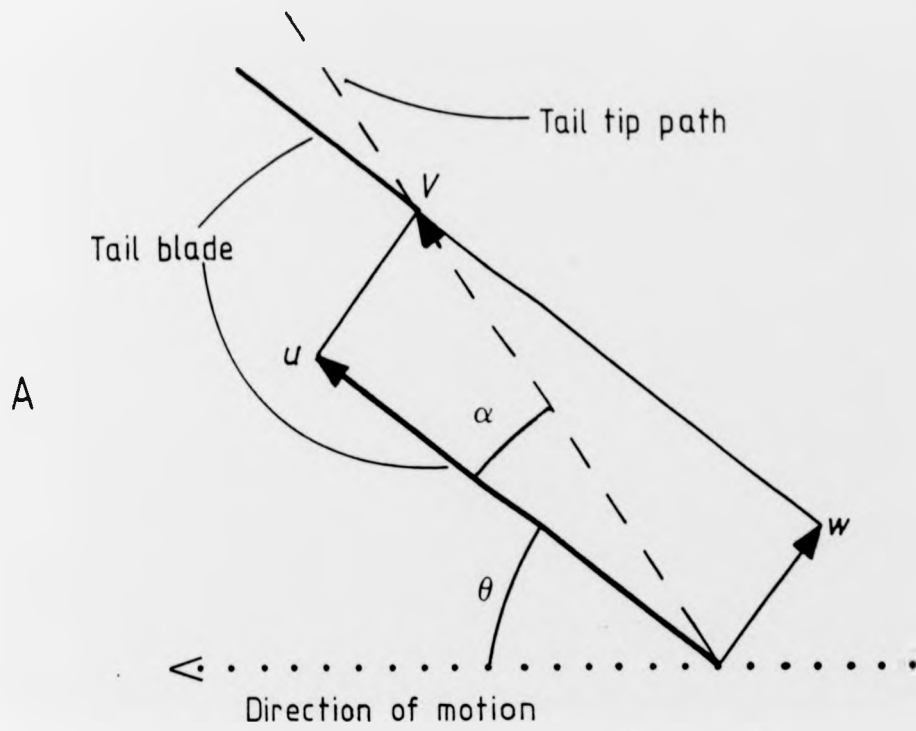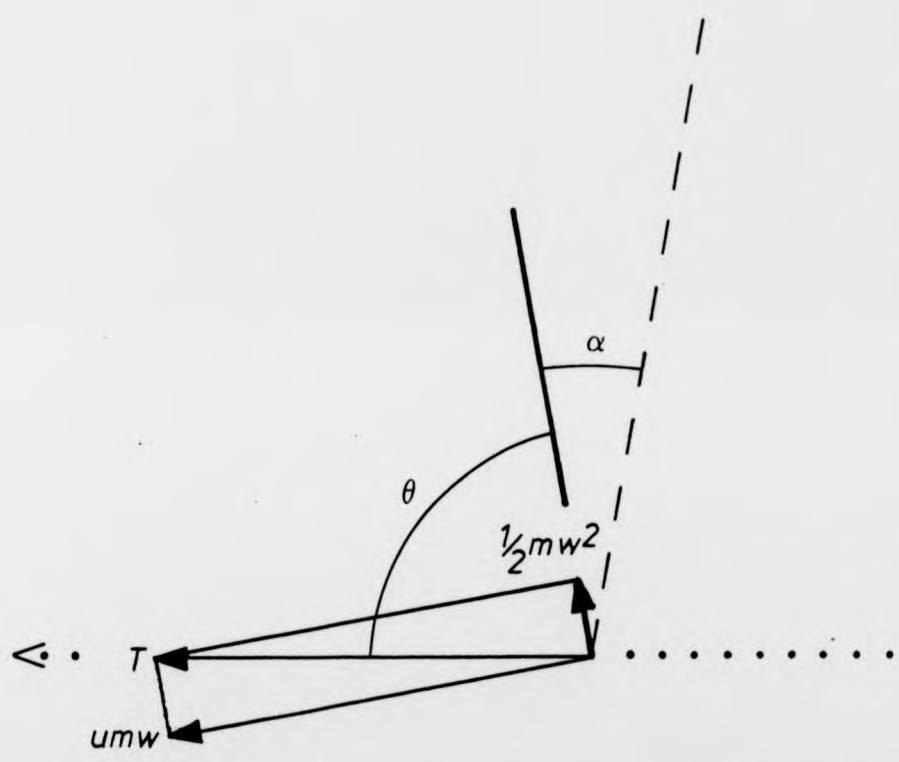
$\partial z/\partial t$, θ and $\partial x/\partial t$, without considering α, the angle of attack

of the tail blade, nor did they calculate Q, the side force

produced by the tail.

The ideal tail blade angle (θ) and direction of movement

($\theta + \alpha$) would be when Q is 0 and P is substantially positive.

To simplify this calculation we calculate $\dfrac{u_p mw}{P}$ and $1/2\ mw^2$ and then

using the equation as written we calculate the total force and its

direction relative to the tail blade as in Fig. 35. If this

direction becomes θ then Q will be zero. A constant tail tip

velocity is used and angle of attack varied to give different

values of u_p and w. Fig. 36 contains a plot of such a simulation.

θ is plotted for increasing values of between 0° and 90°. It

shows that as α increases the ideal θ decreases. The direction of

movement of the tail tip ($\alpha + \theta$) is also plotted and remains

greater than 90°, showing that the tail tip would have to move

slightly tailwards during the lateral stroke. Thrust force is also

included in the graph. The vertical line on the graph at 20°

indicates the possible limiting value of α, the angle of attack at

which the tail blade would 'stall'. This value (Webb, 1975) is taken

from the theory of aerofoils. At this stall angle the model would

no longer apply. In Viderler and Wardle's (1978) prediction, where

they concluded that θ should be 10° or less, α (which they did

not calculate) was between 30° and 61° where the model is not

likely to apply.

It is interesting that herring larvae come close to this

Fig. 35.   A plot of possible values of θ and α which result in
the special case when Q is zero (Fig. 34). In this
prediction a larva would have been swimming at a
speed of 40 mm.s^{-1}, with V = 0.12 mm.s^{-1} and
s = 0.004 m. The vertical pecked line indicates the
range of values of α to which the model may be limited.
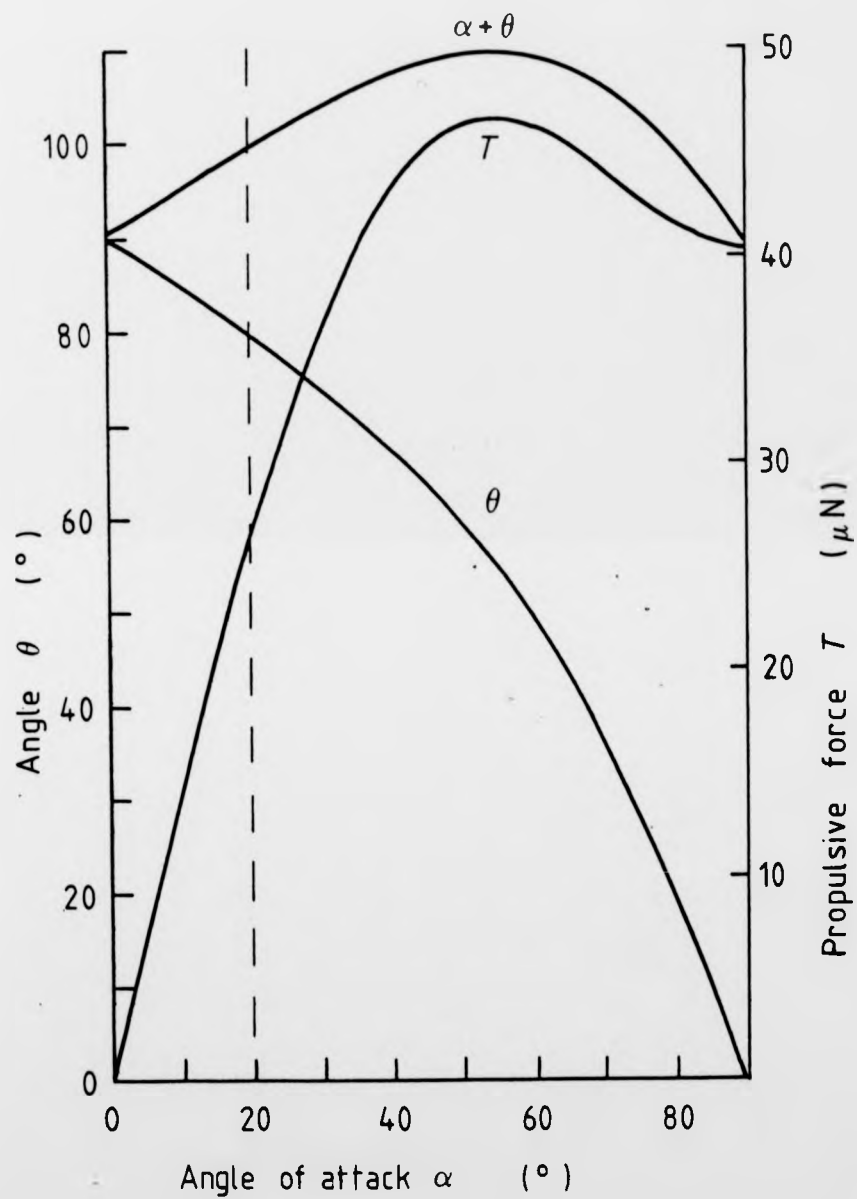
predicted ideal. During a tail beat the angle θ is close
to 90° during the fastest part of the stroke and the tail-tip
also has a negative $\partial x/\partial t$ for a substantial part of the stroke.
This must be a mechanism to reduce recoil, simply by minimizing
it at source, i.e. by reducing lateral forces

Model of larval fish swimming.

By fitting a standing wave equation to each of a series of
frames it has been possible to detect changes in wavelength and
speed of the propulsive wave within the tail beat cycle. The
shortening of body wavelength at the beginning of alternate tail
strokes may be seen as a way of transmitting the propulsive
effort of the anterior myotomes to the tail tip where propulsive
force acts on the water. Wardle and Videler (1980) suggest that
this transmission of effort may be facilitated by the combined
effects of muscle myosept structure and skin elasticity. The
wavelength shortening seen in rightward going strokes of the caudal
fin of a 22 mm larva in Fig. 31B combined with an acceleration of
the wave shown in Fig. 31D, may be a further way of helping this
necessary transmission of propulsive force. Electromyographical
evidence in adult tench (*Tinca tinca*) (see Blight, 1976, 1977)
has shown that contraction is not stimulated strictly in waves
but at certain phases of the tail beat cycle complete muscle blocks
are stimulated together either on the right or left side. Work by
Grillner and Kashin (1976) on various species, showed that waves of

contraction pass down the body at burst speeds but at cruising speeds there was considerable overlap in stimulation so that at just after the beginning of the tail stroke all the muscle on one side of the body would be stimulated to contract together. This simultaneous stimulation occurs at the beginning of the tail stroke, the same time that wavelength shortening is seen in herring larvae.

Distribution of red muscle in larval fish.

A distribution of red aerobic muscle fibres similar to that reported here has been described in larval zebra fish *Brachydanio rerio* by Waterman (1969) using SDHase staining and by van Raamsdonk et al. (1978) using immunological techniques. Both studies showed a single layer of red fibres in newly hatched larvae, developing to an adult distribution similar to that of adult herring.

Development of muscle and respiration.

The development of respiration in herring larvae was studied by de Silva (1973, 1974). Her results for gill and body surface area are plotted in Fig. 27, together with the percentage of red muscle. A vertical dashed line indicates the body length at which the adult distribution or red muscle fibres starts to develop. The gills develop very rapidly from a length of 22 mm onwards, the most rapid development occurring at around 30 mm. The maximum gill area to body weight ratio attained was 1.2 $mm^2.mg^{-1}$ at metamorphosis (length 35-40 mm). It thus appears that cutaneous respiration is

more important than gill respiration during most of the larval

stage. Gill respiration only becomes important when the gill

area has increased at a length of 25 mm. Up to this length,

the red muscle is distributed peripherally, enabling it to

utilise cutaneous respiration. Subsequently, new red fibres appear

away from the periphery but by this time gill respiration has been

established.

REFERENCES

Aleev, Yu.G. 1958.   Adaptation for movement and the turning
    ability of fish. Doklady Biol. Sci. (Transl.) 120, 299-302.

Aleev, Yu.G. 1963.   Function and Gross Morphology in Fish.
    Moscow. (Transl. from Russian, Isr. Program. Sci. Transl.
    No. 1773, Jerusalem, 1969).

Alexander, R. McN. 1969.   The orientation of muscle fibres in
    the myomers of fishes. J. mar. biol. Ass. U.K. 49, 263-290.

Arnold, G.P. 1969.   The orientation of plaice larvae
    (*Pleuronectes platessa* L.) in water currents. J. exp. Biol.
    50, 785-801.

Arnold, G.P. & Nuttall-Smith, P.B.N. 1974.   Shadow cinematography
    of fish larvae. Mar. Biol. 28, 51-53.

Aronson, W. & Pharmakis, T. 1962.   Enhancement of neotetrazoleum
    staining for succinic dehydrogenase activity with cyanide.
    Stain Technology 37, 321-

Bailey, K.M. & Batty, R.S. 1983.   A laboratory study of predation
    by *Aurelia aurita* on larval herring (*Clupea harengus*):
    experimental observations compared with model predictions.
    Mar. Biol. 74, (in the press).

Bainbridge, R. 1958.   The speed of swimming of fish as related
    to size and to the frequency and amplitude of the tail beat.
    J. exp. Biol. 35, 109-133.

Bainbridge, R. 1963.   Caudal fin and body movement in the
     propulsion of some fish.   J. exp. Biol. 40, 23-56

Batty, R.S. 1981.   Locomotion of plaice larvae.   Symp. zool.
     Soc. Lond. 48, 53-69.

Bishai, H.M. 1960.   The effect of water currents on the survival
     and distribution of fish larvae.   J. Cons. int. Explor. Mer.,
     25, 134-146.

Blake, R.W. 1979.   The mechanics of labriform locomotion I.
     Labriform locomotion in the Angelfish (*Pherophyllum eimekei*):
     an analysis of the power stroke.   J. exp. Biol. 82, 255-271.

Blake, R.W. 1980.   Mechanics of drag-based mechanisms of
     drag-based mechanisms of propulsion in aquatic vertebrates.
     Symp. zool. Soc. Lond. 48, 29-52.

Blaxter, J.H.S. 1962.   Herring Rearing-IV.   Rearing beyond the
     yolk-sac stage.   Mar. Res. Scot. 1962 No. 1.

Blaxter, J.H.S. 1968.   Rearing herring larvae to metamorphosis
     and beyond.   J. mar. biol. Ass. U.K. 48, 17-28.

Blaxter, J.H.S. & Staines, M.E. 1971.   Food searching potential
     in marine fish larvae.   In: Fourth European Marine Biology
     Symposium.(ed. D.J. Crisp), pp. 467-485.   Cambridge University
     Press.

Blight, A.R. 1976.   Undulatory swimming with and without waves of
     contraction.   Nature, Lond. 26, 352-354.

Blight, A.R. 1977.   The muscular control of vertebrate swimming
     movements.   Biol. Rev. 52, 181-218.

Boyar, H.C. 1961. Swimming speeds of Immature Atlantic Herring with reference to the Passamaquaddy tidal project. Trans. Am. Fish. Soc. 90, 21-26.

Breder, C.M. 1926. The locomotion of fishes. Zoologica (N.Y.) 4, 159-256.

Chayen, J., Bitensky, L., Butcher, R.G. & Poulter, L.W. 1969. A guide to practical histochemistry. Edinburgh: Oliver and Boyd, 261 p.

Culling, C.F.A. 1963. Handbook of histopathological techniques, 2nd edn. London: Butterworths, 553 p.

Currie, R.I., Blaxter, J.H.S. & Joyce, J. 1976. The aquarium at the Dunstaffnage Marine Laboratory. J. mar. biol. Ass. U.K. 56, 1049-1061.

Edgerton, H.E. 1977. Silhouette photography of small active subjects. J. Microsc. 110, 79-81.

Ehrlich, K.F. 1972. Morphometrical, behavioural and chemical changes during growth and starvation of herring and plaice larvae. Ph.D. Thesis : Stirling University.

Ehrlich, K.F. 1974. Chemical changes during growth and starvation of herring larvae. In : The Early Life History of Fish (ed. J.H.S. Blaxter), pp. 301-323. Berlin : Springer Verlag.

Everest, F.H. & Edmundson, E.H. 1967. Cold branding for field use in marking juvenile salmonids. Prog. Fish Cult. 29, 175-176.

Glova, G.J. & McInerey, J.E. 1977.   Critical swimming speeds of

coho salmon (*Oncorhynchus kisutch*) fry to smolt stages in

relation to salinity and temperature.   J. Fish. Res. Bd. Can.

34, 151-154.

Gray, J. 1968.   Animal Locomotion. London : Weidenfeld Nicolson,

479 p.

Gray, J. 1933.   The movement of fish with special reference to the

eel.   J. exp. Biol. 10, 88-104.

Gray, J. & Hancock, G.J. 1955.   The propulsion of sea-urchin

spermatozoa.   J. exp. Biol. 32, 802-814.

Gray, P. 1958.   Handbook of basic microtechnique.   New York :

McGraw-Hill, 252 p.

Grillner, S. & Kashin, S. 1976.   On the generation and performance

of swimming in fish.   In : Neural control of locomotion (ed.

R.M. Herman,   S. Grillner, P.S.G. Stein, & D.G. Stuart),

pp. 181-201. New York : Plenum.

Hertel, H. 1966.   Structure, form and movement. New York : Reinhold

Publishing Corp., 251 p.

Hora, S.L. 1935.   Ancient Hindu conception of correlation between

form and locomotion of fishes.   J. Asiatic Soc. Bengal. 1, 1-7.

Houde, E.D. 1969.   Sustained Swimming Ability of larvae of Walleye

(*Stizostedian vitreum vitreum*) and yellow perch (*Perca flavescens*).

J. Fish. Res. Bd. Can. 26, 1647-1659.

Hunter, J.R. 1972.   Swimming and feeding behaviour of larval anchovy

Engraulis mordax. Fish. Bull. U.S. 70, 821-838.

Kashin, S.M., and Smolyaninov, V.V. 1969. Concerning the Geometry of Fish Trunk muscles. Veprosy Ikhtiol. (transl.). 9, 923-925.

Laurence, G.C. 1972. Comparative swimming abilities of fed and starved larval largemouth bass (*Micropterus salmoides*). J. Fish Biol. 4, 73-78.

Lighthill, M.J. 1960. Note on the swimming of slender fish. J. Fluid. Mech. 9, 305-317.

Lighthill, M.J. 1969. Hydromechanics of aquatic animal propulsion. Ann. Rev. Fluid Mech. 1, 413-446.

Lighthill, M.J. 1971. Large-amplitude elongated-body theory of fish locomotion. Proc. R. Soc. B. 179, 125-138.

Lighthill, M.J. 1977. Mathematical theories of fish swimming. In : Fisheries Mathematics (ed. J.H. Steele), pp. 131-144. London : Academic Press.

Marey, E.J. 1895. Movement. London. 323 p.

Neave, D.A. & Batty, R.S. 1982. A simple method for measuring fish larvae using silhouette photography. Aquaculture 29, 165-168.

Pearse, A.G.E. 1968. Histochemistry, theoretical and applied. Vols 1 & 2. London: Churchill 759 pp.

Rosenthal, H. 1968. Schwimmverhalten und Schwimmgeschwindigkeit bei den Larven des Herings *Clupea harengus*. Helgoländer wiss. Meeresunters., 18, 453-486.

Rosenthal, H. and Hempel, G. 1969. Experimental studies in
feeding and food requirements of herring larvae. In : Symp.
Marine Food Chains, Univ. of Aarhus, Denmark 1968 (ed. J.H.
Steele), pp. 344-364. Edinburgh: Oliver and Boyd.

Ryland, J.S. 1963. The swimming speeds of plaice larvae. J. exp. Biol.
40, 285-299.

Shelbourne, J.E. 1956. The effect of water conservation on the
structure of marine fish embryos and larvae. J. mar. biol. Ass.
U.K. 35, 275-286.

de Silva, C.D. 1973. The ontogeny of respiration in herring and
plaice larvae. Ph.D. Thesis. Stirling University.

de Silva, C.D. 1974. Development of the respiratory system in
herring and plaice larvae. In : The Early Life History of Fish
(ed. J.H.S. Blaxter), pp. 465-485. Berlin : Springer-Verlag.

Teissier, G. 1948. La relation d'allometrie: sa signification
statistique et biologique. Biometrics 4, 14-48.

Van Raamsdonk, W., Pool, C.W. & te Kronne, G. 1978. Differentiation
of Muscle Fibre types in the teleost *Brachydanio rerio*. Anat.
Embryol. 153, 137-155.

Van Raamdonk, W., Van der Stelt, A., Diegenbach, P.C., Van de Berg, W.,
de Bruyn, H., van Dijk, J. & Mijzen, P. 1974. Differentiation
of the Musculature of the teleost *Brachydanio rerio*. I. Mytome
Shape and Movements in the Embryo. Z. Anat. Entwickl. Gesch.
145, 321-342.

Videler, J.J. 1981. Swimming movements, body structure and propulsion in cod *Gadus morhua*. Symp. zool. Soc. Lond. 48, 1-27.

Videler, J.J. & Wardle, C.S. 1978. New kinematic data from high speed cine film recordings of swimming cod (*Gadus morhua*). Neth. J. Zool. 28, 465-484.

Vlymen, W.J. III 1974. Swimming energetics of the larval anchovy *Engraulis mordax*. Fish. Bull. U.S. 72, 885-899.

Walker, M.G. & Pull, G.A. 1975. A survey of red and white muscle in marine fish. J. Fish. Biol. 7, 295-300.

Waterman, R.E. 1969. Development of the Lateral Musculature in the Teleost, *Brachydanio rerio*: A fine structural study. Am. J. Anat. 125, 457-494.

Wardle, C.S. 1975. Limit of fish swimming speed. Nature, Lond. 225, 725-727.

Wardle, C.S. & Reid, A. 1977. The application of large amplitude elongated body theory to measure swimming power in fish. In : Fisheries Mathematics (ed. J.H. Steele), 171-191. London : Academic Press.

Wardle, C.S. & Videler, J.J. 1980. Fish Swimming. In : Aspects of Animal Movement. (ed. H.Y. Elder & E.R. Trueman), pp. 125-150. London : Cambridge Univ. Press.

Webb, P.W. 1975. Hydrodynamics and Energetics of Fish Propulsion. Bull. Fish. Res. Board Can. 190, 159 p.

Webb, P.W. 1977. Effects of size on performance and
energetics of fish. In : Scale effects in animal locomotion
(ed. T.J. Pedley), pp. 315-331. London : Academic Press.

Weihs, D. 1980(a). Energetic significance of changes in swimming
modes during growth of larval anchovy Engraulis mordax. Fish.
Bull. U.S. 77, 597-604.

Weihs, D. 1980(b). Respiration and depth control as possible
reasons for swimming of northern anchovy, Engraulis mordax,
yolk-sac larvae. Fish. Bull. U.S. 78, 109-117.

Appendix 1 Digitiser

Introduction

The reasons for using a coordinate digitiser to analyse film of larval fish swimming have been outlined on pages 29-31. Coordinate digitisers are rather expensive computer peripherals (costing in the region of £3000 at the time this work was carried out) and could not be afforded for this project but it was realized that by using some existing hardware it might be practical to build our own in the laboratory. A Hewlett Packard 9825 desktop computer was already in use and was interfaced with a Hewlett Packard 6940B Multiprogrammer. The latter device is fitted with an analogue-to-digital converter and a relay switching card which together allow the computer to control the sampling of a number of independant analogue voltages in a data logger system. To obtain a digitiser all that was necessary was a means of translating pairs of x,y coordinates into voltages to input to the multiprogrammer.

Digitising Tablet

A plan view of the digitising tablet is shown in Fig. A1. Large pulleys (d) are attached to the shafts of each of the two single turn potentiometers (q). The cursor (c) is attached to the pulleys by two nylon cords (a) so that extension of the cords results in anticlockwise rotation of the left-hand potentiometer A and clockwise rotation of the right-hand

Fig. A1.   Plan view of the digitising tablet. d pulleys,

q potentiometers, c cursor, a nylon cord,

e elastic tensioning strap, r reference points,
p guide pins.

50 cm

potentiometer B.   The drive cords are kept in tension by an
elastic strap (e) which connects the two inner pulleys.   This
simple tensioning device results in an equal tension on the
two cords, biasing the cursor to the top of the tablet.

The drive cords run over the guide pins (p) to provide a
constant 'origin' for each cord; this is important for the
calculation of (x,y) coordinates from the two voltages A and
B which correspond to the lengths of the cords.   The 20 cm
diameter pulleys and the positions of the guide pins provide
a digitising area of 452 by 320 mm on the tablet.

Calibration and calculation of (x,y) coordinates

The geometry of the digitising area is set out in Fig. A2.
Two rectangles are shown; the outer one includes the two guide
pins and the inner one joins the four reference points.   The
squares share a common centre and diagonals, such that points
A^- and A^+ represent the minimum and maximum voltages for
potentiometer A respectively.   To calculate (x,y) coordinates
the values of A and B are adjusted after calibration to have
values 0 to 830.5 along the diagonals of the outside square.
Then x and y are calculated using Pythagoras' theorem.
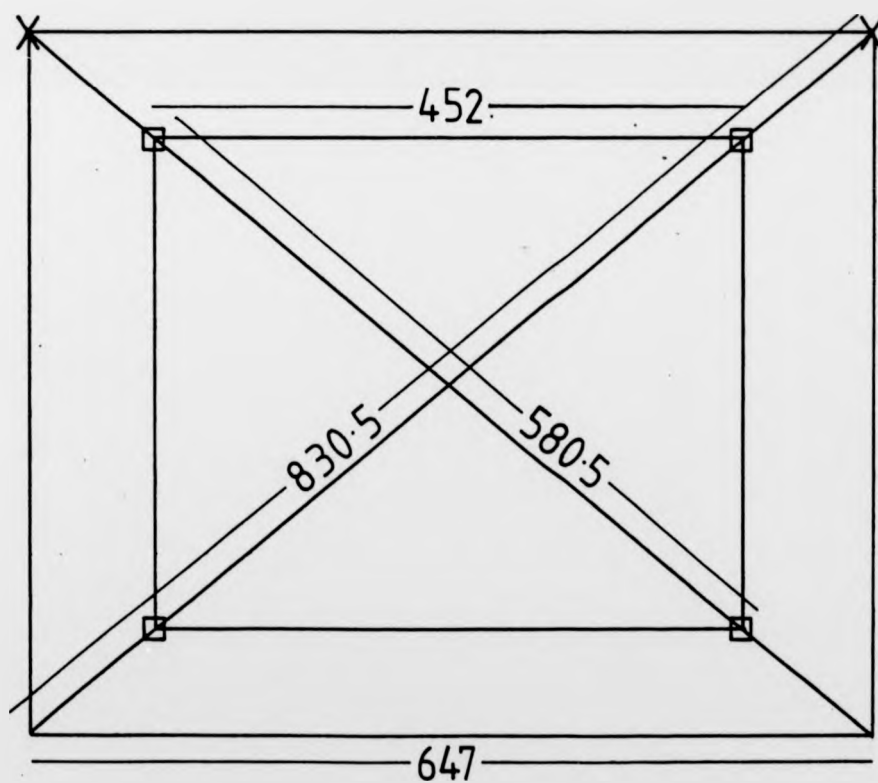
X   Guide pins

□   Reference marks

Fig. A2.   The digitising area: showing reference marks, guide

pins and dimensions used in computing coordinates.

It is seen that:-

$$a^2 = y^2 + x^2 \tag{1}$$

$$b^2 = y^2 + (647-x)^2 \tag{2}$$

rearranging (1) and substituting in (2) we get:-

$$b^2 = a^2 - x^2 + (647-x)^2 \tag{3}$$

which can be simplified to

$$b^2 = a^2 - 1294x + 418609 \tag{4}$$

now x can be found

$$x = (a^2 + 418609 - b^2)/1294 \tag{5}$$

rearranging (1) we get

$$y = \sqrt{a^2 - x^2} \tag{6}$$

and so y can be found.

Control

The means by which the computer demands readings and the operator offers them is as follows. The diagram in Fig. A3 summarises the system and its inter-connections. The computer demands readings from the operator by displaying a prompt and at the same time repeatedly tests for a voltage on the input line to the multiprogrammer which is connected to the footswitch. The operator signals to the computer that a reading is ready by pressing the footswitch. The computer responds by taking readings of the two potentiometer voltages from the multiprogrammer.

In addition to single points, complete curves and outlines can be recorded. This is achieved in a similar way but pairs of

Fig. A3.   The digitising tablet and it's connection

to the computer via the multiprogrammer.

9825S computer

computer

6940B

mutiprogrammer

digitizer
controller

platen

footswitch

9825S computer

computer

6940B

mutiprogrammer

digitizer
controller

platen
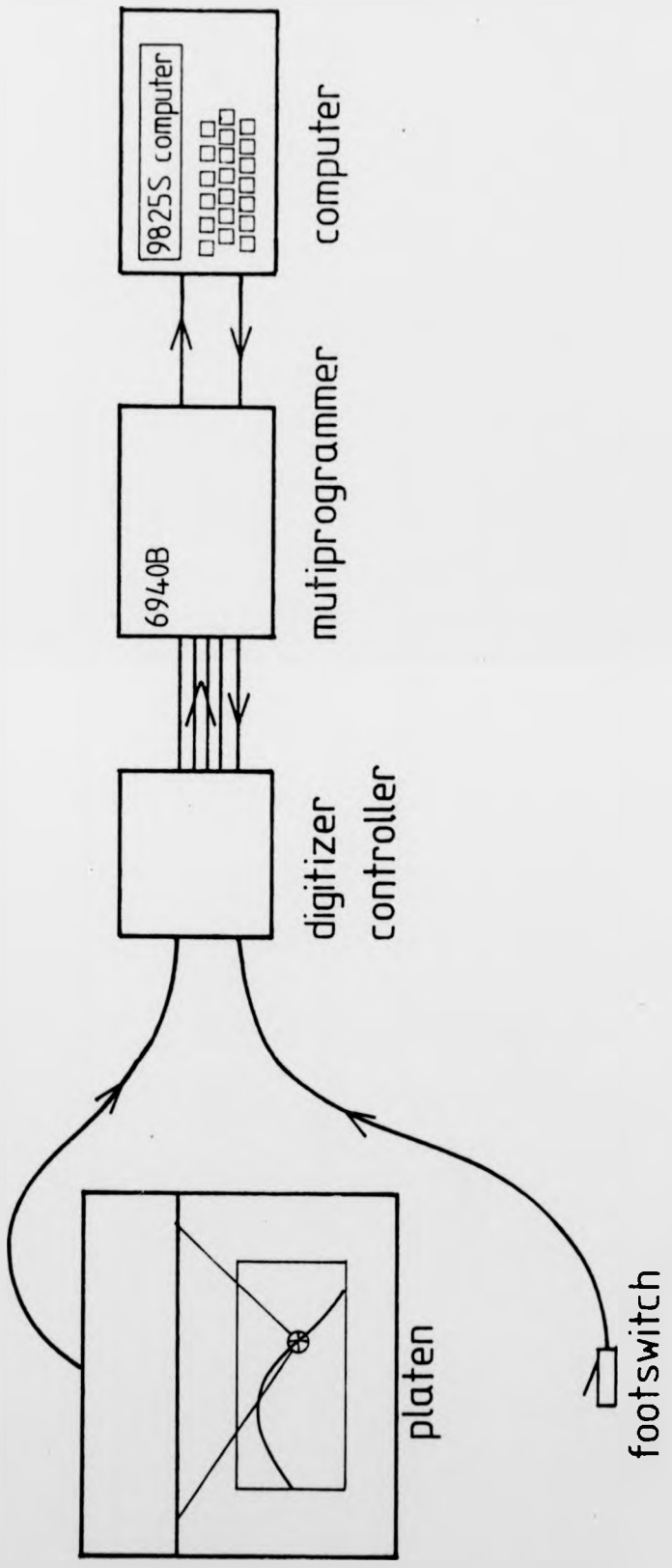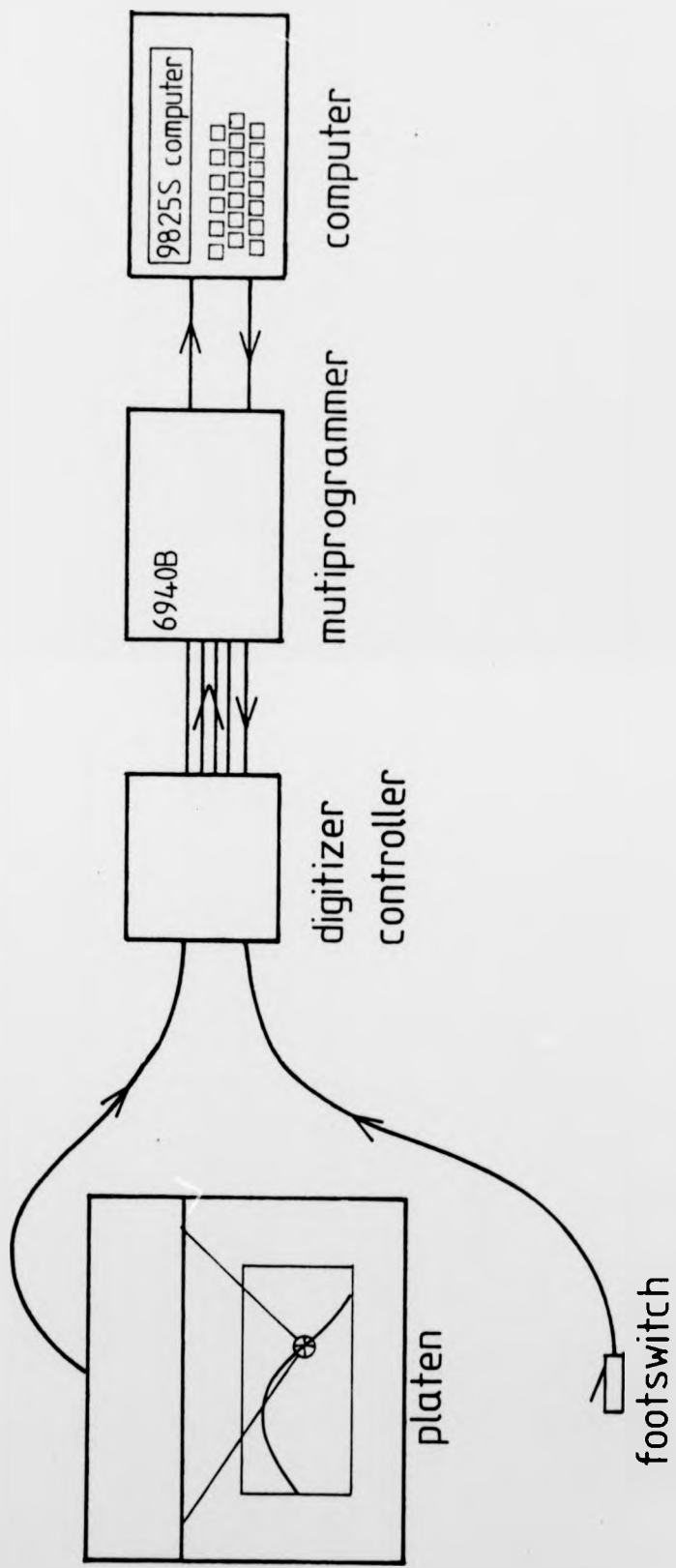
footswitch

(x,y) coordinates are recorded continuously whilst the footswitch is depressed. Software in the computer ensures a minimum spacing between points by ignoring any pair of coordinates within a preset radius of the previous pair.

A circuit diagram of the digitiser control box, which provides the stabilised power supplies for the potentiometers, processes the voltages and connects them to the multiprogrammer, is shown in Fig. A4. Fig. A5 shows the connections of the footswitch and potentiometers to sockets 1 and 2. Connections between the control box and the multiprogrammer relay card are shown in Fig. A6.

The main part of the control circuit is the sample and hold circuits which are needed when tracing lines. They ensure that, although the voltages A and B are tested sequentially they are recorded at the same instant despite a continually moving cursor.

Contact closures of the relay card switches are determined by a 16 bit word sent to the multiprogrammer by the computer. This allows the computer to control the process of taking a reading by sending a series of control words to the multiprogrammer.

Protocol

For single point recording the computer first sends a word (binary 00000011, octal 3) which allows the voltage from the footswitch to be tested. The computer then demands repeated voltage readings from the A/D card until this voltage is high when

Fig. A4.   Circuit diagram of the digitiser control circuit.

R1	100 kΩ
R2	10 kΩ
R3	1 kΩ preset
R4	19 kΩ
R5	220 Ω
R6	68 kΩ
R7	10 kΩ
R8	22 kΩ
R9	33 kΩ
R10	22 kΩ
R11	1 kΩ preset
R12	19 kΩ
R13	220 Ω
R14	68 kΩ
R15	10 kΩ preset
R16	22 kΩ
R17	33 kΩ
C1	0.1 μF polypropylene
C2	"
IC1	LF 398 (sample and hold circuit)
IC2	"
Skt1	standard jack socket
Skt2	5 pin DIN 240°
Skt3-7	4 mm socket
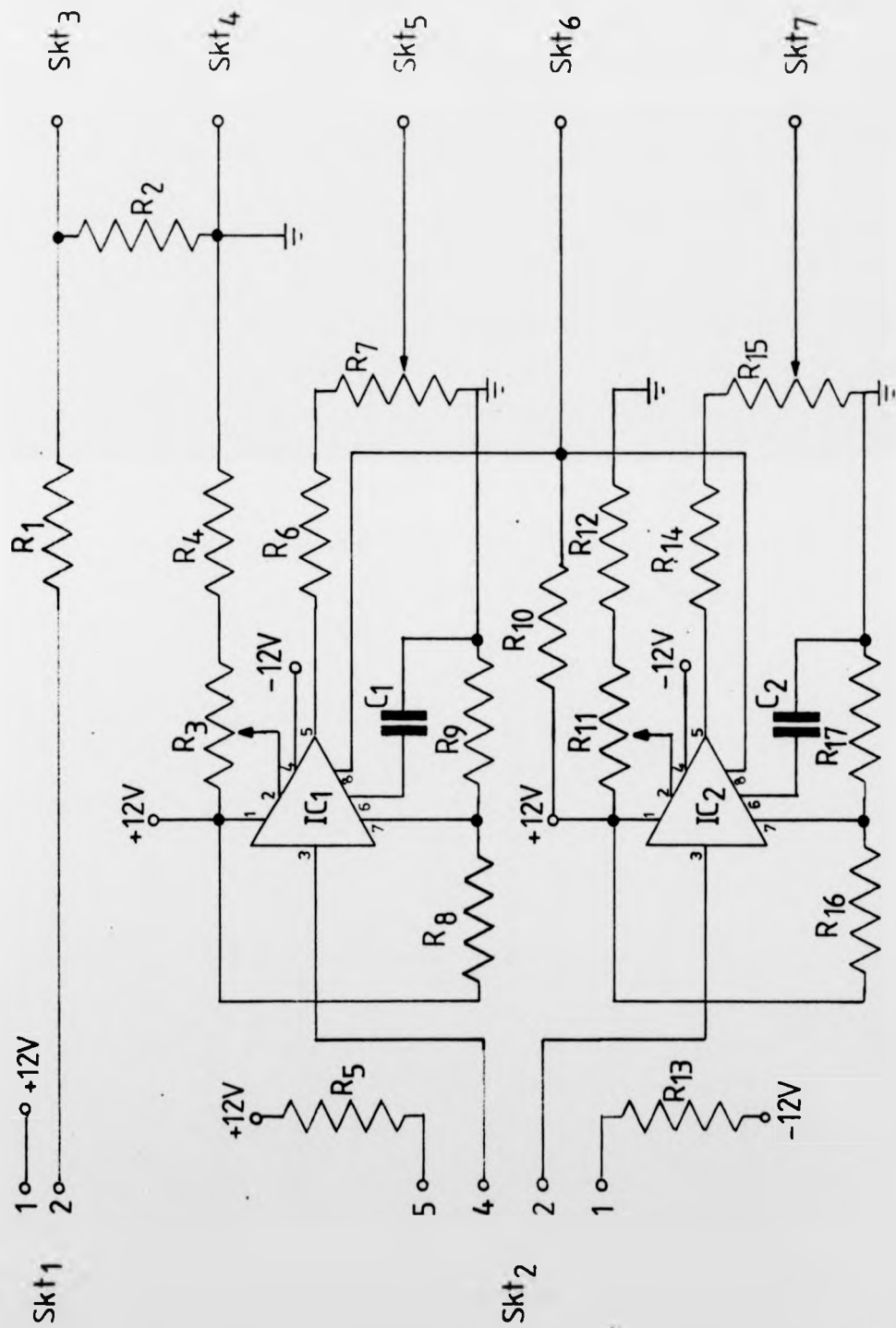
Fig. A5.   Connections of footswitch and potentiometers to

sockets 1 and 2.

footswitch

o 1

to Skt$_1$

o 2

potentiometers

o 5

5K0

o 4

to Skt$_2$

5K0

o 2

o 1
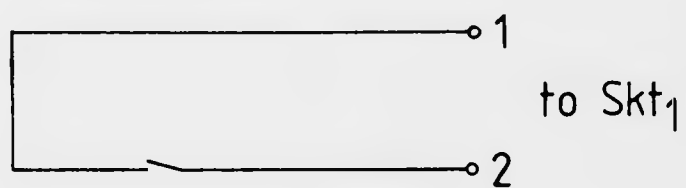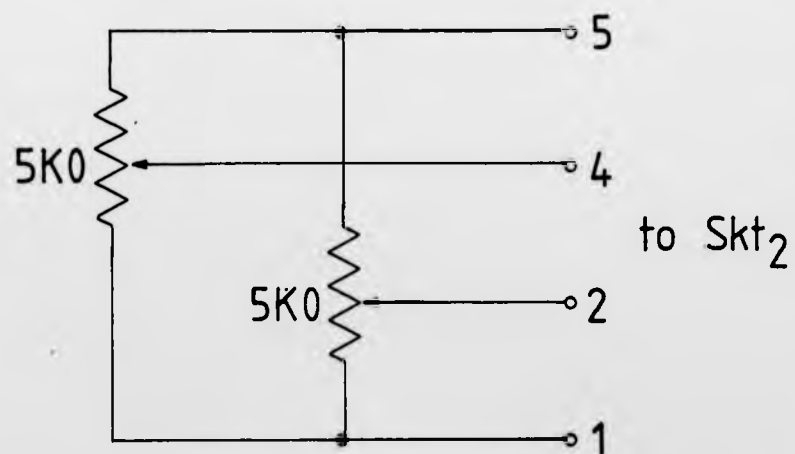
Fig. A6.   Connections between the control box and the

multiprogrammer relay card are shown together

with the bit numbers that close each relay.

Relay Switches
closed by bit no.
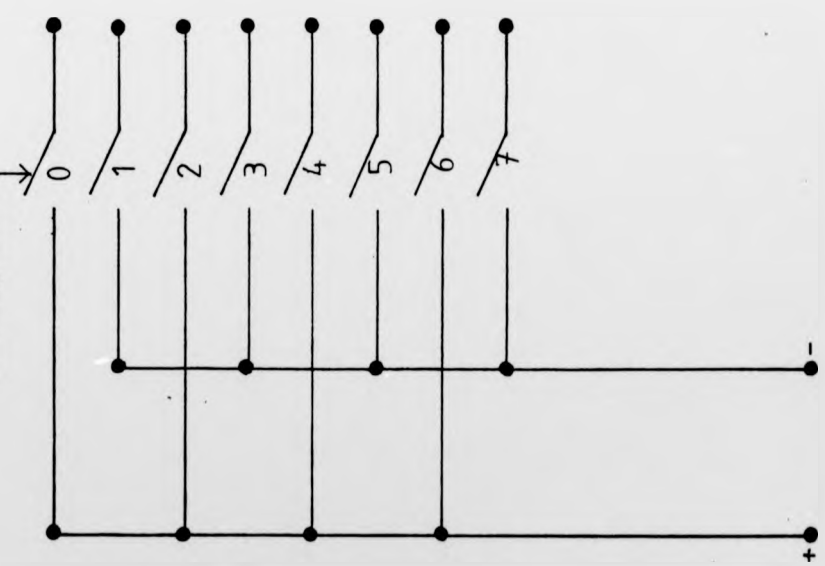
Bit	Wire Colour	Function
0	BLUE	'DATA READY' FOOTSWITCH TRIGGER.
1	RED	COMMON GROUND
2	GREEN	VOLTAGE A.
3	YELLOW	S/H CIRCUIT TRIGGER.
4	BLACK	VOLTAGE B.
5	WHITE	
6	BROWN	
7	PURPLE	

Wire Colour

To Multiprogrammer A/D Card.

another control word is sent. This control word (binary 00001110, octal 16) short circuits the sample and hold circuit trigger and so latches these circuits into the hold mode and connects the voltage from potentiometer A (at the instant the S/H circuit latched) to the A/D card. The computer now demands a voltage reading and repeats this process for potentiometer B using the control word, binary 00011010, octal 32. Finally all the relays are opened by sending the control word binary 00000000.

To make multiple readings a similar procedure is adopted. The series of instructions already described is repeated continuously while the footswitch is depressed.

Programming

The protocol used to take readings and the method used to calculate (x,y) coordinates have already been described. The software is written in HPL, the only language used on the 9825 computer. This programming language is in some ways similar to Basic but its execution is much faster; a feature which is very important in this application.

The programmes are written as subroutines which can be called from any programme. The following routines are used:-

```
"point"

"xy"

"point xy"

"line"

"calibrate"

"I1"

"I2"
```

APPENDIX 2 COMPUTER PROGRAMS

Digitiser Subroutines

```
0:  "line":0}r1}r2;cfg 4
1:  oni 9,"I1"
2:  otdr1}p1;if p1>2047;p1-4096}p1
3:  otdr2}p2;if p2>2047;p2-4096}p2
4:  cfg 1;sfg 2;3}r3
5:  moct;wtb 9,170160,60003;eir 9
6:  if p1=0;gto +8
7:  cll ´xy´(p1,p2)
8:  if p3=0;if p4=0;gto +2
9:  if \((p1-p3)^2+(p2-p4)^2)<r13;gto +5
10: p1}p3;p2}p4
11: p5+1}p5
12: if p0=1;cll ´convert´(p1,p2)
13: cll ´1´(p1,p2,p5)
14: jmp flg1
15: if flg5;gto +2
16: if flg2;gto -15
17: moct;wtb 9,170160,60000;mdec;ret
18: "I1":oni 9,"I2"
19: moct;wtb 9,170260,20000;mdec;eir 9
20: iret
21: "I2":moct;wti 0,11;wti 4,20000;rdi 4}r0;mdec
22: if r3=3;if r0>7700 or r0<10;wait 100;gto +6;if flg4;cfg 2;sfg 1;gto +7
23: if r3=3;16}r3;gto +4
24: if r3=16;r0}r1;32}r3;gto +3
25: if r3=32;r0}r2;3}r3
26: sfg 1,4;gto +3;if flg3;3}r3;gto +1
27: moct;wtb 9,170160,60000+r3;mdec
28: oni 9,"I1";eir 9
29: iret
30: "convert":cll ´polar´(p1-r8,p2-r9,p3,p4)
31: r11p4cos(p3-r10)}p1
32: r12p4sin(p3-r10)}p2;ret
33: "point":cfg 1;sfg 2;sfg 3;cfg 4
34: oni 9,"I1";3}r3
35: moct;wtb 9,170160,60003;eir 9
36: jmp not flg2
37: otdr1}p1;if p1>2047;p1-4096}p1
38: otdr2}p2;if p2>2047;p2-4096}p2
39: cfg 3;ret
40: "xy":(p1-r4)/r6*830.5}p1
41: (p2-r5)/r7*830.5}p2
42: (647^2-p2^2+p1^2)/1294}p3
43: 520-\(p1^2-p3^2)}p4
44: p3-97.5}p1;p4-78.5}p2;ret
```

```
45: "calibrate":
46: dsp "Top Left";cll 'point'(p1)
47: dsp "Bottom Left";cll 'point'(0,p4)
48: dsp "Bottom Right";cll 'point'(p2)
49: dsp "Top Right";cll 'point'(0,p3)
50: fxd 0;dsp "Amin",p1,"Amax",p2,"Bmin",p3,"Bmax",p4;stp
51: .2153(p2-p1)}p5;.2153(p4-p3)}p6
52: p1-p5}r4;p3-p6}r5
53: p2-p1+2p5}r6;p4-p3+2p6}r7;ret
54: "coordinate":
55: dsp "Origin";cll 'point'(r8,r9);cll 'xy'(r8,r9)
56: dsp "x axis reference";cll 'point'(p1,p2);cll 'xy'(p1,p2)
57: dsp "y axis reference";cll 'point'(p3,p4);cll 'xy'(p3,p4)
58: ent "enter x scale",r11,"enter y scale",r12;if flg13;1}r11}r12
59: cll 'polar'(p1-r8,p2-r9,r10,p5)
60: cll 'polar'(p3-r8,p4-r9,p7,p6)
61: p7-r10}p7;if p7<0;-p7-180}p7
62: if p7>89;if p7<91;gto +2
63: beep;dsp "not square xoy=",p7;stp
64: if not flg13;r11/p5}r11;r12/p6}r12;cfg 13
65: ret
66: "pointxy":cll 'point'(p1,p2);cll 'xy'(p1,p2)
67: if p0=3;cll 'convert'(p1,p2)
68: ret
69: "polar":if p1=0;90}p3;gto +4
70: if p2=0;0}p3;gto +2
71: atn(p2/p1)}p3
72: if p1<0;180+p3}p3;gto +3
73: if p2<0;360+p3}p3
74: if p3=450;270}p3
75: \(p1^2+p2^2)}p4;ret
*25684
```

HPL Program for digitising herring outlines

```
0: "REDGE2":
1: avd
2: dim A$[3],D$[17,55],B$[8],X[2,200],Y[2,200]
3: ent "Track?",T,"First file no?",H,"scale factor?",S,"Resolution",r13
4: H-1}Q
5: cll 'calibrate'
6: "R":A+1}A
7: Q+1}Q;if Q>129;0}Q;T+1}T;if T=2;beep;dsp "Change tape";0}T
8: fxd 0
9: prt "N=",A,"F=",Q,"T=",T
10: if T=0;trk 0
11: if T=1;trk 1
12: dsp "ref 1";cll 'pointxy'(C,D)
13: dsp "ref 2";cll 'pointxy'(E,F)
14: dsp "upper edge";cfg 6;cll 'line';pen
15: dsp "lower edge";sfg 6;cll 'line';pen
16: lbl A
17: prt "M=",M,"N=",N;spc 1
18: ent "OK?",A$;if cap(A$)="NO";A-1}A;Q-1}Q;gto "R"
19: for I=1 to 17
20: "      "}D$[I,1,5];str(I)}B$[1];B$[2,len(B$)]}D$[I,6-len(B$)];" "}D$[I,5]
21: next I
22: for I=6 to 40;" "}D$[1,I,I];next I
23: fxd 2
24: str(C)&"      "}D$[1,14-len(str(C))]
25: str(D)&"      "}D$[1,22-len(str(D))]
26: str(E)&"      "}D$[1,30-len(str(E))]
27: str(F)&"      "}D$[1,38-len(str(F))]
28: str(S)}D$[1,46-len(str(S))]
29: 0}P
30: for O=1 to 9 by 8
31: P+1}P
32: 0}K
33: for I=1 to 4
34: for J=6 to 54 by 2
35: K+1}K
36: prnd(KM/100,0)}L;if L=0;1}L
37: X[P,L]*10}X
38: Y[P,L]*10}Y
39: cll 'encode2'(X)
40: A$}D$[I+O,J,J+1]
41: cll 'encode2'(Y)
42: A$}D$[I+4+O,J,J+1]
43: next J
44: next I
45: N}M
46: next O
```

```
47: rcf Q,D$;vfy Z;if Z=1;jmp 0
48: ent "any more frames?",A$
49: if cap(A$)="YES";gto "R"
50: fxd 0
51: spc 4;prt "No. of files",A,"Last file",Q,"Track",T;spc 4
52: end
53: "1":if flg6;2}p4;p3}N;gto +3
54: 1}p4;p3}M
55: if p3=1 and p4=1;scl 0,450,p2-30,p2+270;30}Z
56: p1}X[p4,p3]
57: p2}Y[p4,p3];plt p1+1.5U,p2+(A-V-1)30;ret
58: "encode2":if p1=0;gto +3
59: abs(int(p1))}p2
60: p2/94-(frc(p2/94)}p3)}p2;94p3}p3
61: char(p2+33)}A$[1,1]
62: char(p3+33)}A$[2,2]
63: ret
64: "decode2":
65: num(A$[1,1])-33}p2
66: num(A$[2,2])-33}p3
67: 94p2+p3}p1
68: ret
*4452
```

HPL Program for digitising plaice outlines including pectoral fins

```
0: "PLAICE EDGE":
1: avd
2: dim A$[3],B$[8],X[200],Y[200],X$[4,100],Y$[4,100],W[4],Z[4]
3: ent "Track?",T,"First file no?",H,"scale factor?",S,"Resolution",r13
4: H-1}Q
5: cll ´calibrate´
6: "R":A+1}A
7: Q+1}Q;if Q>129;0}Q;T+1}T;if T=2;beep;dsp "Change tape";0}T
8: fxd 0
9: prt "N=",A,"F=",Q,"T=",T
10: if T=0;trk 0
11: if T=1;trk 1
12: dsp "ref 1";beep;cll ´pointxy´(C,D)
13: dsp "ref 2";beep;cll ´pointxy´(E,F)
14: cll ´polar´(E-C,F-D,W,R)
15: dsp "left edge";beep;1}B;cll ´line´;pen
16: 50}N;cll ´sort´
17: dsp "right edge";beep;2}B;cll ´line´;pen
18: 50}N;cll ´sort´
19: dsp "left fin";beep;3}B;cll ´line´;pen
20: 25}N;cll ´sort´
21: dsp "right fin";beep;4}B;cll ´line´;pen
22: 25}N;cll ´sort´
23: dsp "tail";beep;cll ´pointxy´(W[1],Z[1])
24: dsp "head";beep;cll ´pointxy´(W[2],Z[2])
25: dsp "l pectoral";beep;cll ´pointxy´(W[3],Z[3])
26: dsp "r pectoral";beep;cll ´pointxy´(W[4],Z[4])
27: for I=1 to 4
28: cll ´polar´(W[I]-C,Z[I]-D,G,R);cll ´rect´(W[I],Z[I],G-W,R)
29: next I
30: ent "OK?",A$;if cap(A$)="NO";A-1}A;Q-1}Q;gto "R"
31: rcf Q,X$,Y$,W[*],Z[*];vfy Z;if Z=1;jmp 0
32: ent "any more frames?",A$
33: if cap(A$)="YES";gto "R"
34: fxd 0
35: spc 4;prt "No. of files",A,"Last file",Q,"Track",T;spc 4
36: end
37: "sort":
38: fxd 2
39: 0}P
40: P+1}P
41: for K=1 to N
42: prnd(KM/N,0)}L;if L=0;1}L
43: X[L]}X
44: Y[L]}Y
45: cll ´polar´(X-C,Y-D,G,R);cll ´rect´(X,Y,G-W,R)
46: fti (10X)}X$[B,2K-1,2K]
47: fti (10Y)}Y$[B,2K-1,2K]
48: next K
49: ret
```

```
50: "1":
51: p3}M
52: if p3=1;scl 0,450,p2-30,p2+270;30}Z
53: p1}X[p3]
54: p2}Y[p3];plt p1+1.5U,p2+(A-V-1)30;ret
55: "polar":if p1=0;90}p3;gto +4
56: if p2=0;0}p3;gto +2
57: atn(p2/p1)}p3
58: if p1<0;180+p3}p3;gto +3
59: if p2<0;360+p3}p3
60: if p3=450;270}p3
61: \(p1^2+p2^2)}p4;ret
62: "rect":p4cos(p3)}p1
63: p4sin(p3)}p2
64: ret
*6003
```

HPL Program for computing centre lines

```
0: "HSPINE":
1: ent N,F
2: dim D$[17,80],W[4,50],A$[2]
3: dim L[50],A[N,2,0:10]
4: fxd 0
5: F-1}H
6: for I=1 to N
7: H+1}H
8: ldf H,D$
9: val(D$[1,6,13])}r1
10: val(D$[1,14,21])}r2
11: val(D$[1,22,29])}r3
12: val(D$[1,30,37])}r4
13: val(D$[1,38,45])}S
14: cll 'polar'(r3-r1,r4-r2,r5,r6)
15: 0}r12
16: for J=1 to 9 by 8
17: 0}r11;r12+2}r12
18: for L=1 to 4
19: for K=6 to 54 by 4
20: r11+1}r11
21: D$[L+J,K,K+1]}A$;cll 'decode2'(X);X/10}X
22: D$[L+J+4,K,K+1]}A$;cll 'decode2'(Y);Y/10}Y
23: cll 'polar'(X-r1,Y-r2,V,U);cll 'rect'(X,Y,V-r5,U)
24: X*S/r6}W[r12-1,r11];Y*S/r6}W[r12,r11]
25: if K=54;if L=1 or L=3;r11-1}r11
26: next K
27: next L
28: next J
29: for J=1 to 50
30: W[1,J]+.5(W[3,J]-W[1,J])}W[3,J];W[2,J]+.5(W[4,J]-W[2,J])}W[4,J]
31: next J
32: W[3,1]}W[1,1];W[3,50]}W[1,50];W[4,1]}W[2,1];W[4,50]}W[2,50]
33: for J=2 to 49
34: .25(W[3,J-1]+2W[3,J]+W[3,J+1])}W[1,J]
35: .25(W[4,J-1]+2W[4,J]+W[4,J+1])}W[2,J]
36: next J
37: W[1,1]}P;W[1,2]}X;W[2,1]}Q;W[2,2]}Y
38: for J=3 to 48
39: (P+2X+3(W[1,J]}X)+2W[1,J+1]+W[1,J+2])/9}W[1,J]
40: (Q+2Y+3(W[2,J]}Y)+2W[2,J+1]+W[2,J+2])/9}W[2,J]
41: X}P;Y}Q
42: next J
43: 0}L
44: for J=1 to 50;L+\(W[1,J]^2+W[2,J]^2)}L}L[J];next J
45: for J=1 to 50;L[J]/L}L[J];next J
46: W[1,1]}A[I,1,0];W[2,1]}A[I,2,0]
```

```
47: for A=.1 to 1 by .1
48: 0}J
49: J+1}J;jmp L[J]>=A
50: if L[J]=A;W[1,J]}A[I,1,10A];W[2,J]}A[I,2,10A];gto +4
51: L[J]-A}D
52: W[1,J]-(W[1,J]-W[1,J-1])*D/(L[J]-L[J-1])}A[I,1,10A]
53: W[2,J]-(W[2,J]-W[2,J-1])*D/(L[J]-L[J-1])}A[I,2,10A]
54: next A
55: next I
56: cll 'regression'(11N,B,R,Z);fxd 4;prt B,R,Z
57: cll 'polar'(1,B,T)
58: for A=0 to 10
59: 0}M
60: for I=1 to N
61: cll 'polar'(A[I,1,A],A[I,2,A]-Z,U,V);cll 'rect'(A[I,1,A],A[I,2,A],U-T,V)
62: next I
63: next A
64: dsp "insert tape";stp
65: ent "track no.",T,"file no.",F
66: trk T;rcf F,A[*]
67: end
68: "polar":if p1=0;90}p3;gto +4
69: if p2=0;0}p3;gto +2
70: atn(p2/p1)}p3
71: if p1<0;180+p3}p3;gto +3
72: if p2<0;360+p3}p3
73: if p3=450;270}p3
74: \(p1^2+p2^2)}p4;ret
75: "rect":p4cos(p3)}p1
76: p4sin(p3)}p2
77: ret
78: "X":if p1=1;ret A[1,1,0]
79: int((p1-1)/11)}p2;p1-11p2-1}p3;p2+1}p2;ret A[p2,1,p3]
80: "Y":if p1=1;ret A[1,2,0]
81: int((p1-1)/11)}p2;p1-11p2-1}p3;p2+1}p2;ret A[p2,2,p3]
82: "regression":
83: 0}p4}p5}p6}p7}p8}p9}p10
84: p4+1}p4
85: 'X'(p4)}p2;'Y'(p4)}p3
86: p6+p2}p6;p8+p3}p8
87: p7+p2^2}p7;p9+p3^2}p9
88: p10+p2p3}p10
89: if p4#p1;gto -5
90: p9-p8^2/p1}p9
91: p7-p6^2/p1}p7
92: p10-p6p8/p1}p10
93: p10/p7}p2
94: abs(p10/\(p7p9))}p3
95: p8/p1}p12;p6/p1}p11
```

```
96:  p12-p2*p11}p4
97:  p10^2/p7}p5
98:  p9-p5}p6
99:  \(p6/(p1-2)/p7)}p7
100: \(p6/(p1-2)/p1)}p8
101: p11}p9;p12}p10
102: ret
103: "decode2":
104: num(A$[1,1])-33}p2
105: num(A$[2,2])-33}p3
106: 94p2+p3}p1
107: ret
*30990
```

Fortran Program for fitting larval fish swimming model, with

tail as an arc of constant radius.

```
C     BENDY2 IS A PROGRAMME TO FIT BENDY2 MODEL TO MANY FRAMES
      COMMON/FISH/ X(100),Z(100),A(100),PED
      INTEGER N,IBOUND,IW(15),LIW,LW,IFAIL,FIRST,LAST
      DOUBLE PRECISION BL(6),BU(6),XC(6),F,W(150),PIE
      IBOUND=0
      LIW=15
      LW=150
      N=6
      WRITE(6,70)
      READ(5,61)FIRST
      WRITE(6,71)
      READ(5,61)LAST
      WRITE(6,72)
      READ(5,69)PED
      PIE=3.1415927
      DO 20 I=1,N
      READ(9,60)BL(I),BU(I),XC(I)
      IF(I.GT.2)GOTO 20
      BL(I)=BL(I)*PIE/180
      BU(I)=BU(I)*PIE/180
      XC(I)=XC(I)*PIE/180
   20 CONTINUE
      DO 100 J=1,LAST
      READ(9,61)IFRAME
      DO 10 I=1,100
      READ(9,60)A(I),X(I),Z(I)
   10 CONTINUE
      IF(J.LT.FIRST)GOTO 100
      IFAIL=0
      GOTO 51
   50 XC(4)=0.1
   51 CALL E04JAF(N,IBOUND,BL,BU,XC,F,IW,LIW,W,LW,IFAIL)
      IF(XC(4).EQ.1.0D0)GOTO 50
      WRITE(6,62)IFAIL
      WRITE(6,63)J,XC(1),XC(2),XC(3),XC(4),XC(5),XC(6),F
      WRITE(10,63)J,XC(1),XC(2),XC(3),XC(4),XC(5),XC(6),F
  100 CONTINUE
      STOP
   60 FORMAT(3F10.5)
   61 FORMAT(I5)
   62 FORMAT(7H IFAIL=,I2)
   69 FORMAT(F5.3)
   70 FORMAT(11H       FIRST)
   71 FORMAT(11H        LAST)
   63 FORMAT(I5,6F10.5,E15.4)
   72 FORMAT(11H         PED)
      END
```

```
      SUBROUTINE FUNCT1(N,XC,FC)
      COMMON/FISH/ X1(100),Z1(100),A1(100),PED
      INTEGER N,I
      DOUBLE PRECISION FC,XC(N),A,F,X,Z,SSQ,T,THETA,THETAP
      T=6.2831853
      Z=0
      X=0
      P=0
      SSQ=0
      DO 10 I=1,100
      A=A1(I)
      F=A1(I)-P
      IF(A.GT.PED)GOTO 20
      THETA=XC(1)+(XC(2)+XC(3)*A+XC(4)*A*A)*SIN(T*A/XC(5)-T*XC(6))
      THETAP=THETA
      GOTO 30
   20 THETA=THETAP+10.0D0*XC(7)*(A-PED)
   30 X=X+F*COS(THETA)
      Z=Z+F*SIN(THETA)
      P=A1(I)
   10 SSQ=SSQ+(X-X1(I))**2+(Z-Z1(I))**2
      FC=SSQ
      RETURN
      END
```

APPENDIX 3

"Locomotion of Plaice Larvae"

Symp. zool. Soc. Lond. (1981) No. 48, 53-69.

Locomotion of Plaice Larvae

R. S. BATTY

Scottish Marine Biological Association, Dunstaffnage
Marine Research Laboratory, P.O. Box 3, Oban, Argyll, Scotland

SYNOPSIS

The locomotion of larval plaice is demonstrated using a new technique — silhouette cinematography. This method, which uses no lenses, gives a very high contrast which is necessary to photograph the almost transparent fins of fish larvae.

Kinematic analyses of cruising speed swimming from the films show many differences from adult swimming. The pectoral fins are used together with body waves at cruising speeds, but pectoral fins are not important in producing propulsive thrust. Their purpose is to counteract recoil caused by lateral tail movements and therefore prevent yaw of the head. This is achieved by synchronized tail and fin movements with a 180° phase difference between the strokes of the left and right pectoral fins. Body wave speed v and swimming speed u were measured and show low values of u/v (0.2 to 0.4) which are positively correlated with swimming speed. Other parameters of the body waves (wavelength, amplitude, frequency) were also measured.

Recordings of burst speeds showed very high tail beat frequencies and a change in swimming style. The pectoral fins are no longer used at these speeds, at which the wavelength of the body wave appears to increase.

INTRODUCTION

The kinematics and hydrodynamics of adult fish swimming have been extensively studied by biologists and physical scientists. This effort, which has been concentrated on undulatory propulsion, has been reviewed by Gray (1968) and Webb (1975). "Paddling" has received much less attention, which is surprising since its use for slow swimming speeds and manoeuvering is so widespread, but it is the subject of another paper in this volume (Blake, this volume).

Little is known, however, about the kinematics of larval fish swimming. This is not so surprising when it is realized that, owing to the transparency of the larvae, special techniques have to be employed to photograph their movements (Hunter, 1972; Arnold & Nuttall-Smith, 1974). Most attention has been given to clupeoid larvae, either

anchovy (*Engraulis mordax*) by Hunter (1972) and Vlymen (1974), or herring (*Clupea harengus*) by Rosenthal (1968) and Rosenthal & Hempel (1969). Clupeoid larvae are typical of one group of larvae that have relatively long slender bodies. Other larvae, with shorter, deeper bodies, have not been studied at all. The plaice larva (*Pleuronectes platessa* L.) is typical of this shorter, deeper body shape. This species is bilaterally symmetrical on hatching at a length of 5 mm and during the larval stages until it metamorphoses at a length of approximately 12 mm to lie on the left side.

Preliminary work with plaice larvae had shown that they swim with body undulations and by moving their pectoral fins, a type of swimming that turbot and lemon sole larvae also employ, which indicates that this may be typical of all flatfish larvae. This chapter describes a new photographic technique called silhouette cinematography which has been used to make a kinematic analysis of the swimming of plaice larvae.

METHODS

Source of Animals

Eggs were stripped from a brood stock kept in the laboratory and fertilized artificially. The eggs were incubated and larvae reared to metamorphosis in 20-litre round black plastic tanks. Temperature was not controlled and the ambient sea water temperature in the aquarium rose from 6 to 12°C during the season. Larvae were fed on a mixture of *Artemia salina* nauplii and natural plankton.

Post yolksac larvae of 7–11 mm body length were used for these experiments.

Silhouette Cinematography

Preliminary work, using closed circuit television and a "Scotchlite" background illumination technique similar to that used by Wardle & Reid (1977), showed that the pectoral fins were used simultaneously with body movements. These fins are nearly transparent and were not always clearly visible using this technique.

Edgerton (1977) had shown that high speed silhouette photography, a simple technique using no lenses, could give high resolution photographs of small rapidly moving subjects. This method would, in theory, give the highest possible contrast and was thought to be the ideal method to demonstrate larval plaice swimming.
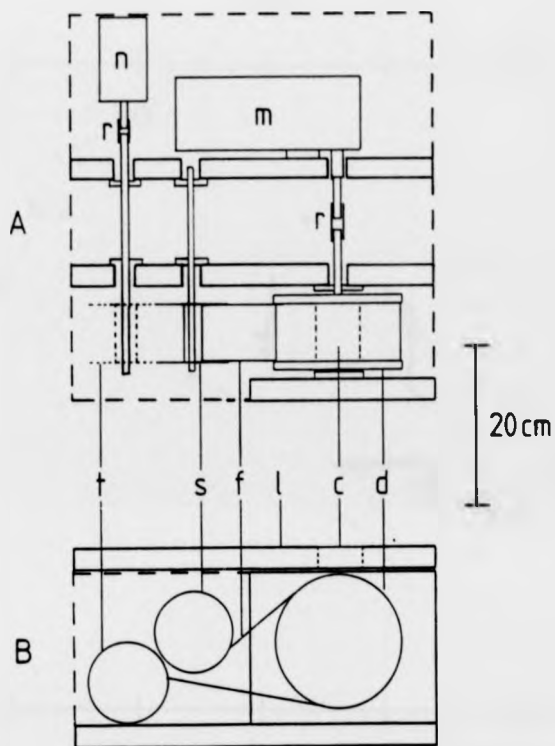
FIG. 1. The silhouette "camera". (A) plan view, (B) side view. c, container for subjects; d, drum; f, 70 mm film; l, lid; m, drum motor; n, take up spool motor; r, rubber coupling; s, supply spool; t, take-up spool.

Edgerton's technique was modified so that the film moved beneath the subject while a strobe flashlight, 2.2 m vertically above the subject in a dark room, gave a series of separate exposures along the length of the film.

The field of view is determined by the area of film exposed and is limited by the film format used. Therefore, to allow a large 57 mm × 57 mm field of view, 70 mm (Kodak TriXpan) film was used. A diagram of the apparatus is shown in Fig. 1. The supply spool contains the film to be exposed preceded by a 10 m leader of scrap film. With the 10 μs, 0.15 J strobe running at 70 Hz and the subjects in place, both motors are started together. The take-up spool motor tends to tension the film against the drum and the drum motor determines the maximum speed of film movement of 4.9 m s^{-1} at which the
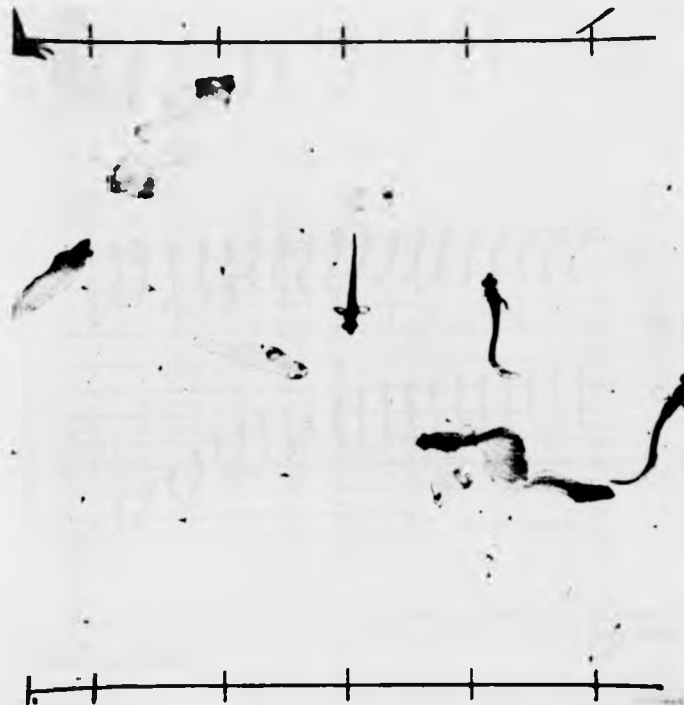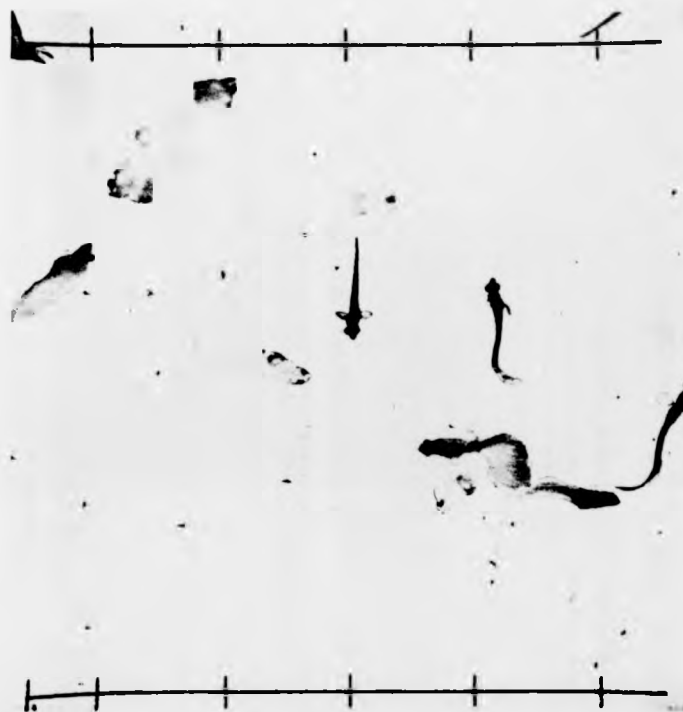
FIG. 2. A print from one frame of a silhouette film showing plaice larvae at various stages. The reference scales have 1 cm divisions and are 5 cm long.

70 Hz strobe gave separate images on the film. After exposure the film was developed in Kodak D 76 developer for 9 min. A print from one frame of a resulting negative is shown in Fig. 2.

Analytical Techniques

The films were analysed by a computer-aided method. Individual frames were projected and traced onto sheets of paper which were then fixed to a digitizing table linked to a Hewlett Packard 9825 desktop computer. Whole outlines of the body and pectoral fins were traced with the digitizer's cursor (Fig. 3), recorded by the computer and stored on magnetic tape for subsequent analysis.

Body waves
The first step was to reduce the data to a number of points centred

FIG. 2. A print from one frame of a silhouette film showing plaice larvae at various stages. The reference scales have 1 cm divisions and are 5 cm long.

70 Hz strobe gave separate images on the film. After exposure the film was developed in Kodak D 76 developer for 9 min. A print from one frame of a resulting negative is shown in Fig. 2.

Analytical Techniques

The films were analysed by a computer-aided method. Individual frames were projected and traced onto sheets of paper which were then fixed to a digitizing table linked to a Hewlett Packard 9825 desktop computer. Whole outlines of the body and pectoral fins were traced with the digitizer's cursor (Fig. 3), recorded by the computer and stored on magnetic tape for subsequent analysis.

Body waves
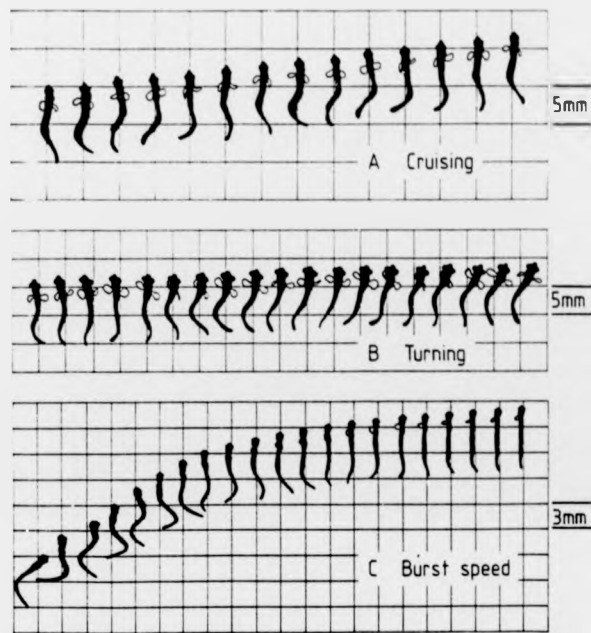The first step was to reduce the data to a number of points centred

FIG. 3. Computer plotted outlines of plaice larvae swimming, derived from silhouette photographs. (A) an example of cruising swimming; (B) turning; (C) burst speed swimming. There are 14 ms between frames.
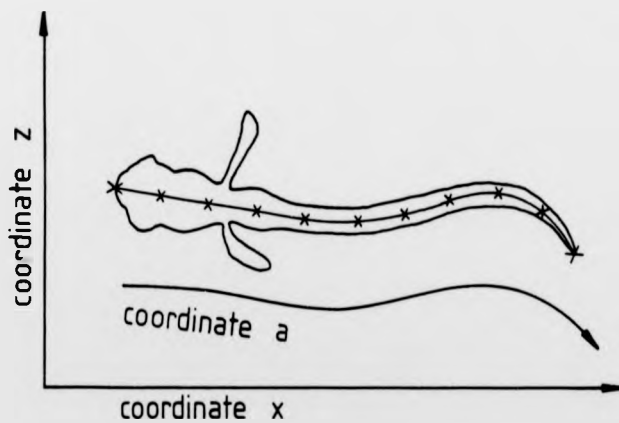

FIG. 4. A diagram showing the co-ordinate system and the 11 points on the co-ordinate a at fixed 0.1 a increments from the head ($a = 0$) to the tail ($a = 1$).

on the notochord of fixed position along a length co-ordinate a (see Fig. 4). To achieve this a series of points making up a line midway between the two sides of the larva was found. This was done by taking pairs of points, one from each side of the body at a similar distance from the head and then finding the co-ordinates of the point midway between these two points. The a co-ordinate of each of these points was found. The x and z co-ordinates for 11 points at 0.1 a increments, along a from head = 0 to tail = 1 were found by interpolation. It was then possible to follow similar methods to those used by Videler & Wardle (1978) to find the various parameters of the body waves, which are summarized by Fig. 5. These authors estimated wave speed v from wave crest da/dt, i.e. speed along the co-ordinate a. This value was found by plotting z against time for each a increment and so finding the time at which a wave crest (maximum or minimum) passes through each point. These values were then plotted as graphs of a against time (Fig. 6). Videler & Wardle (1978) multiplied the value for da/dt, found by fitting regression lines, by a factor to correct for the effect of body bending on the distance occupied by the body along the x axis.
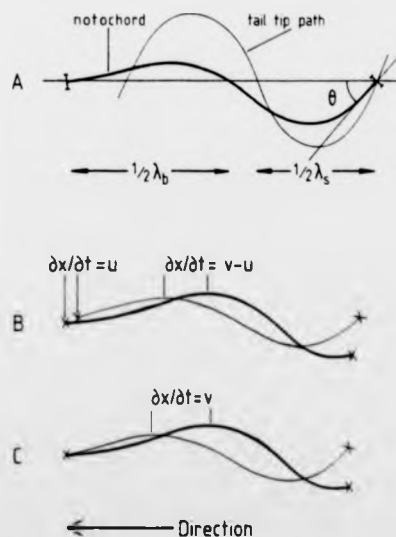

FIG. 5. Diagrams demonstrating body wave parameters. (A) shows λ_b, λ_s, and θ (the angle between any part of the body and the direction of motion. (B) and (C) define swimming speed u and wave speed v from the passage of wave crests down the body. In (B) the two consecutive notochord lines are in their real positions and in (C) they are moved so that the heads are superimposed.
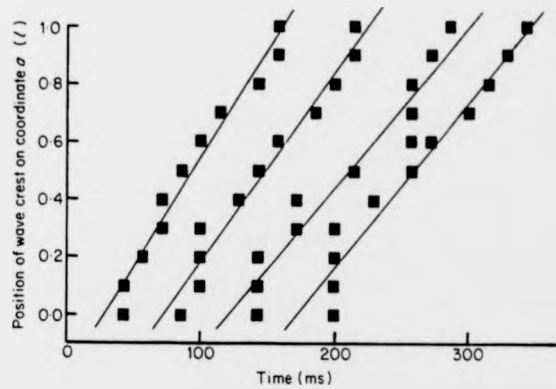
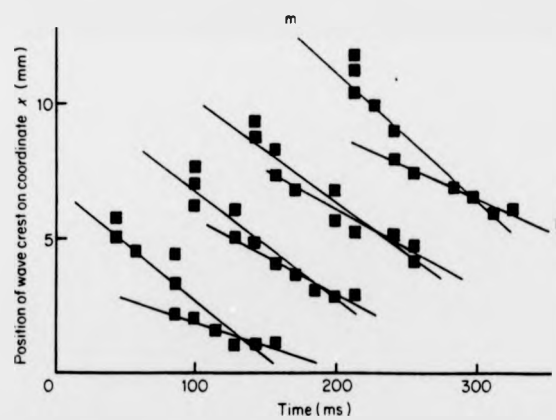FIG. 6. *a* co-ordinate positions against time for a series of wave crests with fitted regression lines.

FIG. 7. *x* co-ordinate positions (corresponding to *a* co-ordinates plotted in Fig. 6) against time. The slopes of fitted regression lines (m) to all points and (p) to the last 6 points give mean and posterior values for $v - u$.

In the present case this shortening was increased by the larger body angles θ, and therefore it was considered better to measure actual wave crest dx/dt and then find the corresponding x co-ordinate for each a co-ordinate found by Videler & Wardle's (1978) method. Figure 6 shows that plots of a against time are straight lines and contrast with Fig. 7, showing plots of x against time (for calculation of dx/dt on the same sequence). This value of dx/dt is equal to $v - u$. Figure 7 shows that $v - u$, and therefore v, can

decrease along the length of the larva and demonstrates the value of using this method for calculating v.

Two values for v were calculated from each wave, using either all the points on a or the last six; in other words a mean or posterior v (v_m, v_p).

Pectoral fin movements

A simple analysis was made in order to describe pectoral fin movements. It was not possible to distinguish and follow individual fin rays through a fin stroke cycle as Blake (1979) did. Left and right fin tip co-ordinates were defined for each frame as the point on the fin outline furthest from the base of the fin (the first pair of co-ordinates recorded for each fin). Having found the fin tip, the fin angle was defined as the angle between the tip of the larva's head, the fin base and the fin tip. The phase and frequency of fin movements and body movements could now be compared. Since it was not possible to find the positions of individual fin rays the three-dimensional shapes of the fins were not known, and for this reason a measurement of angle of attack to the water flow, could not be made. An estimation of this angle of attack was taken as the projected area of the fin seen from above. When this projected fin area was low, angle of attack to the water flow was high and vice versa.

RESULTS

Cruising Speeds

Cruising swimming of plaice larvae is characterized by the simultaneous use of pectoral fins and body waves. On the only recorded occasion when pectoral fins were used alone no forward progress was made. Body waves without the use of pectoral fins were only used at burst speeds.

Body waves

Wave characteristics were analysed for two sizes of larvae, 7 mm and 11 mm. An example of amplitude of z displacement along the body is shown in Fig. 8, together with angle θ for the intervals between each a increment. These amplitude curves are very similar to those for adult fish swimming in the subcarangiform mode (Grillner & Kashin, 1976). There is a major difference between larval and adult fish in the body angle θ curve. A much larger tail θ occurs at the moderate cruising speed employed here than has been found in
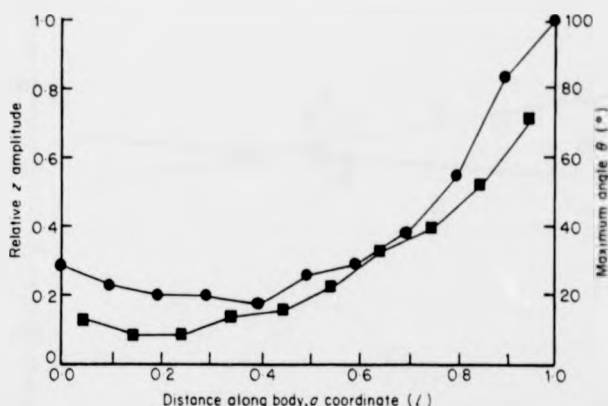
FIG. 8. Maximum relative amplitudes for each length co-ordinate a point ●, and maximum angle θ of each interval between the points ■, for a 10 mm larva.

similar analyses of adult fish cruising. Indeed, in larvae, tail angles of greater than $90°$ have been observed at higher cruising speeds and during acceleration. It is notable that the measured wave speeds v show no positive correlation with forward swimming speed u (Fig. 9). In adult fish u/v is relatively constant (Videler & Wardle, 1978). The technique used to find v has some bearing on the result since v varies with position on the body (Fig. 7), decreasing from head to tail, when u was above $30\,\mathrm{mm\,s^{-1}}$. For this reason both v_m and v_p are plotted in Fig. 7 showing the changing swimming style at higher cruising speeds. Figure 10, a plot of u/v against speed u, shows a clear increase in u/v with swimming speed and the change in style.

If v does vary along the body then so must wavelength λ_b, otherwise the larvae would be ripped apart if frequency changed. Since frequency is equal to v/λ_b, when speed v decreases the wavelength λ_b must get shorter.

Tail tip amplitude varies little with speed, therefore maximum tail θ must increase with swimming speed as tailwards decrease in v becomes more pronounced. This may be the means of increasing thrust force with speed. Unfortunately, maximum measured values for θ at the tail are not very close to the true maximum value since the technique did not provide sufficient frames per second. Films at a higher frame rate would be necessary to confirm this conclusion.

Mean values of λ_b/L (body wavelength in units of body length), the number of waves included on the body and amplitude (A), are
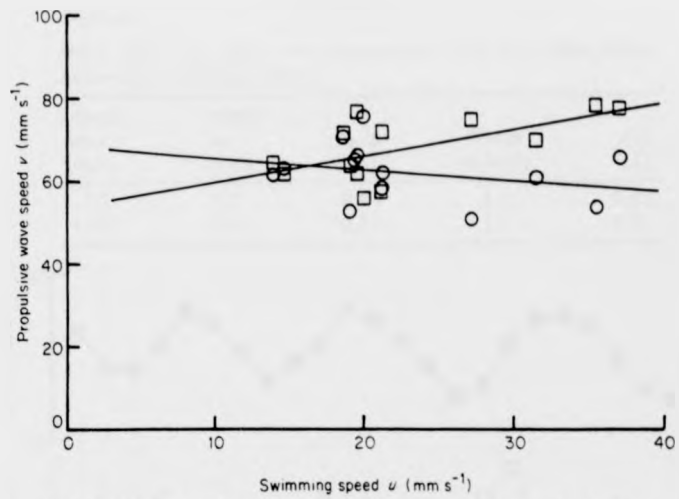
R. S. Batty

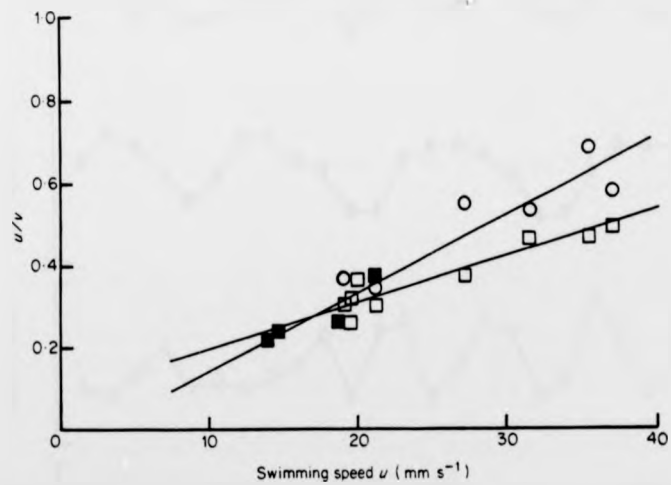FIG. 9. Plots of v_m (□) and v_p (○) against u with fitted regression lines.

FIG. 10. u/v_m (□) and u/v_p (○) against swimming speed u, with fitted regression lines. ■ indicates where values for u/v_m and u/v_p coincide.

shown in Table I, for two body lengths, 7.2 mm and 10.0 mm. There is little difference between the two sizes of larva and both include slightly more than one wave on their body when swimming at cruising speeds.

TABLE I

Mean values of body wave parameters from two plaice larvae swimming at cruising speeds

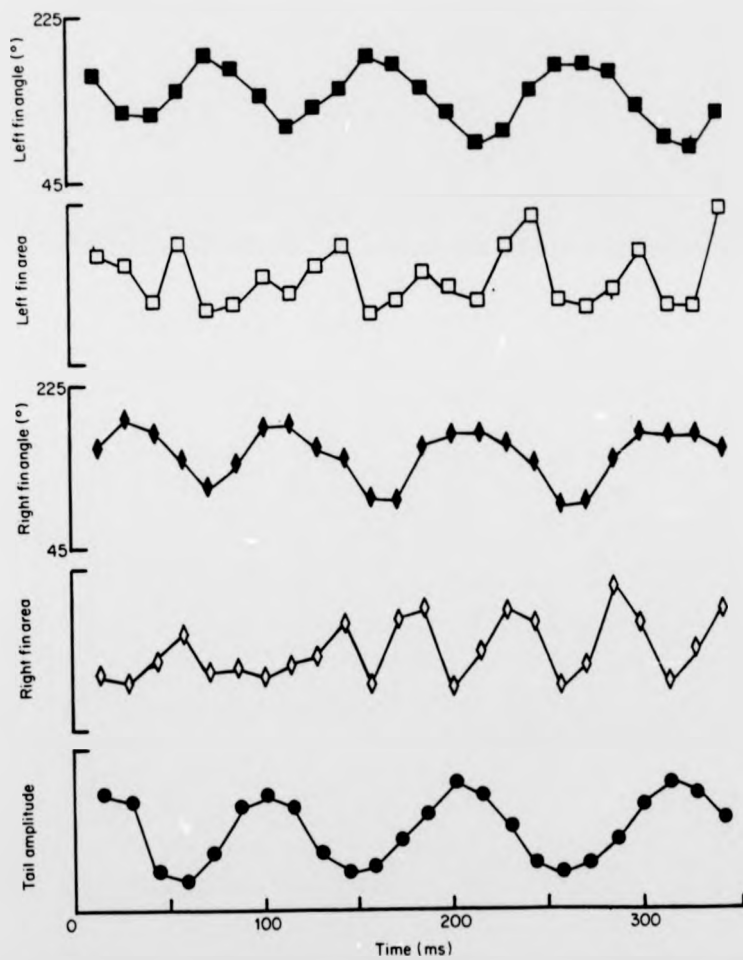| Length on a (mm)	Length on x (mm)	λ_b/L (L)	Waves on body	A/L (L)
7.2	6.7	0.84	1.1	0.32
10.0	9.2	0.82	1.1	0.35

FIG. 11. Pectoral fin movements during straight swimming of a 10 mm larva. ■, left fin angle; □, left fin area; ♦, right fin angle; ◊, right fin area; ●, tail amplitude.

Pectoral fin movements

An example of an analysis of pectoral fin movements during steady
forward swimming is shown in Fig. 11. This diagram clearly shows
the synchronization of pectoral fins with body waves. Their move-
ments are of the same frequency but there is a 180° phase difference
between the left and the right pectoral fin. Projected fin areas are
plotted on the same axis as fin angle and give an indication of angle
of attack. The projected fin area (an indication of angle of attack)
varies at twice the frequency of fin beating, showing that lift or
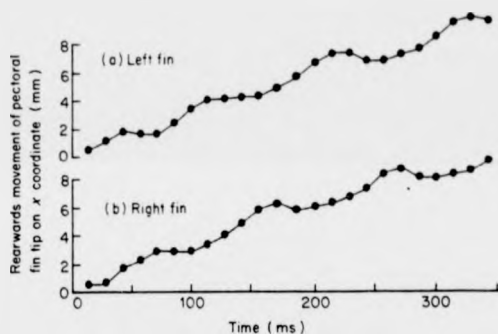negative lift may be produced on both strokes.

FIG. 12. Pectoral fin tip x co-ordinate position against time for the same sequence shown in
Fig. 11.

Rearward strokes of the pectoral fins may have little propulsive
effect. Figure 12, a graph of fin tip x co-ordinate against time demon-
strates the low or zero effect on the water of rearward strokes; but
the synchronization of pectoral fin strokes with propulsive waves will
tend to counteract head yaw by counteracting the recoil effect pro-
duced by the tail fin strokes. The pectoral fin strokes are perfectly
timed to do this and improve efficiency by reducing drag induced by
swimming movements.

Turning

Pectoral fin movements change during turning. In the example shown
in Fig. 3, the larva is turning to the right. The right fin moves be-
tween a point perpendicular to the body and a point 180° from the
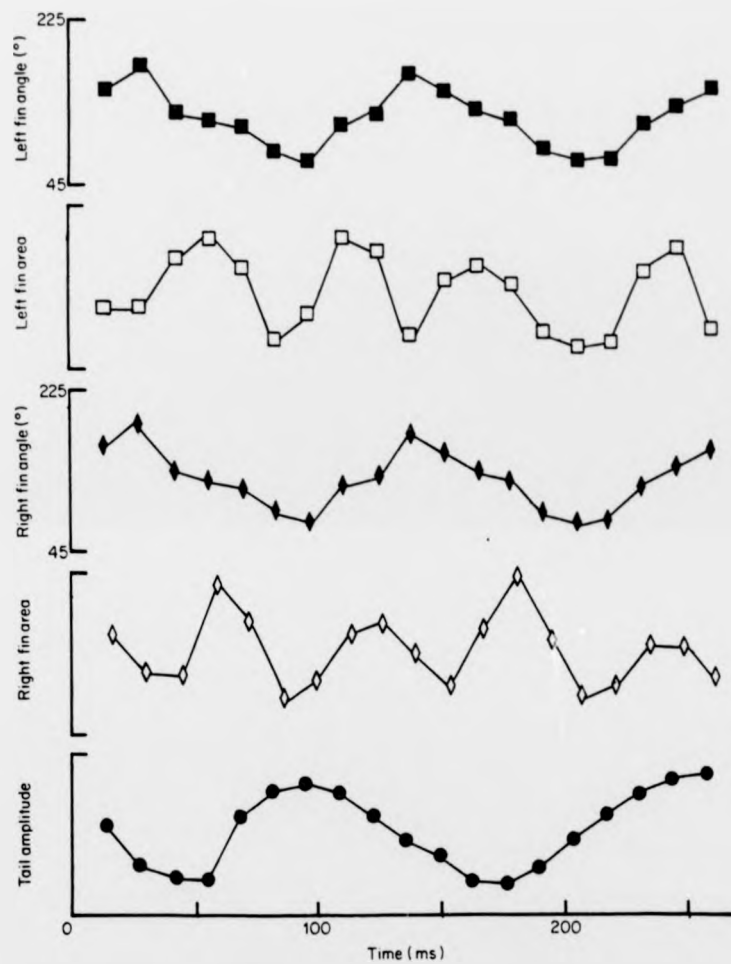head as in straight swimming, but the left fin moves between 0 and

FIG. 13. Pectoral fin movements during a right turn. Labelled as in Fig. 11.

90° from the head; this situation is reversed in left turns. An analysis of this turn (Fig. 13) shows a movement similar to straight swimming except for this change in the stroke of the left fin to move in the range 0 to 90° from the head.

The part played by the pectoral fins during turning is not clear, especially since the turning couple on the head would tend to rotate the head against the desired direction.

R. S. Batty

Burst Speeds

At burst speeds only body waves are used (Fig. 3c) and are apparently of a different form to cruising speed swimming. Unfortunately the photographic method used has limited the number of frames per tail beat to two, at this speed, so that a proper analysis of the propulsive waves cannot be made. An examination of the outlines of a 7 mm larva shown in Fig. 4 indicates that wavelength λ_b is longer than one body length (L) and that amplitude is much greater than during cruising. These two changes cause less than one complete wave to be included on the body. It seems that the larva has "changed gear" in order to swim at this higher speed of $140\,\mathrm{mm\,s^{-1}}$ ($20\,L\,\mathrm{s^{-1}}$) whilst using a very high tail beat frequency of 35 Hz. A considerable yaw of the head is seen in this sequence, compared with cruising swimming (Fig. 4a) when pectoral fin movements are used. Measurements of maximum tail beat frequencies of the plaice larvae are plotted in Fig. 14 together with similar data obtained by Bainbridge (1958) for adult fish and by Hunter (1972) for anchovy larvae.
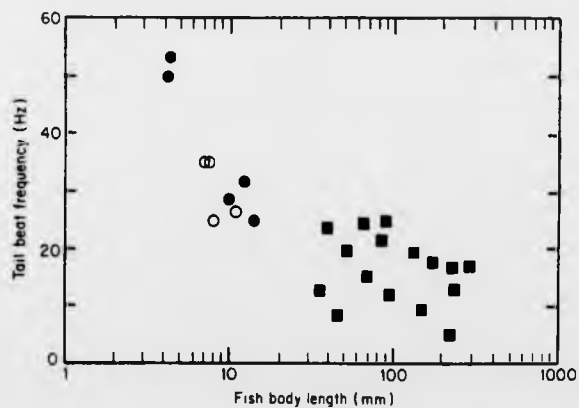

FIG. 14. Maximum tail beat frequencies of different sizes of fish. ○, plaice larvae; ●, anchovy larvae (Hunter, 1972); ■, adult fish (Bainbridge, 1958).

The graph demonstrates that maximum tailbeat frequency is strongly dependent on size, increasing as size decreases. This observation is confirmed by the findings of Wardle (1975) on the contraction time of adult muscle which shows the same type of size effect.

DISCUSSION

The results indicate that the pectoral fins are not important for producing thrust to propel the larva forward. It seems that their role is to produce lift, which is important since the larvae are negatively buoyant (Ehrlich, 1972), and at the same time, during cruising, to reduce head yaw.

Head yaw is caused by angular recoil forces which are generated by the lateral movements of the tail (Lighthill, 1977). The opposite forces generated by the pectoral fins of the larvae form a couple tending to turn the head against the recoil caused by the tail. Any reduction in head yaw should lead to a decrease in drag caused by swimming movements (Lighthill, 1977), but in this case the improvement in swimming movements is due in part to an increase in drag caused by the forward movement of one of the fins.

If alternating fin movements were not used lift would be produced by a pair of fixed fins, resulting in some drag. The plaice larva's alternating pectoral fin movements increase swimming efficiency by using energy spent in producing lift to reduce the amount of drag that is induced by swimming movements.

The one disadvantage is that roll might be induced, but this was too small to be observed in the films made in this study and would be expected to be very small in a deep-bodied fish larva which will have a large resistance to forces producing roll.

If the body waves of larvae are compared with those of adult fish, they are most like adult fish swimming in the subcarangiform mode (Breder, 1926). But there are many differences between larvae and adults. Speed of the propulsive wave v and tail beat frequency are not firmly linked to swimming speed at cruising speeds as in adults. This means that u/v, found to decrease only slightly with increasing speed for an adult fish, actually increases in the larval plaice: u/v is much lower (0.2 to 0.4) than in adult fish where it is in the range 0.6 to 0.8.

Values of u/v may be used to calculate propeller efficiency η_p (Lighthill, 1960) provided that amplitude increases from near zero at the head to a maximum at the tail tip.

$$\eta_p = \tfrac{1}{2}(1 + u/v) \qquad (3.1)$$

Using this formula, η_p would be in the range 0.6 to 0.7 for plaice larvae or 0.8 to 0.9 for most adult fish. Webb (1977) used results obtained by C. C. Lindsey to make estimates of propeller efficiency for a wide range of sizes. He showed a size dependence of propeller efficiency of similar magnitude to the results presented here.

ACKNOWLEDGEMENTS

REFERENCES

Arnold, G. P. & Nuttall-Smith P. B. N. (1974). Shadow cinematography of fish larvae. *Mar. Biol.* 28: 51–53.

Bainbridge, R. (1958). The speed of swimming of fish as related to size and to the frequency and amplitude of the tail beat. *J. exp. Biol.* 35: 109–133.

Blake, R. W. (1979). The mechanics of labriform locomotion. I. Labriform locomotion in the Angelfish (*Pherophyllum eimekei*): an analysis of the power stroke. *J. exp. Biol.* 82: 255–271.

Blake, R. W. (1981). Mechanics of drag-based mechanisms of propulsion in aquatic vertebrates. In *Vertebrate locomotion*: 29–52. Day, M. H. (Ed.). London and New York: Academic Press.

Breder, C. M. (1926). The locomotion of fishes. *Zoologica, N.Y.* 4: 159–256.

Edgerton, H. E. (1977). Silhouette photography of small active subjects. *J. Microsc.* 110: 79–81.

Ehrlich, K. F. (1972). *Morphometrical, behavioural and chemical changes during growth and starvation of herring and plaice larvae.* Ph.D. Thesis: Stirling University.

Gray, J. (1968). *Animal locomotion*. London: Weidenfeld & Nicolson.

Grillner, S. & Kashin, S. (1976). On the generation and performance of swimming in fish. In *Neural control of locomotion*: 181–201. Herman, R. M., Grillner, S., Stein, P. S. G. & Stuart, D. G. (Eds). New York: Plenum Press.

Hunter, J. R. (1972). Swimming and feeding behavior of larval anchovy *Engraulis mordax*. *Fish. Bull.*, *U.S.* 70: 821–838.

Lighthill, M. J. (1960). Note on the swimming of slender fish. *J. Fluid Mech.* 9: 305–317.

Lighthill, M. J. (1977). Mathematical theories of fish swimming. In *Fisheries mathematics*: 131–144. Steele, J. H. (Ed.). London & New York: Academic Press.

Rosenthal, H. (1968). Schwimmverhalten und Schwimmgeschwindigkeit bei den Larven des Herings *Clupea harengus*. *Helgoländer wiss. Meeresunters.* 18: 453–486.

Rosenthal, H. & Hempel, G. (1969). Experimental studies in feeding and food requirements of herring larvae. In *Symp. Marine Food Chains, Univ. of Aarhus, Denmark 1968*: 344–364. Steele, J. H. (Ed.). Edinburgh: Oliver and Boyd.

Videler, J. J. & Wardle, C. S. (1978). New kinematic data from high speed cine film recordings of swimming cod (*Gadus morhua*). *Neth. J. Zool.* 28: 465–484.

Vlymen, W. J. (1974). Swimming energetics of the larval anchovy, *Engraulis mordax*. Fish. Bull., U.S. **74**: 36–51.

Wardle, C. S. (1975). Limit of fish swimming speed. *Nature, Lond.* **225**: 725–727.

Wardle, C. S. & Reid, A. (1977). The application of large amplitude elongated body theory to measure swimming power in fish. In *Fisheries mathematics*: 171–191. Steele, J. H. (Ed.). London & New York: Academic Press.

Webb, P. W. (1975). Hydrodynamics and energetics of fish propulsion. *Bull. Fish. Res. Bd Can.* **190**: 1–159.

Webb, P. W. (1977). Effects of size on performance and energetics of fish. In *Scale effects in animal locomotion*: 315–331. Pedley, T. J. (Ed.). London & New York: Academic Press.

II